

**BIOSYNTHESIS OF COPPER NANOPARTICLES USING
Senna didymobotrya ROOT EXTRACT AND THEIR EFFICACY
ACTIVITY AGAINST *Escherichia coli* and *Staphylococcus aureus***

BY

BERNARD OTIENO SADIA

**A THESIS SUBMITTED IN PARTIAL FULFILMENT OF THE
REQUIREMENTS FOR THE AWARD OF A MASTER OF SCIENCE
IN ANALYTICAL CHEMISTRY OF MOI UNIVERSITY**


NOVEMBER, 2021

DECLARATION

Declaration by the Candidate

This thesis is my original work and has not been presented for a degree in any other University. No part of this thesis may be reproduced without the prior written permission of the author and/or Moi University.


Sadia Bernard Otieno

Signature  Date28/11/2021.....

MSC/ACH/01/18

Declaration by Supervisors:


This thesis has been submitted for examination with our approval as University Supervisors.

Signature ...  Date ...29/11/2021.....

Dr. Jackson Cherutoi

Department of Chemistry & Biochemistry

Moi University

Signature ...  Date ...29/11/2021.....

Dr. Cleophas Achisa Mecha

Department of Chemical and Process Engineering

Moi University

DEDICATION

I dedicate this thesis report to my parents, Mr. Michael Sadia Menya and Phibi Achieng' Sadia, for both emotional and financial support without which I would not have completed this Master's program.

The author sincerely praises and honor the Lord for provision of good health, strength, wisdom and protection to achieve this success.

ACKNOWLEDGEMENTS

Special recognition goes to the various individuals and organizations for the support accorded to me during my thesis progress. Special appreciation to Africa Centre of Excellence in Phytochemicals, Textile, and Renewable Energy (ACE II-PTRE) for the master's scholarship without which, my studies would have been impossible. I thank Moi University, School of Sciences and Aerospace Studies and School of Engineering staff especially my Supervisors Dr. Jackson Cherutoi and Dr. Cleophas Achisa Mecha for the technical guidance and support throughout my thesis research period. You indeed offered valuable educational insights.

Not forgetting my classmates, Mr. Calvince Ondijo, Mr. Vincent Rotich, Mr. Evans Kapkea, Miss Merab Lilian Ndiege, Mrs Alide Tandi, Miss Winnie Nassazi, Miss Linet Jelagat Kipkulei and Mrs Immaculate Mbabazi whom I consulted often during my research work.

ABSTRACT

The economic burden and high mortality associated with multi-drug resistance in *Escherichia coli* and *Staphylococcus aureus* is a major public health concern. This study investigated nanomaterials as antimicrobial agents. Copper (Cu) nanoparticles exhibit better antimicrobial efficacy than copper in bulk form. Cu nanoparticles can offer a solution to antibiotic resistance. *Senna didymobotrya* roots contain phytochemicals capable of synthesizing Cu nanoparticles. The aim of this study was to synthesize Cu nanoparticles using *S. didymobotrya* plant root extract and test their efficacy against *E. coli* and *S. aureus*. The specific objectives were to: perform extraction, qualitative and quantitative phytochemical screening; synthesis and characterization of Cu nanoparticles; and evaluation of the antimicrobial efficacy of Cu nanoparticles. All the experiments were performed at the Chemistry laboratory in Moi University, Kenya. Extraction was done by soxhlet method. Phytochemical screening was done. Total flavonoid content and total phenolic content was determined. GC-MS analysis was performed to identify compounds in *S. didymobotrya* root extracts. Cu-nanoparticles were synthesized by adding 10 mL of *S. didymobotrya* root extracts to 90 mL of 0.0125-0.05 M aqueous $\text{CuSO}_4 \cdot 5\text{H}_2\text{O}$ solution at varying temp of 40-80 °C and pH of 3-10. Box Behnken design was used to obtain optimal synthesis conditions as determined using Nanotrak particle analyzer. Characterization was done using UV-Vis, Particle size analyzer, X-ray diffraction, Zeta potentiometer, GC-MS and FT-IR. Antibacterial tests were conducted using Kirby-Bauer disk diffusion susceptibility test involving 30 μL solution of Cu nanoparticles. Amoxicillin clavulanate was positive control and dimethyl sulfoxide was negative control. Extraction yield of *Senna* root methanol extract was 9.94 %. Phytochemical screening showed positive for phenols, tannins, saponins, gladiac glycosides, anthraquinones, alkaloids, and flavonoids; and negative for steroids and terpenoids. Total Flavonoid Content was 48.3 ± 1.5 mgQE/g dry weight while Total Phenolic Content was 34.5 ± 0.1 mg GAE/g dry weight. The major compounds identified by GC-MS in reference to NIST library were; Benzoic acid, Thymol, N-Benzyl-2-phenethylamine, Vanillin, Phenyl acetic acid, and Benzothiazole. UV-Vis spectrum showed characteristic peak at 571 nm indicating the formation of Cu-nanoparticles. The optimum synthesis conditions were temperature of 80 °C, pH 3.0 and Cu ion concentration of 0.0125 M. FT-IR spectrum showed absorptions in the range $3500\text{-}3100\text{ cm}^{-1}$ (N-H stretch), $3400\text{-}2400\text{ cm}^{-1}$ (O-H stretch), $988\text{-}830\text{ cm}^{-1}$ (C-H bend), peak at 1612 cm^{-1} (C=C stretch), and 1271 cm^{-1} (C-O bend). Cu- nanoparticles sizes ranged between 5.55 and 63.60 nm. The zeta potential value was -69.4 mV indicating that they were stable. The nanoparticles exhibited significant antimicrobial activity on *E. coli* and *S. aureus* with Zone of Inhibition 26 ± 0.58 mm and 30 ± 0.58 mm compared to amoxicillin clavulanate (standard) with 20 ± 0.58 mm and 28 ± 0.58 mm, respectively. In conclusion, *Senna* has high amounts of flavonoids and phenols; the biosynthesized Cu nanoparticles are stable and displayed better antimicrobial activity against *E. coli* and *S. aureus* compared to amoxicillin clavulanate (standard). The study recommends the testing of biosynthesized Cu nanoparticles against other potential multi-drug resistant microbes to enable their development into antimicrobial agents.

TABLE OF CONTENTS

DECLARATION.....	i
DEDICATION.....	ii
ACKNOWLEDGEMENTS.....	iii
ABSTRACT.....	iv
ABBREVIATIONS.....	xiii
CHAPTER 1: INTRODUCTION.....	1
1.1 Background of the Study.....	1
1.2 Statement of the Problem.....	4
1.3 Justification of the study.....	5
1.4 Significance of the study.....	6
1.5 Objectives of the study.....	7
1.5.1 Main objective.....	7
1.5.2 Specific objectives:.....	7
1.6 Hypothesis.....	7
CHAPTER 2: LITERATURE REVIEW.....	9
2.1 <i>Senna didymobotrya</i>	9
2.1.1 Phytochemical Evaluation.....	11
2.1.2 Isolation and Characterization.....	12
2.1.3 Gas Chromatography – Mass Spectrometry.....	13

2.2.0 Nanotechnology	13
2.3.0 Copper Nanoparticles.....	15
2.4.0 Methods of Synthesis	15
2.4.1 Chemical reduction method.....	16
2.4.2 Biosynthesis method.....	16
2.5 Application of Copper Nanoparticles.....	18
2.6 Kinetics and Stability of biosynthesized Copper Nanoparticles	20
2.6.1 Optimization of synthesis process	20
2.7.0 Characterization technique.....	21
2.7.1 Ultraviolet – Visible Spectrophotometry.....	22
2.7.2 Fourier Transform Infrared Spectroscopy	22
2.7.3 Particle size determination	23
2.7.4 X – Ray Diffraction Spectroscopy	23
2.7.5 Zeta potential measurement.....	24
2.8.0 Antimicrobial resistance.....	24
2.9 Summary of main findings and gaps.....	26
CHAPTER 3: MATERIALS AND METHODS	29
3.0 Introduction	29
3.1 Materials and Equipment	30
3.1.1 Chemicals and Reagents.....	30

3.1.2 Equipment.....	30
3.2. Sample Collection	31
3.2.1 Extraction of phytochemicals from <i>Senna didymobotrya</i> roots	31
3.2.2 Preparation of <i>Senna didymobotrya</i> roots Extract.....	31
3.3 Qualitative and quantitative phytochemical evaluation	32
3.3.1 Qualitative phytochemical analysis	32
3.3.2 Determination of total flavonoid content	34
3.3.3 Determination of total phenolic content	35
3.3.6 Gas chromatography mass spectrophotometry.....	36
3.4 Optimized Biosynthesis of Copper nanoparticles and Characterization.....	37
3. 4. 1 Synthesis of copper Nanoparticles	37
3.4.2 Optimization of biosynthesis process	38
3.5 Characterization of Copper Nanoparticles.....	39
3.5.1 Ultra-Violet Spectroscopy	39
3.5.2 Particle Size Analysis	39
3.5.3 X-Ray Diffraction.....	40
3.5.4 Zeta Potential.....	40
3.5.5 FT–IR Spectroscopy Analysis.....	40
3.6 Anti-microbial Activity of <i>Senna didymobotrya</i> Copper nanoparticles.....	41
CHAPTER 4: RESULTS AND DISCUSSION.....	43

4.0 Introduction	43
4.1 Extraction of compounds of <i>Senna didymobotrya</i> roots	43
4.2 Qualitative and Quantitative phytochemical evaluation	43
4.2.1 Phytochemical screening of <i>Senna didymobotrya</i> root extract	43
4.2.2 Total Flavonoid and Phenol content determination.....	44
4.2.5 Gas Chromatography-Mass Spectrometry	47
4.3 Biosynthesis of Copper nanoparticles	53
4.3.1 Design of Experiments and optimization Analysis	56
4.4 Characterization of Copper Nanoparticles	66
4.4.1 Particle Size Analysis	66
4.4.2 X-Ray Diffraction Analysis.....	68
4.4.3 Zeta Potential Analysis.....	69
4.4.4 FT –IR Analysis	70
4.5 Anti-microbial activity of <i>Senna didymobotrya</i> copper nanoparticles.....	71
CHAPTER 5: CONCLUSIONS AND RECOMMENDATIONS.....	76
5.1 Conclusions	76
5.2 Recommendations	77
REFERENCES	78
APPENDICES	91
Appendix A: Particle Size Analyzer Data	91

Appendix B: Growth Inhibition Zones of Cu NPs biosynthesized at different conditions of temperature, pH and Copper ion Concentration	93
---	----

LIST OF TABLES

Table 1: Results of phytochemical screening of aqueous extract of <i>Senna didymobotrya</i> . .44	44
Table 2: Preparation of calibration curve of quercetin.....46	46
Table 3: Calculation procedure for total flavonoid.46	46
Table 4: Preparation of calibration curve of garlic acid.....46	46
Table 5: Calculation procedure for total phenolic.....47	47
Table 6: Compounds identified by Gas Chromatography-Mass Spectrometry analysis of <i>Senna didymobotrya</i> root extracts.49	49
Table 7: Box behnken design and response variables.....56	56
Table 8: Calculated values of the coefficients of the model.57	57
Table 9: Analysis of variance (ANOVA) for Size of Cu NPs Versus Temp (°C), Conc (M), pH.....58	58
Table 10: Regression table - Model Summary.....59	59
Table 11: Antimicrobial activity of Cu NPs synthesized at different parameters.....74	74

LIST OF FIGURES

Figure 1: Some compounds isolated from the root and the stem bark extracts of Senna didymobotrya	10
Figure 2: Relationship between the number of cubes from a 1-m cube and the surface area produced.....	14
Figure 3: General procedure for the nanoparticle synthesis	17
Figure 4: Methodological process relating to research objectives.....	29
Figure 5: Photographs showing colours of Copper (II) Sulphate (a), pure root extract of S. didymobotrya (b), initial colour change (c), final colour change (d).....	38
Figure 6: Calibration curve of quercetin.....	45
Figure 7: Calibration curve for Gallic acid.....	45
Figure 8: Total ion chromatogram of Senna didymobotrya extracts.	48
Figure 9: Some compounds identified from Senna didymobotrya root extract using GC-MS analysis.....	52
Figure 10: UV-Visible spectra of Senna didymobotrya root extract.	54
Figure 11: UV-Vis spectra of Cu NPs synthesized by Senna root extract.....	55
Figure 14: Main effects plot for mean particle size.	60
Figure 15: Interaction effects plot for mean particle size.	61
Figure 16: Probability plot for average size of copper nanoparticles.	61
Figure 17: Normality plot of residual for mean particle size.....	62
Figure 18: Plot of residual versus fitted values of mean particle size.	63
Figure 19: 3D Surface graph for mean particle size versus Copper ion concentration and pH of the mixture.....	64

Figure 20:3D Surface graph for mean particle size versus temperature and pH of the mixture.	64
Figure 21: 3D Surface graph for mean particle size versus temperature and concentration of Copper ion.....	65
Figure 22: Response optimization for average particle size of Cu NPs.	65
Figure 23: Particle Size of Cu NPs prepared at Temp 80 °C, pH 3.0 and Copper ion Concentration 0.03125 M.	66
Figure 24: X-Ray Diffraction pattern of Cu NPs biosynthesized by Senna root extracts. ...	69
Figure 25: Zeta Potential Distribution of Cu NPs synthesized by Senna root extracts.	70
Figure 26: FT-IR Spectrum of Cu NPs synthesized by Senna root extract.	71
Figure 27: Graph of antimicrobial activity of Copper nanoparticles, Standard drug, copper sulphate solution and Senna root extract.	75
Figure 28: The growth inhibition zones of CuNPs biosynthesized at different conditions of temperature, pH and copper ion concentration against Escherichia coli in Luria betani (LB) disk diffusion.....	93
Figure 29: The growth inhibition zones of CuNPs biosynthesized at different conditions of temperature, pH and copper ion concentration against Staphylococcus aureusi in Luria betani (LB) disk diffusion.....	94

ABBREVIATIONS

μL – micro Liter

°C – Degree Celsius

CC – Column Chromatography

Cu NPs – Copper Nanoparticles

Da – Dalton

DCS – Differential Centrifugal Sedimentation

DLS – Dynamic Light Scattering

DOE – Design of Experiment

EPLS – Elliptically Polarised Light Scattering

EPM – Electrophoretic Mobility

EU – European Union

eV – Electron Voltage

EXAFS – Extended X-ray Absorption Fine Structure

FMR – Ferromagnetic Resonance

FTIR – Fourier Transform Infrared Spectroscopy

GC – Gas Chromatography

GC-MS – Gas Chromatography – Mass Spectroscopy

HRTEM – High Resolution Transmission Electron Microscopy

ICDD – International Centre for Diffraction Data Database

ICP-MS – Inductively Couple Plasma – Mass Spectrometry

LB – Lauria Bertani

LC – Liquid Chromatography

M – Molarity

MDR – Multidrug Resistance

MRSA – Methicillin-Resistant Staphylococcus aureus

mV – micro Voltage

NCCLS – National Committee for Clinical Laboratory

NTA – Nanoparticle Tracking Analysis

OFAT – One Factor at a Time

pH – $-\log$ of Hydrogen ion Concentration

PTA – Particle Tracking Analysis

R_f – Retention factor

rpm – Revolution per minute

SANS – Small Angle Neutron Scattering

SAXS – Small Angle X-Ray Scattering

SIMS – Secondary Ion Mass Spectrometry

STEM – Scanning Transmission Electron Microscopy

TEM – Transmission Electron Microscopy

TGA – Thermal Gravimetric Analysis

TLC – Thin Layer Chromatography

UTI – Urinary Tract Infection

UV-Vis – Ultra violet-Visible spectroscopy

v/v – Volume by Volume

XPS – X-ray Photoelectron Spectroscopy

XRD – X-ray Diffraction

XRF – X – Ray Fluorescence Spectroscopy

CHAPTER 1: INTRODUCTION

1.1 Background of the Study

Nanotechnology is of profound interest to scientists due to its extensive application in pharmaceutical products, electronics, biotechnology and medicine (Poinern *et al.*, 2015; Nair *et al.*, 2010). Nanoparticles (NPs) are solid particles with size approximately extending from 1 nm to 100nm in length in at least one dimension (Padma *et al.*, 2018). Metallic nanoparticles have good stability compared to organic nanostructures, which still encounter unsolved problems, such as their low chemical and mechanic stability and agglomeration (Patra *et al.*, 2018).

Biosynthesis of metal nanoparticles involves using bacteria, algae, fungi plant and plant products and is often referred to as green-synthesis. This approach is considered to be a bottom up method, where the reduction or oxidation is the main reaction that occurs during the fabrication of nanoparticles (Caroling *et al.*, 2015). In this method, the phytochemicals composed in plant parts or microorganism itself act as reductant and capping agents for synthesizing metal nanoparticles (Umer *et al.*, 2014; Honary *et al.*, 2014; Bashir *et al.*, 2011 and Arya, 2010). Biosynthesized inorganic nanoparticle is preferred in applications in various fields, including chemistry because it is an eco-friendly approach. Currently, application of phytochemicals to synthesize nanoparticles is being explored. Green-synthesis of nanoparticles allow for a nanomaterial to be synthesized in a way that is environmentally friendly and can be utilized by human without side-effects. This synthesis approach minimizes toxic chemicals that pose risks to the environment (Adewale *et al.*, 2020).

Nanoparticles application in the field of biotechnology is growing very fast. This is because of various reasons including: nanoparticles are in the same size scale as organic molecules hence can interact easily with them and allow the control and participate in biotic processes; they have high specific surface area and for this reason accommodation of a high concentration of drugs or required molecules in them is possible. Nanotechnology has laid a base for the discovery of new drugs and diagnosis tools (Patra *et al*, 2018).

Inorganic nanoparticles synthesized using biological methods can offer solutions to emergence of multi-drug resistance microbes. This can act as substitute to the traditional organic agents that have limited application due to high rate of decomposition and low heat resistance. The physical and chemical properties are unique, high surface-to-volume ratio, less cost of fabrication, and low toxicity to the environment makes CuNPs desirable as an outstanding gas sensors, dye absorbents, photo-catalysts, antioxidant, antimalarial, antimicrobial and antitumor proxy in comparison to nanoparticles prepared from zinc, gold, silver and iron compounds (Al-Hakkani, 2020; Williams *et al*, 2006; Sathiyavimal *et al*, 2018).

Senna didymobotrya belongs to the genus *Senna* and family *Fabaceae*. It is a hairy, aromatic shrub 5-9 m high. The plant flowers in each inflorescence are arranged sequentially in raceme of bright yellow petals. The fruit is a flat brown legume pod. Different ethnic communities in Kenya have various names for species *didymobotrya*, for example in Meru, it is called Murao/Kirao (Gakuubi *et al*, 2012), Nandi and Kipsigis communities call it Senetwet (Jeruto *et al*, 2008), Owinu/Obino in Luo, and Ithaa/Muthaa in Kamba (Wagate *et al*, 2012). The plant is used to stimulate lactation and to induce uterine contraction and abortion, for treatment of bacterial and fungal infections,

haemorrhoides, sickle-cell anaemia, hypertension, a variety of diseases affective to women such as fibroids and backache, inflammation of fallopian tubes (Nyamwamu *et al*, 2015).

Preceding authors reported that aqueous and organic extracts and fractions of different parts (leaves, flowers, twigs, roots, stem bark, immature pods and root bark) of *S. didymobotrya* elicited antipyretic activity (Mworia *et al*, 2019), hypolipidemic activity (Ochieng' *et al*, 2013), antimicrobial activity against bacteria (such as *Escherichia coli*, *Bacillus cereus*, *Bacillus subtilis*, *Enterobacter aerogenes*, *Lactobacillus acidophilus*, *Klebsiella pneumoniae*, *Proteus vulgaris*, *Ralstonia solanacearum*, *Salmonella typhi*, *Serratia liquefaciens* and *Streptococcus mitis*) (Anthoney *et al*, 2014; Mutuku *et al*, 2015; Hussein *et al*, 2019; Mining *et al*, 2014) and fungi (such as *Aspergillus niger*, *Candida albicans*, *Candida glabrata*, *Candida krusei*, *Candida parapsilosis*, *Candida tropicalis*, *Candida duabus haemulonii*, *Candida haemulonii*, *Candida auris*, *Candida famata*, *Candida orientaris*, *Cryptococcus neoformans*, *Trichophyton mentagrophyte* and *Microsporum gypseum*) (Jeruto *et al*, 2015; Korir *et al*, 2012; Ocharo, 2005; Orwa and Njue, 2019; Igunza *et al*, 2019). It has been reported that the plant has Insecticidal activity against *Acanthoscelides obtectus* and fleas, anthelmintic and anti-amoebic activities as well as toxicity of the extracts (McGaw *et al*, 2000; Nyamwamu *et al.*, 2015; Maina *et al*, 2018).

Classical phytochemical screening of various extracts of *S. didymobotrya* has indicated that anthraquinones, terpenes, saponins, naphthoquinones, tannins, steroids, alkaloids, flavonoids, phenols and terpenoids are the major secondary therapeutic secondary metabolites (Nyamwamu *et al.*, 2015; Alemayehu *et al.*, 2015; Maema *et al.*, 2020). Compounds such as 2, 6, 4'- trihydroxy-trans-stilbene (a stilbenoid derivative) and 4-(2'-oxymethylene-4'-hydroxyphenyl) chrysophanol (a phenyl anthraquinone) were isolated and

characterized for the first time from chloroform/methanol extract of *S. didymobotrya* roots (Alemayehu *et al.*, 2015). Mining *et al.* (2014) performed chromatographic separation of the hexane and dichloromethane extracts of *S. didymobotrya* roots and identified terpenoids (3 β -sitosterol and stigmasterol) and anthraquinones (chrysophanol and physcion) (Mining *et al.*, 2014). Recently, Mworira *et al.*, (2019) reported alpha pinene and terpinolene in dichloromethane extract of *S. didymobotrya* leaves as the main antipyretic compounds.

Reports on pharmacological activities and toxicity of different extracts of *S. didymobotrya* parts exist, however, there was no scientific data on use of *S. didymobotrya* to the synthesis of CuNPs and antimicrobial activity of nanoparticles synthesized from this plant. The current study therefore investigated, for the first time, the synthesis of CuNPs using roots extracts and their antimicrobial efficacy against *E. coli* and *S. aureus*. Synthesis of nanoparticles of smaller, stable and uniform size distribution, crystalline structure requires control of experimental conditions (Maema *et al.*, 2020; Biswas *et al.*, 2017), and for that reason synthesis conditions (concentration of copper ions, temperature and pH) for the CuNPs were optimized.

1.2 Statement of the Problem

The economic burden and high mortality associated with multi-drug resistance in *Escherichia coli* and *Staphylococcus aureus* is a major public health concern. High levels of antimicrobial resistance to commonly used antibiotics have been reported, for instance Ampaire *et al.*, (2016) found resistance among Gram-negative infections to cotrimoxazole and ampicillin infections in the range of 50%-100%, gentamicin (20% – 47%) and ceftriaxone (46% – 69%) with *Klebsiella* species and *Escherichia coli* exhibiting relatively high resistance (Tuem *et al.*, 2018; Tadesse *et al.*, 2012). Gram-positive infections report

shows wide resistance to ampicillin (100%), gentamicin and ceftriaxone (50% – 100%), with methicillin-resistant *Staphylococcus aureus* prevalence ranging from 2.6% – 4.0%. The resistance to antibiotics complicates treatment of diseases caused by these microorganisms, increasing the cost of treatment, and in addition limits the therapeutic options as some of the most effective drugs lose their efficiency (Dromigny *et al.*, 2005). The increase in prevalence of multiple drug resistance has slowed down the development of new synthetic antimicrobial drugs, and has necessitated the search for new antimicrobials from alternative sources (Barak *et al.*, 2016).

Nanotechnology has laid a base for the discovery of new drugs and diagnosis tools (Deepak *et al.*, 2020). Wet chemical reduction methods in nanoparticle synthesis in most cases utilize organic solvents and reducing agents such as hydrazine, dimethyl formamide, sodium borohydride, potassium bitartrate, formaldehyde, hydroxylamine hydrochloride or sodium hypophosphite, among others which are toxic to living organisms and environmentally hazardous (Hsiao *et al.*, 2006). Biosynthesis of nanoparticles allow for a nanomaterial to be synthesized in a way that is environmental friendly and can be utilized by human without side-effects. This synthesis approach eliminates toxic chemicals that pose risks to the environment. Therefore, this study investigated antimicrobial efficacy activity of copper nanoparticles synthesized from *Senna didymobotrya* root extracts on *E. coli* and *S. aureus*.

1.3 Justification of the study

Human health is of great significance and with the current prevalence of multidrug resistance in *E. coli* and *S. aureus*, the cost of treatment of diseases caused by these bacteria is high. This necessitate the search for better antibiotics with unique

bactericidal mechanism to help control cases of drug resistance. Copper nanoparticles inactivate cell surface protein necessary for transport of materials across cell membranes, thus affecting membranes integrity and membrane lipids (Espirito *et al.*, 2008). Copper ions inside bacterial cells also disrupt biochemical process (Shobba *et al.*, 2014). This antimicrobial mechanism of copper nanoparticles is promising approach to help deal with resistant *E. coli* and *S. aureus* thus the need for their investigation.

Biosynthesized copper nanoparticles using plant extracts is preferable since it can solve the problem of the high toxicity of chemical synthesized copper nanoparticles, offer low cost since plants are available in the environment, allow eco-friendly methods of metal nanoparticle synthesis (Abd-Elkarem *et al.*, 2016). Since *Senna didymobotrya* root extracts contain compounds such as of steroids, terpenoids, anthraquinones, tannins, saponins, glycosides, flavonoids, alkaloids and phenols (Nyamwamu *et al.*, 2015), root extracts from this plant was used to synthesize effectively copper nanoparticles to solve the problem of resistance of *E. coli* and *S. aureus* to antibiotics.

1.4 Significance of the study

The results from this research may trigger the processing of new antimicrobial drugs or lead compounds to be developed into new antimicrobial drugs. The results may be a step in dealing with ever increasing number of microbes developing resistance to present antimicrobial drugs.

The findings will direct future formulation of herbal concoctions that are scientifically validated not only at home but also for commercial production hence increasing the base of antimicrobial drugs.

The findings in the study could provide an insight into the biosynthesis of nanoparticles that are cheap, stable, uniform morphology and eco-friendly hence eliminating environmentally biohazard chemicals from chemical synthesis of copper nanoparticles.

The results from this research may support applications of copper nanoparticles in waste water treatment, coating of hospital equipment, in cosmetics as preservatives eliminating health hazard chemicals, and in food industry as low cost biosensors that detect pathogens and monitor different stages of contaminant.

1.5 Objectives of the study

1.5.1 Main objective

To synthesize copper nanoparticles using *Senna didymobotrya* plant root extracts and to test their efficacy against *Escherichia coli* and *Staphylococcus aureus*.

1.5.2 Specific objectives:

The specific objectives were to:

1. Perform qualitative and quantitative phytochemical evaluation of *Senna didymobotrya* root extracts
2. Synthesize copper nanoparticles using *Senna didymobotrya* root extracts
3. Characterize Copper nanoparticles
4. Evaluate antimicrobial efficacy of the copper nanoparticles against *E. coli* and *S. aureus*.

1.6 Hypothesis

H₀: *Senna didymobotrya* root extracts do not possess phytochemicals at statistically significant quantities

H₀: *Senna didymobotrya* root extracts will not effectively synthesize copper nanoparticles with optimum characteristics

H₀: Characterization will not confirm presence of copper nanoparticles

H₀: Copper nanoparticles will not show statistically significant antimicrobial efficacy against *E. coli* and *S. aureus*.

CHAPTER 2: LITERATURE REVIEW

2.1 *Senna didymobotrya*

Senna didymobotrya is a prospective plant of therapeutic advantages which are explored well worldwide by traditional practitioners (Nagappan, 2012). Kenyan communities such as the Kipsigis use this plant to manage malaria as well as diarrhoea (Korir *et al.*, 2012), the Pokot peel the bark, dry the stem and burn it into charcoal for milk preservation (Tabuti, 2007). Njoroge and Bussmann, (2007) as well reported its use in treatment of skin ailment of humans and livestock infections. The concoction from the plant has been used in removal of ticks from livestock (Njoroge and Bussmann, 2006).

In Rwanda, Congo, Burundi, Kenya, Tanzania, and Uganda decoction of this plant root has been used for the management of malaria, ringworm, jaundice and intestinal worm (Nagappan, 2012). The plant is also useful for the treatment of fungal, bacterial infections, hypertension, haemorrhoids, sickle cell anaemia, a range of women's diseases such as inflammation of fallopian tubes, fibroids and backache, to stimulate lactation and to induce uterine contraction and abortion (Tabuti, 2007). Korir *et al.*, (2012) reported antibacterial activities of hexane extract against *Microsporium gypsum*.

According to Reddy *et al.*, (2010), presence of phenols, flavonoids and carotenoids in the ethyl acetate extract of leaves are responsible for antibacterial activities. Root decoction made from the plant is used as an antidote for poisoning, to oust a retained placenta, and to control East Coast fever and blackleg in cattle (Njoroge and Bussmann, 2007).

Nyamwamu *et al.*, (2015) reported the presence of steroids, terpenoids, anthraquinones, tannins, saponins, glycosides, flavonoids, alkaloids and phenols from the root extracts of *Senna didymobotrya*.

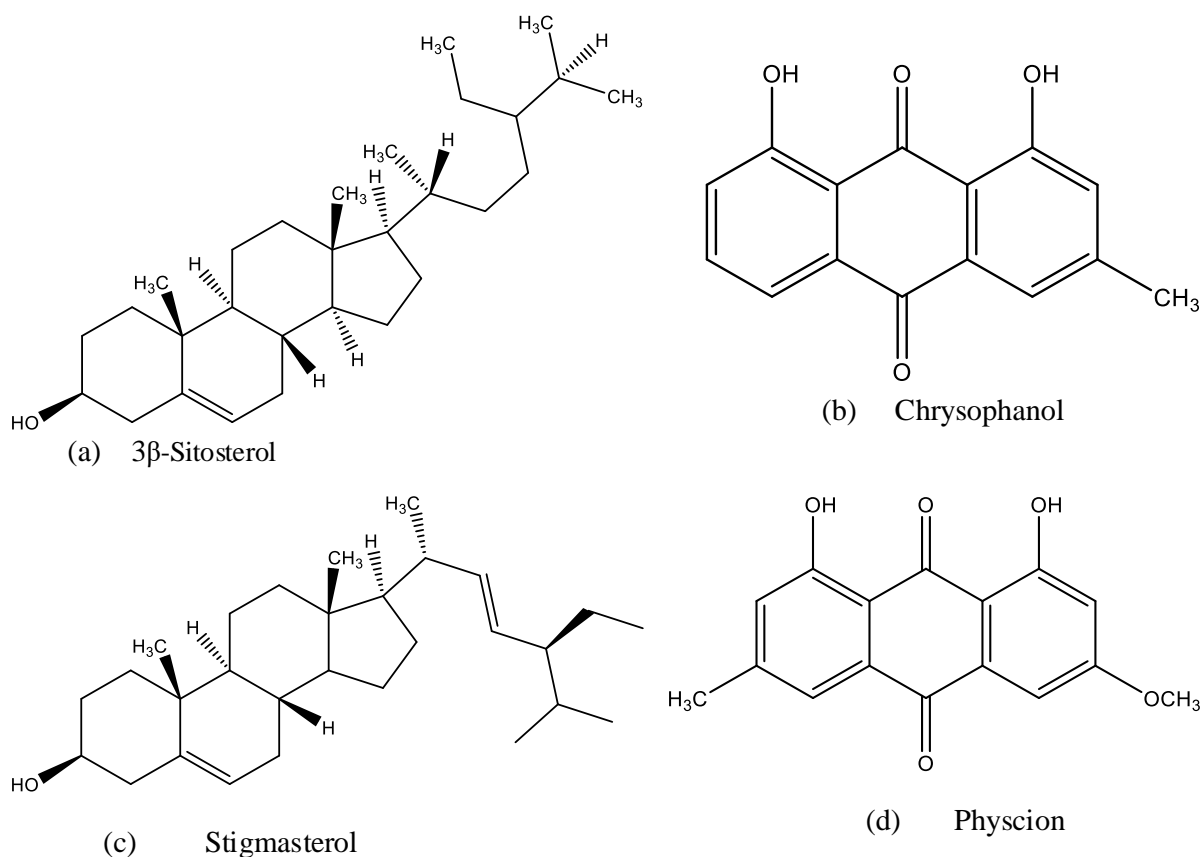


Figure 1: Some compounds isolated from the root and the stem bark extracts of *Senna didymobotrya* (Mining *et al.*, 2014).

Jeruto *et al.*, (2017) investigated the antimicrobial efficacy extracts from leaves, stem bark, flowers, immature pods and root backs of *Senna didymobotrya* on *E. coli* and *S. aureus*. The study revealed that root extracts showed best inhibition at lower concentration of extract, followed by stem bark and limited inhibition by leaves, flowers and immature pods. This could have due to higher concentrations of phytochemicals on the roots as opposed to stem bark, leaves, flowers and immature pods. This informed the choice of *Senna* roots for extraction of phytochemicals to be used in the synthesis of Cu NPs.

2. 1. 1 Phytochemical Evaluation

Herbal medicines contain active ingredients that are present in complex mixtures formulated as crude fractions of plants or combination of plants. Herbal drugs are widely accepted as an alternative treatment for primary health care requirements in both developing and developed populations. However, herbal medicines have a range of limitations including lack of evidence of safety, efficacy, standardization, varying production practices and absence of regulatory standards and implementation protocols (Chawla *et al.*, 2013). The quality issue of herbal drugs can be ensured by conducting some important tests such as; micro and macroscopic investigation, moisture content, exclusion of foreign organic matter, extractive values, ash value, qualitative and quantitative chemical tests, chromatographic characterization, toxicological test, phytochemical evaluation, and microbial tests (Chawla *et al.*, 2013; Sahil *et al.*, 2011; Yadav *et al.*, 2011).

Quality control of the medicinal plants starts right at the source of the plant material. The composition of phytochemical of a plant and the medicinal value can vary due to several factors including a number of environmental factors such as geographical location, temperature and rainfall, soil quality, taxonomy, the time of collection, method of collection, cultivation, harvesting, storage and drying conditions, preparation and processing methods can also affect composition. Contamination by chemical agents such as pesticides, heavy metals and microbes as well as by insects and animals during any of these stages can also contribute to poor quality of the end products (Sahil *et al.*, 2011).

The first step in phytochemical evaluation is the extraction of desired phyto-constituents, followed by phytochemical screening, isolation and characterization. The preliminary steps include pre-washing with running water, drying the plant sample at room temperature under shade, and grinding to obtain homogenous powder sample. Solvents of varying polarities at

different conditions such as time and temperature are utilized during extraction of phytochemicals. The extraction process should be carried out within specific guidelines such that potential active biomolecules are not lost or distorted. The solvent system for extraction depends on the nature of the bioactive compound of interest. The extraction of polar compounds requires use of solvents such as diethyl-ether, methanol, ethanol among polar solvents. Various methods for extraction are available, including soxhlet extraction, sonication, microwave-assisted extraction, maceration, among others (United States Pharmacopeia and National Formulary, 2002). Phytochemical screening assay is a simple, fast and relatively low cost and is carried out to determine the class of phytochemicals in the extract. The screening is conducted on the extract as per the standard method (United States Pharmacopeia and National Formulary, 2002).

2.1.2 Isolation and Characterization

Crude extract always contains complex mixture containing various types of natural products with different polarities. Further separation and purification is needed to obtain pure bioactive compounds (Rasul, 2018). The separation and purification of plant metabolites can be achieved by one, or a combination, of various separation techniques available. These include thin layer chromatography (TLC), column chromatography, gas chromatography (GC), liquid chromatography (LC) and electrophoresis. The choice of technique depends largely on phytochemical compounds properties such as solubility and volatility, the stage of purity of the extract and the final use of the isolated compound (Liu *et al.*, 2019). In identifying plant metabolites, it is necessary to determine first the class of compounds and then to find out which particular compounds constituting that class. The

class of phytochemical can be determined by colour tests, its solubility and Retention factor (R_f) properties and UV-Vis spectra.

Previous studies have isolated Anthraquinones such as chrysophanol, physcion, emodin, tarosachryson, aloe-emodin, fallacinol, rhein and parientinic acid; Flavonoids such as quercetin, ombuin, apigenin, kaemferol, A pigenin-5,7,4-trimethyl ether; flavonoid glycosides such as isoguercitrin and kaempferol-3-rhamnoside from *Senna* (Mahadevan *et al.*, 2002; Alemayehu *et al.*, 1989). In the past, researchers have used only one solvent in the *S. didymobotrya* extraction for example methanol (Jeruto *et al.*, 2017); solvent ratios using methanol : water 9 : 1 (Thangiah *et al.*, 2013), Dichloromethane: methanol 1 : 1 (Alemayehu *et al.*, 2015); sequential extraction using hexane, ethylacetate, dichloromethane, and methanol (Nyamwamu *et al.*, 2015; Mining *et al.*, 2014). Research on total phenolic and flavonoid content of *Senna didymobotrya* plant roots is not available in the publications searched.

2.1.3 Gas Chromatography – Mass Spectrometry

Gas chromatography separates compounds based on their volatilities. It provides both qualitative and quantitative information for pure compounds. The advantages of GC are high separation efficiency, good selectivity, high sensitivity, and stability (Liu *et al.*, 2019). Gas chromatography – mass spectrometry has been used for identification of hundreds of compounds present in natural and biological systems.

2.2.0 Nanotechnology

European Union (EU) Commission Recommendation defines nanoparticle as manufactured or incidental material comprising particles, in an unbound state or as an aggregate or as an agglomerate and where, for 50 % or more of the particles in the number size distribution,

one or more external dimensions is in the size range 1 nm-100 nm (European commission, 2011).

The properties of materials at the nanometer scale are strongly correlated to the size and shape of the particular element or compound. Materials in their bulk form have significantly different properties from those they have at the atomic scale. At this scale, atoms, molecules, and assemblies of these atoms and molecules are dominated by quantum effects. For example, the surface area greatly changes with relation to size as illustrated in Figure 2 (Poinern, 2015).

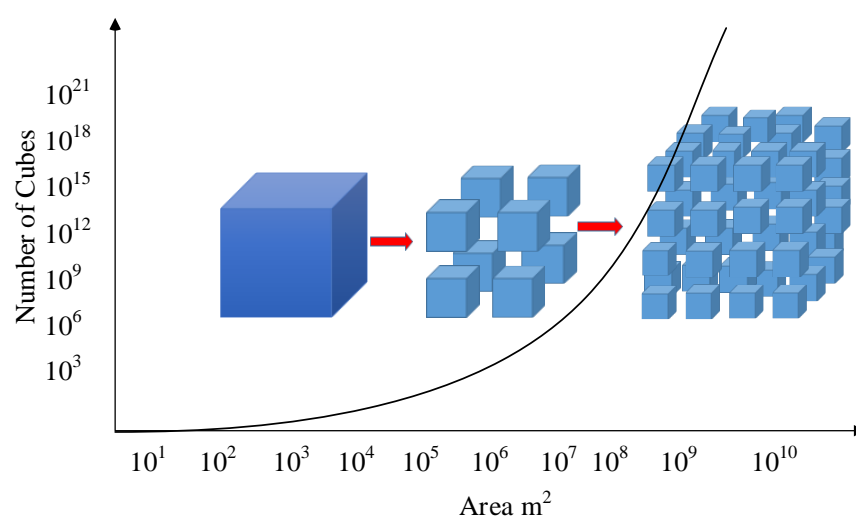


Figure 2: Relationship between the number of cubes from a 1-m cube and the surface area produced (Poinern, 2015).

2.3.0 Copper Nanoparticles

Synthesis of Copper nanoparticles (Cu NPs) has gained a lot of interest in scientific research due to the excellent physical and chemical properties of Cu NPs such as high electrical conductivity and chemical activity (Liu *et al.*, 2012). Cu NPs are known to perform better than silver and gold nanoparticles in applications such as catalysis and as conductive pastes (Wu *et al.*, 2004). Previous studies have reported that it's hard to produce pure copper nanoparticles, unless the synthesis is conducted under inert atmosphere (Khan *et al.*, 2016; Mott *et al.*, 2007). Capping agents have been used to protect Cu NPs, these capping agents decrease the surface energies of Cu NPs and hence minimise oxidation and control growth of a crystal. Since these stabilizers are always in constant molecular motion, they cannot completely prevent Cu NPs from oxidation (Kobayashi *et al.*, 2009).

2.4.0 Methods of Synthesis

Copper nanoparticles have been synthesized by physical and chemical methods. Physical methods such as thermal reduction (Betancourt *et al.*, 2014), pulse laser ablation, photolytic (Gondal *et al.*, 2013). Chemical methods include: microemulsion techniques (Wang *et al.*, 2012), sonochemical reduction (Wonpisutpaisana *et al.*, 2011), microwave method (Blosi *et al.*, 2011), electrochemical method (Tamilvanan, 2015). Physical methods experience low production of nanoparticles and high energy consumption to maintain high temperature and pressure utilized during synthesis process makes the process expensive. Chemical methods are known to use noxious precursor chemicals, harmful synthesis by-products and toxic solvents (Thakkar *et al.*, 2010, Kavita *et al.*, 2018).

2.4.1 Chemical reduction method

Wet chemical reduction methods in most cases utilize organic solvents and use reducing agents such as hydrazine (Granata *et al.*, 2016), dimethyl formamide, sodium borohydride (Liu *et al.*, 2012), potassium bitartrate, formaldehyde, hydroxylamine hydrochloride or sodium hypophosphite, triphenylphosphine (Aazam and El-Said, 2014), among others which are toxic living organisms and environmentally hazardous. The method is complex and utilizes very expensive reducing agents and capping agents such as cetyl trimethyl ammonium bromide, sodium dodecyl sulphate, polyvinylpyrrolidone. These disadvantages limit the use of nanoparticles synthesized using chemical reduction method in biological, medicine and clinical applications (Awwad *et al.*, 2014).

2.4.2 Biosynthesis method

Due to the limitations of the physical and chemical methods of Cu NPs synthesis, the search for a safer method of nanoparticle synthesis has led to the development of biological methods. Copper nanoparticles (Cu NPs) reduction process involve three key factors: the solvent medium, the reducing agent and the capping agent as shown in Figure 3 (Gopi *et al.*, 2017) and proposed reduction of copper nanoparticle is given in scheme 1 (Din *et al.*, 2017) and scheme 2 (Nasrollahzadeh *et al.*, 2018). Infra-red spectroscopy data has shown that the reducing agents involved in formation of nanoparticles comprise a range of plant metabolites such as steroids, phenolic compounds, terpenoids, flavonoids, saponins, alkaloids, tannins and other nutritional compounds and co-enzymes (Sheilesh *et al.*, 2018; Nasrollahzadeh *et al.*, 2018). Previous studies indicate that polysaccharides, carboxylic acids, proteins and lipids present in the plant cell membranes act as capping agents

(Kolekar *et al.*, 2015) and thus limit the use of non-biodegradable commercial surfactants, which are difficult to remove after the synthesis of metal nanoparticles.

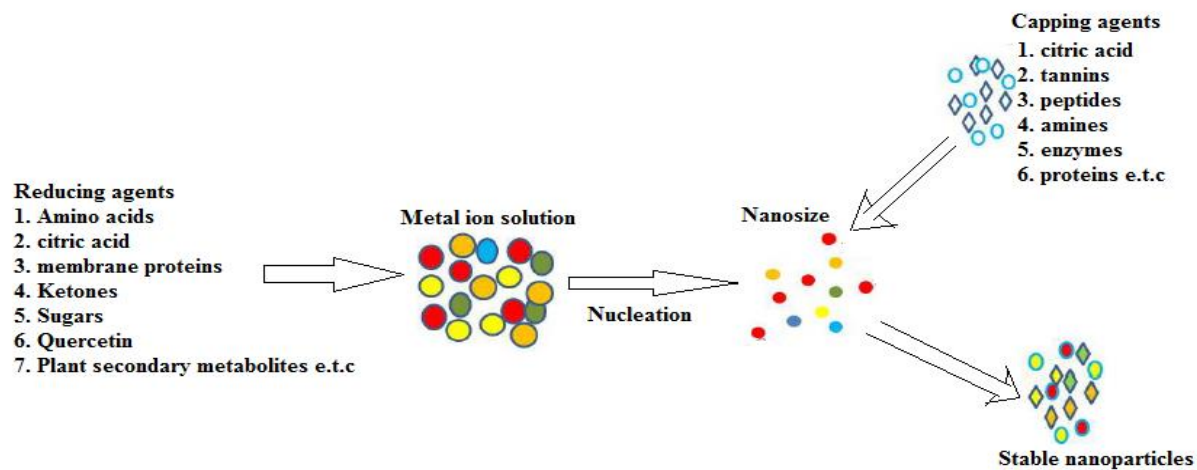
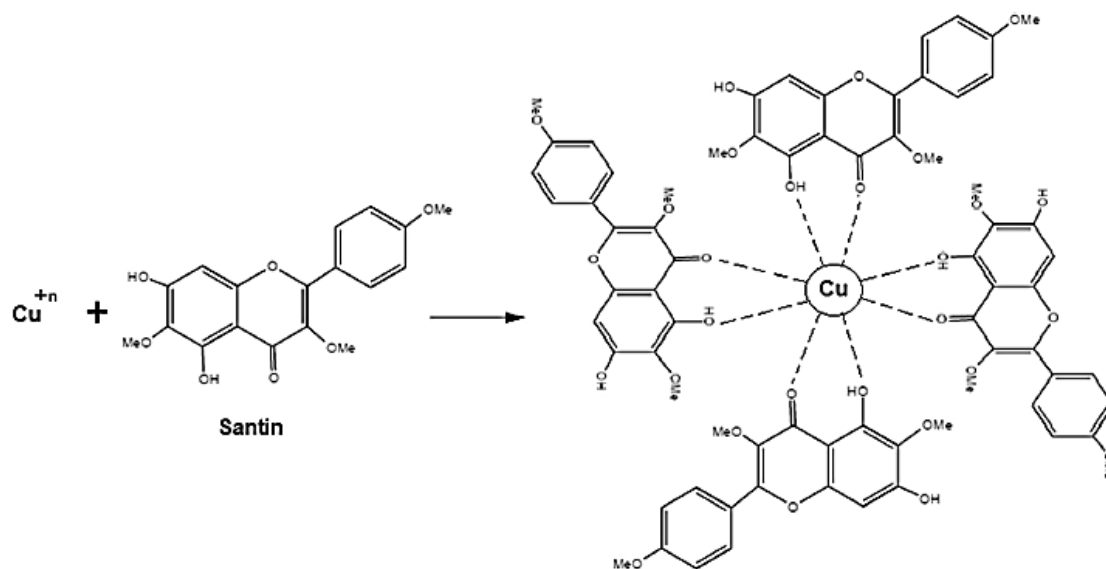
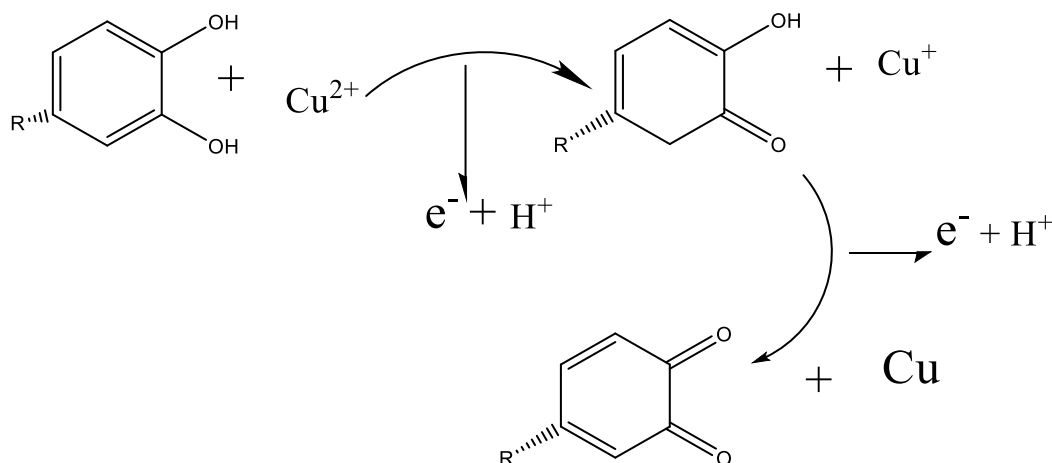


Figure 3: General procedure for the nanoparticle synthesis (Gopi *et al.*, 2017)



Scheme 1: Stabilization of copper nanoparticles by Santin (Din *et al.*, 2017).



Scheme 2: Proposed Mechanism of Biosynthesis of Copper Nanoparticle (Nasrollahzadeh et al., 2018).

Biosynthesis method is fast, for instance *Aloe vera* flower extract was used to prepare Cu NPs of 40 nm size within thirty (30) minutes (Karimi *et al.*, 2015). *Datura* leaf extract synthesized CuNPs within 8 – 10 minutes (Makwana *et al.*, 2014). The method also synthesizes Cu NPs of smaller sizes as reported by Rozina *et al.*, (2016), *Vitis vinifera* leaf extracts biofabricated crystalline Cu NPs of average size ranged between 3 nm and 6 nm. Makwana *et al.*, (2014) reported synthesis of Cu NPs of size ranged between 15 nm and 20 nm using *Datura metel* leaf extract. *Citrus medica* Linn juice synthesized Cu NPs of 20 nm has been reported (Rai *et al.*, 2015). The green method also produce stable Cu NPs as reported on *Magnolia Kobus* leaf extract bio-reduced Cu NPs which showed stability over thirty (30) days (Lee *et al.*, 2011).

2.5 Application of Copper Nanoparticles

Copper nanoparticles have received a wide range of applications as anti-fouling, biocidal, gas sensor, wound dressing and solar cells (Jung *et al.*, 2006) lubricators, catalysts (Nasrollahzadeh *et al.*, 2015; Han *et al.*, 2006), dye degradation (Rajeswari *et al.*, 2016)

and as antimicrobial (Ashwini and Gayathri, 2018; Renganathan *et al.*, 2014; Gopinath *et al.*, 2014; Kote *et al.*, 2014; Bhaskar *et al.*, 2014). However, the main challenge with the copper nanoparticles include aggregation and oxidation, copper nanoparticles are very reactive due to their surface-to-volume ratio and can easily interact with other particles (Kanninen *et al.*, 2008).

The release of ions by Cu Nps is considered the main link to its antimicrobial activity. The activity is further improved by its nano size which corresponds to high surface area to volume ratio, this allows them to interact easily with cellular membranes of microbes. Copper nanoparticles' antimicrobial activity is due to its tendency to alternate between its cuprous – Cu^+ , and cupric – Cu^{2+} , oxidation states differentiating Copper (Cu) from other trace metals. The alternation from cuprous to cupric state results in the production of hydroxyl radicals that subsequently bind with DNA molecules and lead to damage of the helical structure by cross-linking within and between the nucleic acid strands and damage essential proteins by binding to the sulfhydryl amino and carboxyl groups of amino acids. This denatures the protein making the enzymes ineffective (Yoon *et al.*, 2007). It inactivates cell surface proteins necessary for transport of materials across cell membranes, thus affecting membrane integrity and membrane lipids (Espirito *et al.*, 2008). Copper ions inside bacterial cells also disrupt biochemical processes. The exact mechanism behind is not known and needs to be further studied. Based on all of these studies, the denaturing effect of Cu ion on proteins and enzymes in microbes gives Cu its antimicrobial characteristics (Shobha *et al.*, 2014).

2.6 Kinetics and Stability of biosynthesized Copper Nanoparticles

Synthesis of nanoparticles of smaller and uniformly distributed size, crystalline, and stable require control of experimental conditions. Physical parameters such as time, temperature, pH, concentration of copper ion salt determine the size, shape, dispersion, and stability of Cu NPs (Biswas *et al.*, 2017; Asemani *et al.*, 2019).

2.6.1 Optimization of synthesis process

Optimization of an experimental process is always of prime significance, especially at a point where an enormous accomplishment can be attained with a slightest improvement in the response value. Previous studies have utilized computer software such as SAS, Design Expert, Matlab, Monte Carlos and Minitab to achieve modern design of experiments, regression analysis and optimization of various responses (Chakraborty and Biswas, 2016). Minitab software is used widely as it is user friendly and easy to access compared to other software mentioned. Topological and parametric optimizations are the two types of optimization usually employed. Design of experiments (DOE) is utilised in exploitation of different experimental designs, establishment of a relationship on the basis of polynomial mathematics and representation of response within the scopes of the experiments to attain the optimum level of process parameters for the formulations (Chakraborty and Biswas 2016). DOE allows using a minimum number of experiments, in which several experimental parameters are varied systematically and simultaneously to obtain sufficient information. Based on the obtained data, a mathematical model of the process under investigation is generated. The model can be used to comprehend the impact of the experimental parameters on the product and to generate the optimum for the process (Mohammad, 2015).

Response surface methodology has several advantages as opposed to one factor at a time (OFAT), in that it can generate valuable data using minimum experiment runs, can estimate the interactions of independent variables on the responses (Asemani *et al.*, 2019). Optimization studies of synthesis parameters could yield a more viable biosynthesis to be applied in large scale production of nanoparticles.

2.7.0 Characterization technique

Determination of the size distribution and whether a material fulfils the recommended definition of nanoparticle few considerations have to made. Determination of whether a material consist of particles, characterize the constituent particles and the external dimensions of the (constituent) particles and finally the median value of the particle size distribution based on the external dimension (Linsinger *et al.*, 2011).

Characterization techniques for measuring nanoparticles size and structural properties include Transmission electron microscopy (TEM), Scanning electron microscopy (SEM), Dynamic light scattering (DLS), X-ray diffraction (XRD), Nanoparticle tracking analysis (NTA), SAXS, High resolution Transmission electron microscopy (HRTEM), ICP-MS, UV-Vis, Nuclear magnetic resonance (NMR), and Elliptically polarized light scattering (EPLS). Determination of shape, instruments such as TEM, HRTEM, Atomic force microscopy (AFM), Elliptically polarized light scattering (EPLS), FMR, and 3D-tomography; for crystal structure include XRD, Extended X-ray Absorption fine structure (EXAFS), HRTEM, Scanning TEM (STEM). Size distribution can be characterized by DLS, Differential centrifugal sedimentation (DCS), Small angle X-ray scattering (SAXS), NTA, FMR, SEM, Particle tracking analysis (PTA), and superparamagnetic relaxometry.

Analysis of Ligand binding nanoparticles can be determined using X-ray photoelectron spectroscopy (XPS), FTIR, NMR, Secondary ion mass spectrometry (SIMS), Ferromagnetic resonance (FMR), Thermal gravimetric analysis (TGA), small angle neutron scattering (SANS). Surface charge and stability of the nanomaterials can be investigated using Z-potential, and Electrophoretic mobility (EPM).

2.7.1 Ultraviolet – Visible Spectrophotometry

Ultraviolet-Visible spectroscopy (UV-Vis) records the intensity of light reflected from a sample and compares it to the intensity of light reflected from the reference material. UV-Vis is an important tool in identifying, characterizing and investigate nanoparticles due to the fact that nanoparticles have optical properties that are sensitive to size, shape, concentration, agglomeration state and refractive index near the nanoparticle surface (Mourdikoudis *et al.*, 2018). Cooper, gold, and silver nanoparticle solutions exhibit characteristic UV-Vis spectra due to the existence of a Surface Plasmon Resonance (LSPR) signal in the visible part of the spectrum.

2.7.2 Fourier Transform Infrared Spectroscopy

Fourier-transformed infrared spectroscopy (FT-IR) measures absorption of infrared radiation ($4000 - 400 \text{ cm}^{-1}$) by a molecule with a covalent bond. It gives information on surface composition and ligand binding of the nanoparticle. It reveals the nanoparticle stabilizer interaction and confirmation of the stabilizer type. Previous studies have assigned various vibration modes for most of the common groups present on the surface of nanoparticles, they include; methyl C-H asymmetric and symmetric stretch appearing at about $2970-2950 \text{ cm}^{-1}$ and $2880-2860 \text{ cm}^{-1}$ respectively; Methyl C-H asymmetric and symmetric bend around $1470-1430$ and $1380-1370 \text{ cm}^{-1}$ respectively; C=C alkenyl stretch

around 1680-1620 cm^{-1} ; aromatic C-H stretch around 3130-3070 cm^{-1} ; O-H hydroxyl group, H-bonded OH stretch about 3570-3200 cm^{-1} ; C-O stretch, primary alcohol at approximately 1050 cm^{-1} ; N-H aliphatic primary amine in the range of 3400-3380 cm^{-1} ; C-N stretch around 1090-1020 cm^{-1} ; carboxylate group band around 1610-1550 or 1420-1300 cm^{-1} ; and organic phosphates (P=O stretch) in the range of 1350-1250 cm^{-1} .

2.7.3 Particle size determination

Dynamic light scattering (DLS) measures size of nanoparticles in colloidal suspensions in the nano and sub-micro meter ranges. Nanoparticles dispersed in a colloidal solution are in continuous Brownian motion. DLS measures the light scattering as a function of time, this combined with the Stokes-Einstein assumption are used to determine the nanoparticle hydrodynamic diameter in solution. To avoid multiple scattering in DLS size measurement, low concentration of nanoparticle is needed (Kato *et al.*, 2012). Factors such as suspension concentration, particle shape, colloidal stability and surface coating of Metal nanoparticles influence the size value obtained by DLS measurements (Lim *et al.*, 2013). The advantages of DLS are that its easy, quick and precise operation for monomodal suspensions, it's also an ensemble technique, yielding a good statistical representation of each nanoparticle sample. Its highly sensitive and reproducible for monodisperse, homogenous samples. The limitation of DLS is that large particles scatter much more light and even a small number of large particles can obscure the contribution from smaller particles. This leads to low resolution for polydisperse, heterogeneous samples.

2.7.4 X – Ray Diffraction Spectroscopy

X-ray diffraction (XRD) provides the information on the crystallinity, the nature of the phase, lattice parameters and size of crystalline grain of nanoparticles. Crystalline grain size

can be estimated by using Scherrer's equation using the broadening of the most intense peak of a XRD measurement for the nanoparticle. The composition of particles can be determined by comparing the position and the intensity of the peaks with the reference patterns available at the International Centre for Diffraction Data (ICDD) database. The technique is not suitable for amorphous material and the peaks are too broad for particles with size below 3 nm. X-ray absorption spectroscopy (XAS) can be used to analyse non-crystalline nanoparticles (Mourdikoudis *et al.*, 2018).

2.7.5 Zeta potential measurement

Measurement of zeta potential of nanoparticles gives information on stability of colloidal dispersions. Particles with high positive or negative charges in the range of 20 to 30 mV tend to repel each other hence reduce their agglomeration and thus stability. Highly charged particles are associated to the pH values which are far from the 'isoelectric point' of a solution. Isoelectric point of a solution is the pH value at which the zeta potential is zero. Low zeta potential value of a colloidal nanoparticle dispersion causes the agglomeration of the colloids. Generally, nanoparticles with zeta potential values ranging between 20 and 30 mV or higher, are said to be stable (Honary *et al.*, 2012).

2.8.0 Antimicrobial resistance

Methicillin-resistant *Staphylococcus aureus* (MRSA) has been known to cause clinical infections with minor skin conditions, such as boils, pustules, and folliculitis. It is also associated to serious illness, such as pneumonia, osteomyelitis, bloodstream infections, brain abscesses, sepsis, meningitis, bacteremia and endocarditis (Sievert *et al.*, 2010; Tong *et al.*, 2015; Sergelidis *et al.*, 2015).

Bacteria are the predominantly multidrug-resistant organisms, they are resistant to one or more classes of antibiotics (Tenney *et al.*, 2017). High levels of antimicrobial resistance to commonly used antibiotics have been reported, for instance cotrimoxazole and ampicillin in the range 50%-100%, gentamicin 20% – 47% and ceftriaxone in the range 46% – 69%, among Gram-negative infections. Much of the resistance was reported to be in *Escherichia coli* and *Klebsiella* species. Gram-positive infections, however, extensive resistance was reported to ampicillin (100%), gentamicin and ceftriaxone (50% – 100%), with methicillin-resistant *Staphylococcus aureus* prevalence ranging from 2.6% – 4.0% (Ampaire *et al.*, 2016). Sergelidis *et al.*, (2015) reported multidrug resistance (MDR) of MRSA, with 100% against penicillin, 74% for tetracycline, 59.3% in case of clindamycin and 51.9% against erythromycin. *S aureus* bacteraemia is linked to high morbidity and mortality (Bassetti *et al.*, 2011; de Kraker *et al.*, 2011; Lambert *et al.*, 2011). High cases of drug resistance have been reported on gram negative extended-spectrum beta lactamase producing enterobacteriaceae. These group of bacteria are known to have potential of causing serious infections which are difficult to treat (Shaikh *et al.*, 2015).

Escherichia coli resistance to modern antibiotics is a major problem to health care system worldwide (Tuem *et al.*, 2018). The resistance of antibiotics complicates treatment of diseases caused by these microorganisms, increasing the cost of treatment, and in addition limits the therapeutic options as some of the most effective drugs lose their efficiency (Dromigny *et al.*, 2005). *Escherichia coli* has become resistant to mostly used antibiotics (Tadesse *et al.*, 2012).

Escherichia coli resistance to antimicrobials in developing countries is reported to be one of the major reasons why infectious diseases such as Urinary Tract Infections (UTI) cannot be treated successfully (Erb *et al.*, 2007). Researchers have observed the emergence and spread of drug-resistant *Escherichia coli* that is causing Urinary Tract Infections (UTI) hence limiting treatment options (Gangcuangco *et al.*, 2015). In developing countries where the capacity for resistance surveillance and access to health care are limited, resistance to antibiotics is of particular concern considering that over-the-counter drug purchase is rampant (Molton *et al.*, 2013).

A study was conducted to determine the resistance rates of *Escherichia coli* isolated from women with uncomplicated urinary tract infection in the Philippines. The results in this study showed that the resistance rates of the 179 *Escherichia coli* isolates were highest for ampicillin (64.2%), trimethoprim–sulfamethoxazole (41.3%) and amoxicillin-clavulanic acid (11.7%) (Gangcuangco *et al.*, 2015).

The main mechanism of quinolone resistance in *Escherichia coli* includes alterations of the molecular target of quinolone action, associated with mutations in the quinolone resistance-determining region of *gyrA* and *parC* genes (Dominguez *et al.*, 2002). Aminoglycoside resistance in *Escherichia coli* is mainly due to the expression of aminoglycoside-modifying enzymes.

2.9 Summary of main findings and gaps

Phytochemical screening of various extracts of *Senna didymobotrya* reveal presence of terpenes, saponins, anthraquinones, tannins, steroids, alkaloids, flavonoids and phenols (Nyamwamu *et al.*, 2015; Alemayehu *et al.*, 2015; Maema *et al.*, 2020). These metabolites

for instance, flavonoids and phenols are of high therapeutic values and require quantification of their contents in this plant. Previous studies on *Senna didymobotrya* have not determined total phenolic and flavonoid content, a gap that the current study fills.

Previous studies have isolated and characterized compounds such as 2, 6, 4'- trihydroxy-trans-stilbene and 4-(2'-oxymethylene-4'-hydroxyphenyl) chrysophanol (Alemayehu *et al.*, 2015), there is also limited information on the volatile compounds of *Senna didymobotrya* roots. The current study provides a comprehensive information on the volatile compounds of *Senna* roots by analysis using Gas Chromatography-Mass spectrometry.

Biosynthesis of Copper nanoparticles have utilized different plant extracts (Karimi *et al.*, 2015; Makwana *et al.*, 2014; Rozina *et al.*, 2016; Lee *et al.*, 2011) with results ease of synthesis, size and stability of the nanoparticles varying depending on the plant used. This means that phytochemical composition of plant extract influence synthesis of copper nanoparticles. *Senna didymobotrya* has been shown to contain biomolecules capable of synthesizing Cu-NPs though its extract has not been used in the past in the synthesis of Cu NPs. The current study fills the gap.

Previous studies have revealed that to synthesize nanoparticles of least mean size, uniform morphology and high stability require control of experimental conditions such as temperature, pH and concentration of salt (Honary *et al.*, 2012; Dang *et al.*, 2011). The study addresses this by optimizing the synthesis process.

High levels of antimicrobial resistance to commonly used antibiotics has been reported on *S. aureus* (Ampare *et al.*, 2016) and *E. coli* (Tenney *et al.*, 2017; Shaikh *et al.*, 2015) which is a major problem to healthcare system worldwide. In the past the researchers have

addressed the problem by testing the antimicrobial efficacy of biosynthesized Cu NPs on these bacteria. The results of efficacy have been varying indicating that the phyto-constituents of the plant extract of the plant influence properties of the synthesized NPs which in turn influence its bioassay (Honary *et al.*, 2012). Antimicrobial efficacy of Senna extract biosynthesized Cu NPs has not been reported. The current study fills this gap.

CHAPTER 3: MATERIALS AND METHODS

3.0 Introduction

This chapter presents the materials and methods used for extraction, phytochemical evaluation, optimization of biosynthesis of copper nanoparticles, characterization and bioassays that were followed to achieve the study objectives.

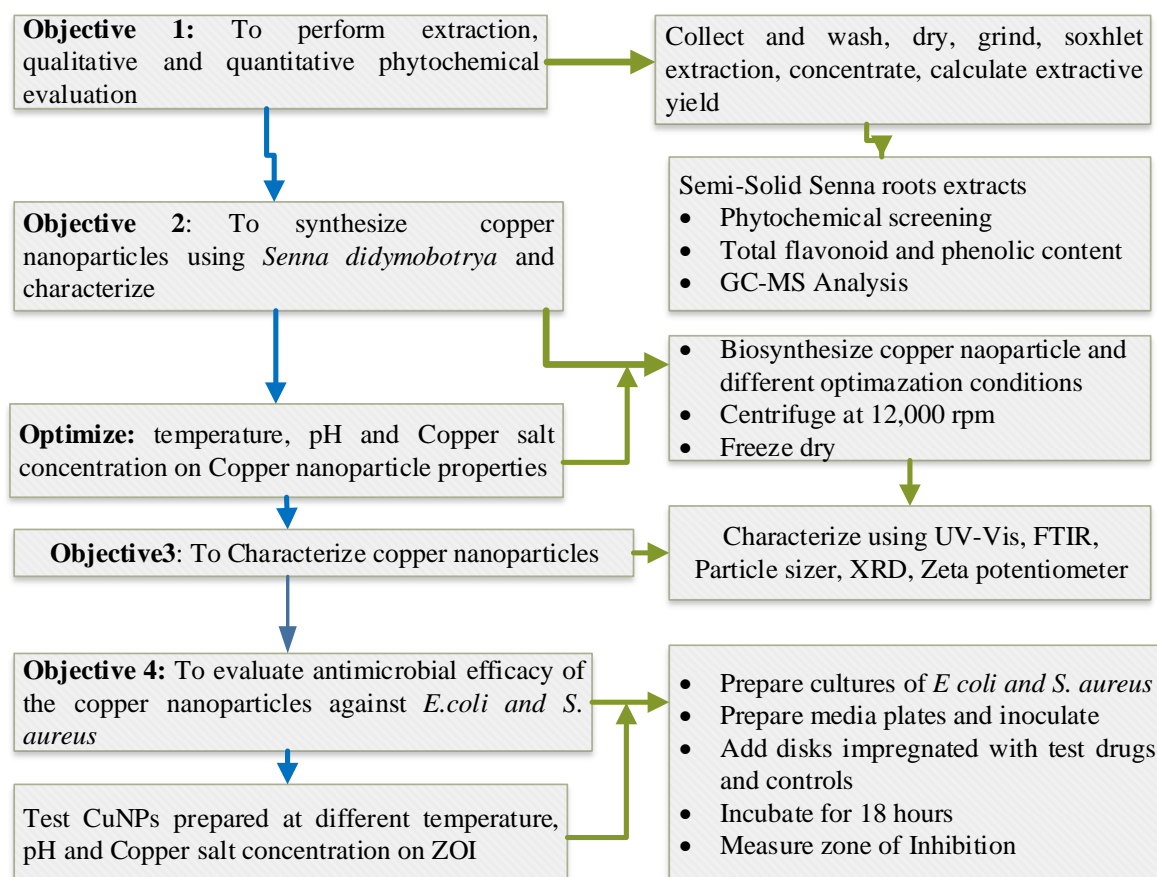


Figure 4: Methodological process relating to research objectives.

3.1 Materials and Equipment

3.1.1 Chemicals and Reagents

Folin Ciocalteu's Phenol reagent, Copper (II) sulphate pentahydrate, acetic acid, Mayer and Wagners reagent, Iron (III) chloride, Hydrochloric acid, dimethyl sulfoxide (DMSO), Chloroform, Sulphuric acid, benzene, Magnesium ribbon, sodium carbonate, ammonia solution, gallic acid, quercetin, and methanol were purchased from Merck Ltd, USA. All the chemicals and reagents were of analytical grade and were used without further purification. Reagents used for standard preparations are quercetin and gallic acid were purchased from Sigma-Aldrich. *Escherichia coli* (ATCC Strain 25922), *Staphylococcus aureus* (ATCC Strain 25923), Kirby-Bauer disks, Amoxicillin clavulanate and 0.5 McFarland Standard were obtained from Cypress diagnostics, Belgium.

3.1.2 Equipment

Sohxlet assembly, Rotary Evaporator (R-200, Buchi Labortechnik), Analytical Balance CITIZEN scale CX-220 (CITIZEN Private Ltd), 20~325 Mesh Grinder Vertical hammer mill pulverizer, Beckman Coulter DU 720 UV-Visible spectrophotometer (700 series (6584) R), Calibrated micropipettes used to accurate measurement and transfer, pH tester HI98107 (HANNA Instruments), Hotplate/Stirrer (Daigger), Ohaus PA213 Pioneer Analytical Balance (Capacity 210g, Readability 0.001g), Centrifuge (Model Microspin 24S, Sorvall Instruments), Agilent GC-MS (Agilent 8890A GC system - 5977B MSD), Nanotrak Wave II (SL-PS-25 Rev. H), Bruker Germany Alpha FT-IR spectrophotometer, XRD, Malvern Zeta potentiometer

3.2. Sample Collection

Senna didymobotrya roots were collected from natural geographical landscapes of West Uyoma Sub-Location, Siaya County, Kenya, GPS location 0°15'8S34°16'02.8E. They were identified and authenticated at the Department of Biological sciences, Moi University where voucher specimen (SD 2018/03) were preserved for future reference.

3.2.1 Extraction of phytochemicals from *Senna didymobotrya* roots

Based on objective one (1), methanol was used for the extraction of *Senna didymobotrya* roots, qualitative and quantitative phytochemical analysis of *S. didymobotrya* root extracts were performed. Although several studies on phytochemical screening of phytochemicals from *Senna didymobotrya* exist, there was no literature on determination of total flavonoid and phenolic content of *S. didymobotrya* root extract, and GC-MS analysis of compounds of phytochemicals contents of the plant root extracts.

3.2.2 Preparation of *Senna didymobotrya* roots Extract

The collected roots were washed several times with distilled water to remove dust. They were dried at room temperature under shade for three weeks, chopped into small pieces (approximately one centimetre) and pulverized using laboratory mill.

The extraction was carried out according to the method described by Kigundu *et al.*, (2009) with slight modifications. Using an electric analytical beam balance, 50 g of powdered dried plant material was weighed, only the appropriate amount fitting the extraction thimble placed in soxhlet apparatus, separately extracted with 250 mL of methanol solvent for 48 hours, the process was repeated until the 50 g are extracted. Methanol was used as the solvent of extraction because it was the best solvent of extraction according to trial extractions done using diethyl ether, methanol and distilled water. The extracted sub

samples were transferred in a conical flask then placed in a rotary vacuum evaporator in a water bath at 40 °C to recover the solvent and concentrate the crude extract. The semi-solid extracts were placed in sterile beakers and were placed in a desiccator containing anhydrous sodium sulphate for 24 hours for complete evaporation of the solvent. The total yield of the solid crude extracts, pooled together from the sub samples, was weighed and put in a tightly screwed capped glass containers and stored in the refrigerator at 4 °C prior to use in the phytochemical screening, determination of total phenol and flavonoid content.

The percentage yield of the crude extract obtained was determined as per Equation 1:

$$\text{Extractive yield value} = \frac{\text{Weight of concentrated extract}}{\text{Weight of plant dried powder}} \times 100 \quad (1)$$

3.3 Qualitative and quantitative phytochemical evaluation

3.3.1 Qualitative phytochemical analysis

The extracts phytochemical analysis for identification of bioactive chemical constituents was

done using standard procedures by Trease (1989) and Sofowara (1983). The test procedures were done in triplicate to eliminate bias. The results were recorded after consistent observation in the three tests.

Tannins

A sample of 0.5 g was put in a test tube and 20 mL of distilled water was added and heated to boiling. The mixture was then filtered and 0.1 % of FeCl₃ was added to the filtrate and observations made. A brownish green colour or a blue black colouration indicate the presence of tannins.

Saponins

The crude *Senna* extract (2 mL) was mixed with 5 mL of water and vigorously shaken. The formation of stable foam indicates the presence of saponins.

Flavonoids

About 1 g of the plant extract was mixed with a few fragments of magnesium ribbon (0.5 g) and a few drops of concentrated hydrochloric acid were added. A pink or magenta red colour development after 3 minutes indicates presence of flavonoids.

Terpenoids

The solvent extracts of the plant material (2 mL) were taken in a clean test tube, 2 mL of chloroform was added and vigorously shaken, then evaporated to dryness. To this, 2 mL of concentrated sulphuric acid was added and heated for about 2 minutes. A grayish colour indicates the presence of terpenoids.

Glycosides**Keller - Kilani test**

The solvent plant material extract was mixed with 2 mL of glacial acetic acid containing 1-2 drops of 2 % solution of FeCl_3 , the mixture was then poured into a test tube containing 2 mL of concentrated sulphuric acid. A brown ring at the interface of the two solutions indicates the presence of cardiac glycoside.

Alkaloids

The crude extract, exactly 0.5 g, was mixed with 1 % of HCl in a test tube. The test tube was then heated gently and a few drops of Mayer's and Wagner's reagents were added by the side of the test tube. A resulting precipitate confirms the presence of alkaloids.

Steroids

Liebermann's Burchard reaction: About 2 g of the solvent extract was put in a test tube and 10 mL of chloroform added and filtered. The filtrate, 2 mL, was mixed with 2 mL of a mixture of acetic acid and concentrated sulphuric acid. Blue green ring indicates the presence of steroids.

Phenols

The plant extract (2 mL) was put in a test tube and treated with a few drops of 2 % of FeCl₃, blue green or black colouration indicates the presence of phenols.

Anthraquinones

Borntrreger's test: A sample of 5 gm of the extract was put in a test tube and 10 mL of benzene added. The mixture was shaken and filtered. Ammonia solution, 5 mL, was added to the filtrate and the mixture shaken. Presence of violet colour in the ammoniacal phase (lower phase) indicates the presence of anthraquinones.

3.3.2 Determination of total flavonoid content

Total flavonoid content (TFC) was determined by aluminium chloride colourimetric assay adapted from Sandip *et al.*, (2014) and Chatatikun *et al.*, (2013) with slight modification. Quercetin was used as standard and the flavonoid content of the extract was expressed as mg of quercetin equivalent per gram of dried extract. Quercetin 10 mg was dissolved in 10 mL 80 % methanol (v/v) and filtered. This was labelled as stock solution. Then serial dilutions were performed: Five 50 mL volumetric flask were cleaned and 10, 20, 30, 40, 50 μ L of the stock solution added to the flask and made to the mark and the final concentrations were 0.2, 0.4, 0.6, 0.8, 1.0 ppm respectively. The blank consisted of all the reagents, except for the extract or quercetin in standard solution which was substituted with 1 mL of methanol. With a pipette 3 mL of plant extract or standard of different

concentration solution was transferred into a test tube. Then 1 mL of 2 % AlCl₃, 80 % methanol solution and 1 mL of 1 M Sodium acetate solution was added to 3 mL of the extract or standard. The test tube of the mixture was then allowed to stand at room temperature for one hour. The extract mixture was diluted to 50 mL to give absorbance below 1.0 in the UV-Vis spectrophotometer. The absorbance of the solution was measured at 446 nm using a UV-Vis spectrophotometer against a blank. The experiments were done in triplicate. The total content of flavonoid compounds in plant extracts in quercetin equivalents was calculated by the following equation

$$C = DF \left(\frac{c \times V}{m} \right)$$

(1)

Where C is the total content of flavonoid compounds in mg/g plant extract, in Gallic equivalents (GAE); DF is the dilution factor; c is the concentration of quercetin established from the calibration curve in mg/mL; V is the volume of the extract in mL; and m is the weight of pure plant extract in gms.

3.3.3 Determination of total phenolic content

Total phenolic content (TPC) of methanol extract of *Senna didymobotrya* was determined by the method involving Folin-Ciocalteu reagent as oxidizing agent and gallic acid as standard (Ahmad *et al.*, 2017; Sembiring *et al.*, 2018). Gallic acid 10 mg was dissolved in 10 mL distilled water, this is 1 mg/mL concentration. It was labelled stock solution. Then serial dilutions were performed: Six 50 mL volumetric flask were cleaned and 20, 40, 60, 80, 100, 120 μ L of the stock solution added to the flask and made to the mark to give the final concentrations as 0.4, 0.8, 1.2, 1.6, 2.0, 2.4 ppm respectively. The blank consisted of

1 mL Folin-Ciocalteu reagent, 3 mL distilled water, and 1 mL Sodium carbonate solution. With a pipette 1 mL of the plant extract or standard of different concentration solution was transferred into a test tube. About 1 mL of Folin-Ciocalteu reagent (diluted 10 times) was added into the test tube. Finally, 1 mL of sodium carbonate (7.5%) solution was added into the test tube. The test tubes were left standing for one hour at 25 °C to complete the reaction. The test tube with extract solution was diluted to 20 mL to get absorbance below 1.0. The absorbance of the solutions was measured at 760 nm using UV-Vis spectrophotometer against a blank. The experiments were repeated three times and average value calculated. The total content of phenolic compounds in plant extracts in gallic acid equivalents was calculated by equation (1) above.

3.3.6 Gas chromatography mass spectrophotometry

GC-MS analysis of crude extract of *S. didymobotrya* were performed using an Agilent 8890A GC system interfaced to a 5977B Mass Spectrometer Detector (GC-MSD) fused a capillary column (30 × 0.25 mm, 0.25 µm). For GC-MS detection, an electron ionization system was operated in electron impact mode with ionization energy of 70 eV. Helium gas (99.999%) was used as a carrier gas at a constant flow mode of 1.2 ml/min, and an injection volume of 2 µL was employed (a split ratio of 10:1). The injector temperature was maintained at 250 °C, the ion-source temperature was 200 °C, the oven temperature was programmed from 60 °C (for 1.5 min), with an increase of 20 °C/min to 220 °C, then 5 °C/min to 280 °C (4 min), ending with a 10 min isothermal at 280 °C. Mass spectra were taken at 70 eV; with Jet-Clean Ion Source temperature at 320 °C, MS Quadrupole at 180 °C a scan interval of 0.5 s. The solvent delay was 0 to 3 min, and the total GC/MS running time was 36 min. The spectrums of the components were acquired using Single Ion

Monitoring mode. Identification of the peaks was based on computer matching of the mass spectra with the National Institute of Standards and Technology (NIST 08) library, direct comparison with the published data was also utilized.

3.4 Optimized Biosynthesis of Copper nanoparticles and Characterization

Based on objective two (2), Copper nanoparticles (Cu NPs) were synthesized under varying temperature, concentration of copper ions, and pH of mixture.

3.4.1 Synthesis of copper Nanoparticles

The synthesis of copper nanoparticles was carried out by adding 10 mL of *Senna didymobrya* roots extract to 90 mL of the (0.0125, 0.03125 and 0.05 M) aqueous $\text{CuSO}_4 \cdot 5\text{H}_2\text{O}$ solution. The reaction mixture was kept in hot magnetic stirrer at 200 rpm and varying temperature (40, 60 and 80 °C) and pH (3, 6.5 and 10 pH). The reduction of Copper ions was measured by UV-Vis spectrophotometer after four hours. Prior to UV-Vis measurement, the reaction mixture was centrifuged at 5000 rpm for 5 min to remove any free biomass residue which are not the capping the ligand of the nanoparticle. The supernatant was again centrifuged at 12,000 rpm for 40 min to obtain pellets. The pellets of copper nanoparticles were re-suspended using distilled water (Olajire *et al.*, 2017). Figure 5 shows the colours of the copper sulphate-containing solution before the reaction (a), aqueous plant leaf extract (b), initial colour change (c) and CuNPs on completion of the reaction (d).

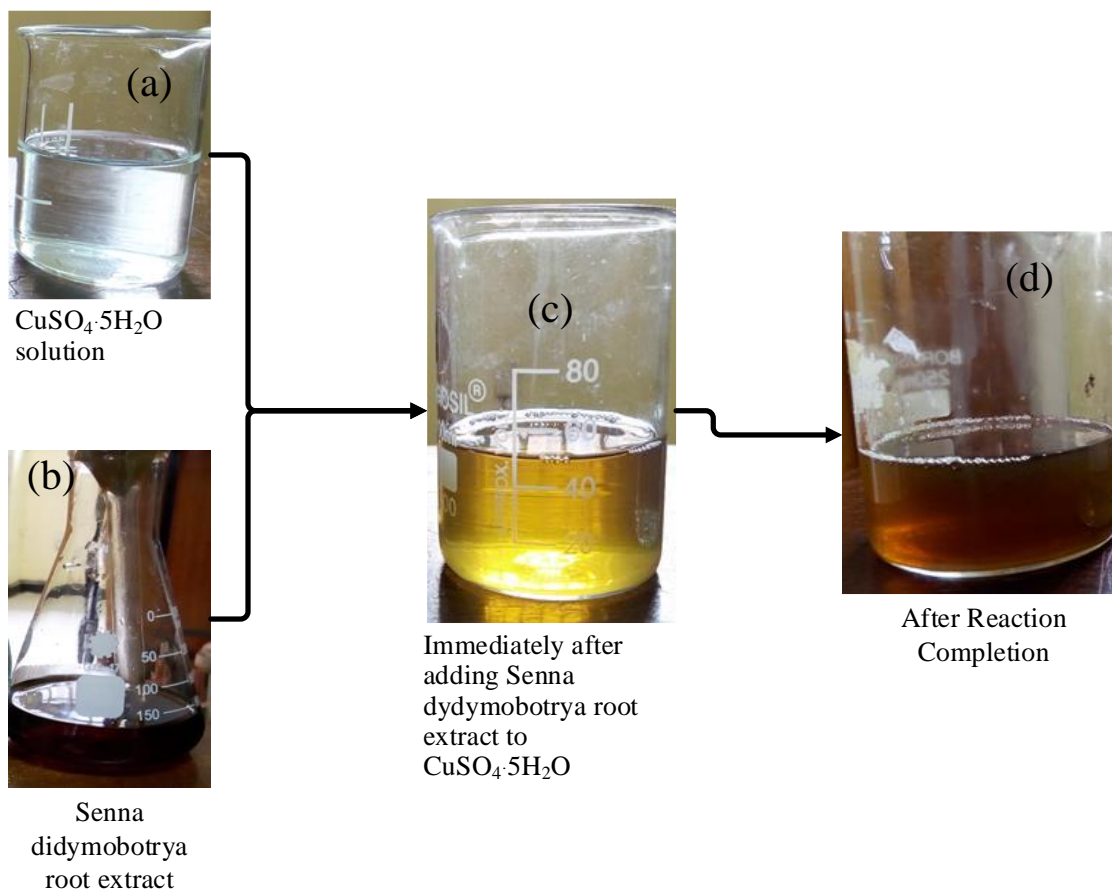


Figure 5: Photographs showing colours of Copper (II) Sulphate (a), pure root extract of *S. didymobotrya* (b), initial colour change (c), final colour change (d).

3.4.2 Optimization of biosynthesis process

A three-level Box–Behnken experimental design was exploited for optimization of analytical parameters affecting the synthesis of copper nanoparticles (Barabadi *et al.*, 2015) using the methanolic root extract of *Senna didymobotrya*. Minitab version 17 was used for experimental design. The selected design matrix from Box-Behnken consisted of 15 trials. The parameters optimized were: concentration of copper ions (0.0125 – 0.05 M); pH of the mixture (3.0 – 10.0); and temperature of the mixture (40 – 80 °C) on the particle size of Cu

NPs. The temperature ranges were prepared prior to the experiment, temperature was adjusted on the hot plate stirrer and monitored on Response variables, as a function of the synthesized parameters, followed a second order polynomial Equation 3.

$$\begin{aligned} \text{Average Size} = & -85.2 + 2.570 \text{ Temp} - 174 \text{ Conc} + 16.97 \text{ pH} - 0.02691 \text{ Temp*Temp} - 5813 \\ & \text{Conc*Conc} - 0.9391 \text{ pH*pH} + 8.41 \text{ Temp*Conc} + 0.0278 \text{ Temp} - 23.1 \text{ Conc*pH} \quad (3) \end{aligned}$$

3.5 Characterization of Copper Nanoparticles

The synthesized Cu NPs were characterized using UV-Vis spectrophotometer, Particle size analyser, zeta potential, X-Ray Diffractometer, and Fourier Transform Infrared Spectroscopy.

3.5.1 Ultra-Violet Spectroscopy

Synthesized Cu NPs sample (300 μ L) were diluted with 3 mL of distilled water, and UV-Vis spectrum analysis was performed using a spectrophotometer device in the range of 200 nm to 700 nm at the resolution of 1 nm. Distilled water was used as blank (Krithiga et al., 2013).

3.5.2 Particle Size Analysis

The sizes of synthesized copper nanoparticles were measured on Particle Size Analyser (Microtrac Nanotrac Wave II, SL-PS-25 Rev. H) with Laser Diode Detector. Dilute solution of copper nanoparticles (0.20 mM), pH of 8 kept constant with borate buffer, were stirred and ultrasonicated for 15 min and then 2 mL was transferred to zeta disposable cell. The solvent used was distilled water. The analysis temperature was 25 $^{\circ}$ C, refractive index of the dispersant was 1.330. Viscosity of the medium was 0.641. (Ghoto *et al.*, 2019). Experiments were repeated three times and mean values calculated.

3.5.3 X-Ray Diffraction

The green synthesized copper nanoparticle (Cu NPs) were subjected to XRD operated at the voltage of 40 kV in the supply of current of about 20 mA with copper $K\alpha$ radiation in the range of θ - 2θ configuration with scanning rate of 0.030 °C/s. The crystallite size (CS) was calculated using Debye-Scherrer equation (**Equation 3**) (Krithiga *et al.*, 2013; Prema, 2010).

$$CS = K\lambda / \beta \cos \theta \quad (4)$$

Where constant (K) = 0.94; $\lambda = 1.5406 \times 10^{-10}$; $\cos \theta$ = Bragg angle; β is the full width at half maximum (FWHM). Full width at half maximum in radius (β) = $FWHM \times \pi/180$.

3.5.4 Zeta Potential

The biosynthesized Cu NPs were subjected to zeta potential measurements using a dynamic laser light scattering method in a Zeta nano instrument from Malvern to investigate copper nanoparticle stability. Briefly, Cu NPs were dispersed for 5 min with an ultrasound using distilled water as dispersion medium (Jardon-Maximino *et al.*, 2021)

3.5.5 FT-IR Spectroscopy Analysis

FT-IR analysis were performed as per Radu *et al.*, 2012, to identify functional groups bound on the surface of the copper nanoparticles. The specimen and KBr granules were powdered together with the ratio of 1 to 100 (1/100 ratio) and then compressed into tablets; subsequently, the analysis was performed and measured using FT-IR spectrophotometer in the range of 400-4000 cm^{-1} and with the resolution of 1-4 cm^{-1}

3.6 Anti-microbial Activity of *Senna didymobotrya* Copper nanoparticles

The antimicrobial efficacy of biosynthesized copper nanoparticles was done using Kirby-Bauer disk Diffusion Susceptibility Test Protocol (Hudzicki, 2009). The test microorganisms were chosen according to the National Committee for Clinical Laboratory Standards, 2010 (NCCLS) protocols. A gram negative *Escherichia coli* ATCC 25922 and a gram positive *Staphylococcus aureus* ATCC 25923 were used for the bioassay of Cu NPs.

The primary culture plate was prepared by rolling saturated swab of test organism on LB agar medium. Using a sterile loop, it was further streaked to facilitate colony isolation. The inoculated primary culture plates were inverted and immediately incubated at 36 °C for 18 hrs. The KWIK-STIK were incinerated.

LB broth was made by mixing 12.5 g of premixed LB Agar with 500 cm³ of distilled water and autoclaved at temperature of 121 °C, pressure of 15 psi for 15 minutes. LB broth at about 55 °C was poured to about 2/3 of the petri dishes and allowed to solidify and then stored in a 4 °C freezer. Four isolated colonies of *E. coli* and *S. aureus* were separately taken from inoculated primary culture plates using sterile loop and suspended in 2 ml of sterile saline and vortexed to create a smooth suspension. The turbidity was adjusted to 0.5 McFarland standard (0.05 mL of 1% BaCl₂ in 9.95 mL of H₂SO₄). The LB Agar plates were inoculated with adjusted suspension of test microorganisms using a sterile swab and left in a lamina flow to dry at room temperature for 3 minutes. Partially removing the lid of the LB Agar plates, impregnated disks were placed on the surface of the agar at least 30 mm from each other using a sterile forceps. The agar plates with antimicrobial impregnated disks were inverted and placed in a 35 °C incubator for 18 hrs. Amoxicillin clavulanate impregnated antimicrobial susceptibility testing discs purchased from Cypress diagnostics

in Belgium were used as positive control on the bioassay for *E. coli* ATCC 25922 and *S. aureus* ATCC 25923. The antimicrobial activity of *Senna* root extracts and that of copper sulphate solution was also tested. All bioassay was done with 30 μ L of solution of Cu NPs resuspended in distilled water, *Senna* root extract and Copper sulphate solution as per the specification of the positive control (Amoxicillin clavulanate). After 18 hours of incubation, zone of inhibition (ZOI) were measured to the nearest millimetre using a ruler and recorded. The susceptibility or resistance of the test organism to each drug tested were determined using the published CLSI guidelines (Clinical Laboratory Standards Institute, 2010). They ZOI were recorded as susceptible (S), intermediate (I), or resistant (R) based on the interpretation chart.

CHAPTER 4: RESULTS AND DISCUSSION

4.0 Introduction

Senna didymobotrya root extract yield obtained from solvents were calculated, qualitative and quantitative phytochemical evaluation was determined. Biosynthesized copper nanoparticles synthesized at optimization parameters were characterized and findings reported. Results of Bioassay of copper nanoparticles on *Escherichia coli* and *Staphylococcus aureus* were analyzed, interpreted and reported.

4.1 Extraction of compounds of *Senna didymobotrya* roots

Fifty (50) grams of *S. didymobotrya* root powder yielded 4.97 g (9.94%) of *S. didymobotrya* crude extracts when extracted with methanol solvent.

4.2 Qualitative and Quantitative phytochemical evaluation

In accordance with objective one (1), qualitative chemical analysis such as phytochemical screening by chemical tests and GC-MS analysis were done, quantitative analysis of the phytochemicals which include total flavonoid and phenolic content were also performed.

4.2.1 Phytochemical screening of *Senna didymobotrya* root extract

Phytochemical screening results in Table 1 showed positive for phenols, tannins, saponins, gladiac glycosides, anthraquinones, alkaloids, and flavonoids; terpenoids and steroids tested negative. The phytochemicals that tested positive are polar and this could be the reason why the yield was highest when water is used as extraction solvent since water is the most polar among the three solvents.

Table 1: Results of phytochemical screening of aqueous extract of *Senna didymobotrya*.

No	Phytochemical	Observation	Test result
1	Phenols	Bluish black colour present	Positive
2	Tannins	Brown colour	Positive
3	Saponins	Formation of stable form	Positive
4	Gladiac glycosides	A brown ring at the interface of the two solutions	Positive
5	Anthraquinones	Violet colour observed in the ammonical phase (lower phase)	Positive
6	Alkaloids	Formation of precipitate	Positive
7	Flavonoids	Magenta red colour observed	Positive
8	Terpenoids	Greyish colour not observed	negative
9	Steroids	Blue ring not observed	negative

The presence of different classes of phytochemicals such as phenols, tannins, saponins, gladiac glycosides, anthraquinones, alkaloids and flavonoids may be the reason why this plant has been used to treat a wide range of diseases traditionally.

4.2.2 Total Flavonoid and Phenol content determination

The total flavonoids content was calculated as quercetin equivalent (mg QE/g dry weight) using the equation based on the calibration curve of Quercetin in Figure 6: $y = 0.1264x - 0.0014$, $R^2 = 0.9973$, where x is the quercetin equivalent (QE) and y is the absorbance. Table 2 was calibration data of quercetin used to obtain calibration curve.

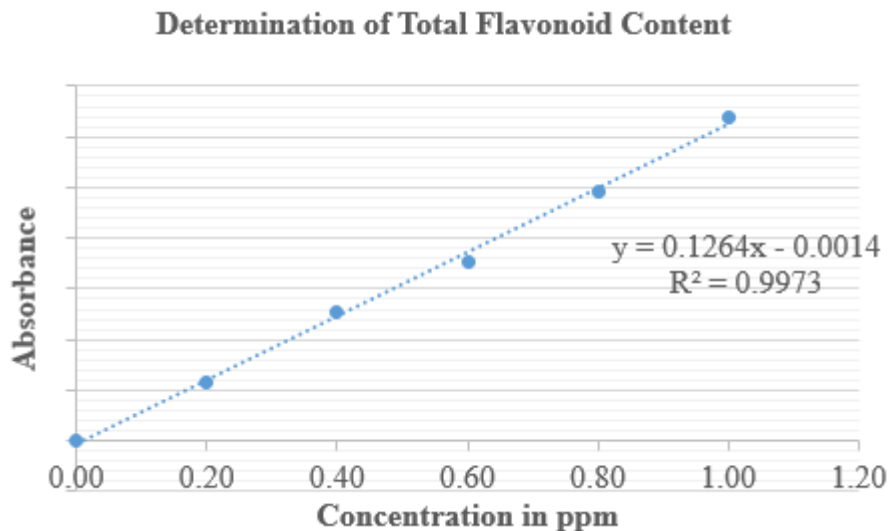


Figure 6: Calibration curve of quercetin.

Total phenolic compound content (TPC) was estimated as gallic acid equivalent (GAE), that is mg GAE per g dry weight, using the equation obtained from the calibration curve of gallic acid in Figure 7: $y = 0.2856x - 0.002$, $R^2 = 0.9966$, where x is GAE and y is the absorbance. Table 4 was calibration data of gallic acid used to obtain calibration curve.

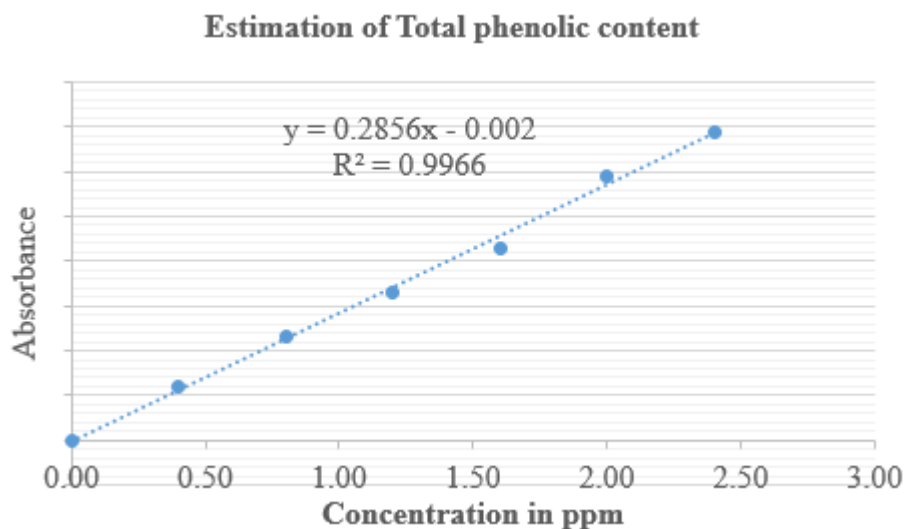


Figure 7: Calibration curve for Gallic acid.

Table 3 shows that the TFC is 48.3354 ± 1.4775 mgQE/g dry weight and Table 5 shows that TPC is 34.4771 ± 0.08734 mg GAE/g dry weight.

Table 2: Preparation of calibration curve of quercetin.

Concentration of Quercetin in (ppm)	Absorbance
0.00	0.000
0.20	0.023
0.40	0.051
0.60	0.071
0.80	0.098
1.00	0.128

Table 3: Calculation procedure for total flavonoid.

Sample solution $\mu\text{g/mL}$	Weight of dry extract in gram	Absorbance	QE Concentration (mg/mL)	TFC as QE $C = DF \left(\frac{c \times V}{m} \right)$	Mean SEM
3000	0.001	0.038	0.3117	46.755	48.335
3000	0.001	0.041	0.3354	50.31	\pm
3000	0.001	0.039	0.3196	47.94	1.4775

Table 4: Preparation of calibration curve of garlic acid.

Concentration of Gallic acid (ppm)	Absorbance
0.00	0.000
0.40	0.120
0.80	0.230
1.20	0.330
1.60	0.429
2.00	0.588
2.40	0.688

Table 5: Calculation procedure for total phenolic.

Sample solution µg/mL	Weight of dry extract in gram	Absorbance	GAE Concentration (mg/mL)	TPC as GAE $C = DF \left(\frac{c \times V}{m} \right)$	Mean SEM
1000	0.001	0.492	1.7297	34.5938	34.4771
1000	0.001	0.489	1.7191	34.382	±
1000	0.001	0.490	1.7226	34.452	0.087341

4.2.5 Gas Chromatography-Mass Spectrometry

The GC-MS analysis on *S. didymobotrya* methanolic root extract was performed to characterize the active phytoconstituents that might take part in the synthesis of CuNPs. The main compounds revealed in the extract were some volatile organic compounds and fatty acids. The compounds along with their retention times, abundances, molecular formulae and molecular weights are presented in Table 7 and Fig. 8. The major compounds identified were benzoic acid, thymol, n-benzyl-2-phenethylamine, benzaldehyde, vanillin, phenyl acetic acid, and benzothiazole.

There is scarcity of literature on volatile compounds in *S. didymobotrya*. This study the first comprehensive report presented on the GC-MS analysis of volatile compounds in *S. didymobotrya* extract. Previously, the presence of terpinolene and alpha pinene was reported as the main antipyretic compounds in dichloromethane extract of *S. didymobotrya* leaves using GC-MS (Mworia *et al.*, 2019). None of the foregoing compounds were identified in this study. Interestingly, some compounds identified in the methanolic extract of *S. didymobotrya* roots in this study have potential to take part in the formation of nanoparticles. For instance, alizarin (a dihydroxyanthraquinone with two hydroxyl groups on a phenyl ring) possess a structure similar to compounds proposed to take part in

chelation and reduction of copper ions to CuNPs (Al-Hakkani, 2020; Nasrolahzadeh *et al.*, 2018).

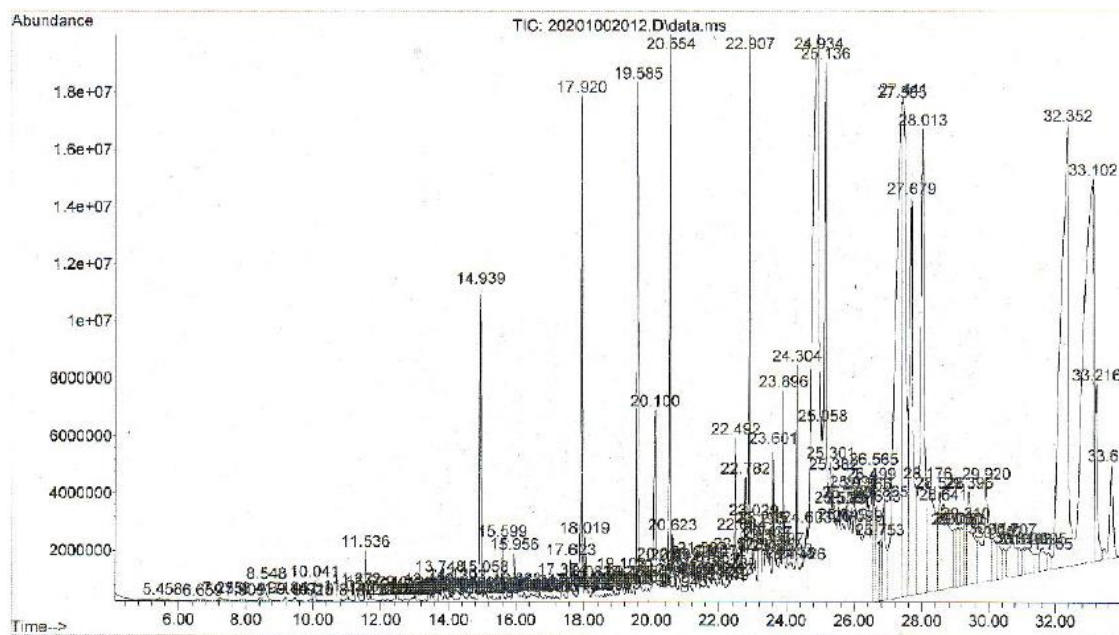
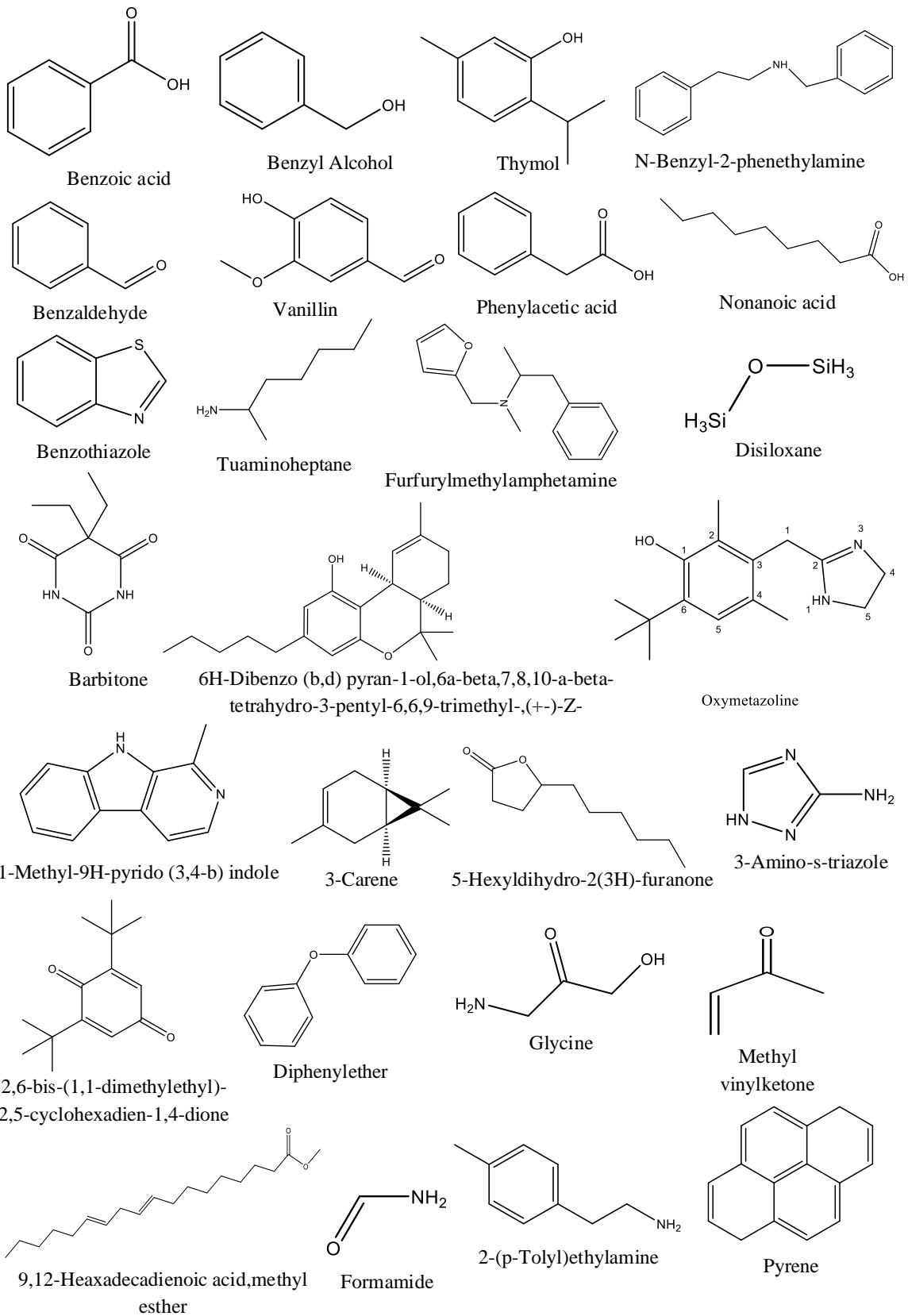


Figure 8: Total ion chromatogram of *Senna didymobotrya* extracts.

Table 6: Compounds identified by Gas Chromatography-Mass Spectrometry analysis of *Senna didymobotrya* root extracts.

S. No	RT	Name of the Compound	Molecular formula	Molecular Weight (g/mol)
1	14.4375	Benzoic acid	C ₇ H ₆ O ₂	122.12
2	12.4726	Benzyl Alcohol	C ₇ H ₈ O	108.14
3	16.7112	Thymol	C ₁₀ H ₁₄ O	150.22
4	11.0757	N-Benzyl-2-phenethylamine	C ₁₅ H ₁₇ N	211.3022
5	17.5703	Benzaldehyde	C ₇ H ₆ O	106.1219
6	18.3040	Vanillin	C ₈ H ₈ O ₃	152.15
7	15.7370	Phenylacetic acid	C ₈ H ₈ O ₂	136.15
8	15.9515	Nonanoic acid	C ₉ H ₁₈ O ₂	158.24
9	16.0344	Benzothiazole	C ₇ H ₅ NS	135.19
10	14.3651	Tuaminoheptane	C ₇ H ₁₇ N	115.2166
11	11.5752	Furfurylmethylamphetamine	C ₁₅ H ₁₉ NO	229.3175
12		Disiloxane	H ₆ OSi ₂	78.22
13	18.6719	Barbital/Barbitone	C ₈ H ₁₂ N ₂ O ₃	184.195
14	30.7212	6H-Dibenzo (b,d) pyran-1-ol,6a-beta,7,8,10-a-beta-tetrahydro-3-pentyl-6,6,9-trimethyl-,(+)-Z-	C ₂₁ H ₃₀ O ₂	314.5
15	33.5783	Oxymetazoline	C ₁₆ H ₂₄ N ₂ O	260.381
16	21.5570	1-Methyl-9H-pyrido (3,4-b) indole	C ₁₂ H ₁₀ N ₂	182.2212
17	10.7265	3-Carene	C ₁₀ H ₁₆	136.2340
18	19.1589	5-Hexyldihydro-2(3H)-furanone	C ₁₀ H ₁₈ O ₂	170.2487
19	19.1900	2,6-bis-(1,1-dimethylethyl)-2,5-cyclohexadien-1,4-dione	C ₁₄ H ₂₀ O ₂	220.3074
20		9,12-Heaxadecadienoic acid,methyl ester	C ₁₉ H ₃₄ O ₂	294.4721
21	12.0521	3-Amino-s-triazole	C ₂ H ₄ N ₄	84.0800
22		Diphenylether	C ₁₂ H ₁₀ O	170.2072
	18.4926			
23		Formamide	CH ₃ NO	45.0406
24		Glycine	C ₂ H ₅ NO ₂	75.0666
25		Thiocyanic acid	CHNS	59.090
26	9.4063	2-(p-Tolyl)ethylamine	C ₉ H ₁₃ N	
27	4.3626	Methyl vinylketone	C ₄ H ₆ O	70.0898
28	28.5117	Pyrene	C ₁₆ H ₁₀	202.2506

29	22.3363	4H-1-Benzopyran-4-one	C ₉ H ₆ O ₂	146.1427
30	16.8355	Methane,isocyanato-/Isocyanic acid/Methyl isocyanate	C ₂ H ₃ NO	57.0513
31	23.6700	Phenanthrene	C ₁₄ H ₁₀	178.2292
32	26.7448	Menthol	C ₁₀ H ₂₀ O	156.269
33	32.1937	Alizarin	C ₁₄ H ₈ O ₄	240.21
34	14.7857	N-Benzylglycine	C ₉ H ₉ NO ₃	169.19
35	13.0157	4-(2-aminoethyl)phenol	C ₈ H ₁₃ NO ₂	155.19
36	14.6250	Benzeneethanamine,N,alpha-dimethyl-N-(phenylmethyl)-,hydrochloride	C ₁₇ H ₂₂ ClN	275.82
37	14.7857	Acetophenone	C ₈ H ₈ O	120.15
38	21.5570	2,4,6-Trimethoxyamphetamine	C ₁₂ H ₁₉ NO ₃ .HC l	261.70
39	32.8342	(2-chlorophenyl)-bis[4-(dimethylamino)phenyl]methanol	C ₂₃ H ₂₅ ClN ₂ O	380.9
40	7.4527	Formamide	CH ₃ NO	45.04
41	8.2517	Aniline	C ₆ H ₇ N	93.13
42	8.6932	4-Methyl-4-hydroxy-2-pentanone	C ₆ H ₁₂ O ₂	116.1583
43	10.1989	Hexylene glycol	C ₆ H ₁₄ O ₂	118.17
44	11.0757	Propylbenzene	C ₉ H ₁₂	120.2
45	11.6747	2-(2-Ethoxyethoxy)ethanol	C ₆ H ₁₄ O ₃	134.17
46	11.8208	1,3,5-trimethylbenzene	C ₉ H ₁₂	164.7
47	12.1959	2-Ethylhexan-1-ol	C ₈ H ₁₈ O	130.2279
48	12.2944	1,3-Dichlorobenzene	C ₆ H ₄ Cl ₂	147.002
49	14.0562	1,2,3,5-Tetramethylbenzene	C ₁₀ H ₁₄	134.22
50	14.1173	2-Hydroxy-3,5,5-trimethyl-2-cyclohexen-1-one	C ₉ H ₁₄ O ₂	154.21
51	22.0834	Methyl tetradecanoate	C ₁₅ H ₃₀ O ₂	242.2
52	22.3954	1-(4-hydroxy-3,5-dimethoxyphenyl)ethanone	C ₁₀ H ₁₂ O ₄	196.1999
53	23.7934	1,2-Benzenedicarboxylic acid, bis(2-methylpropyl) ester	C ₁₆ H ₂₄ O ₄	278.3435
54	15.1598	4-tert-butylphenol	C ₁₀ H ₁₄ O	150.22



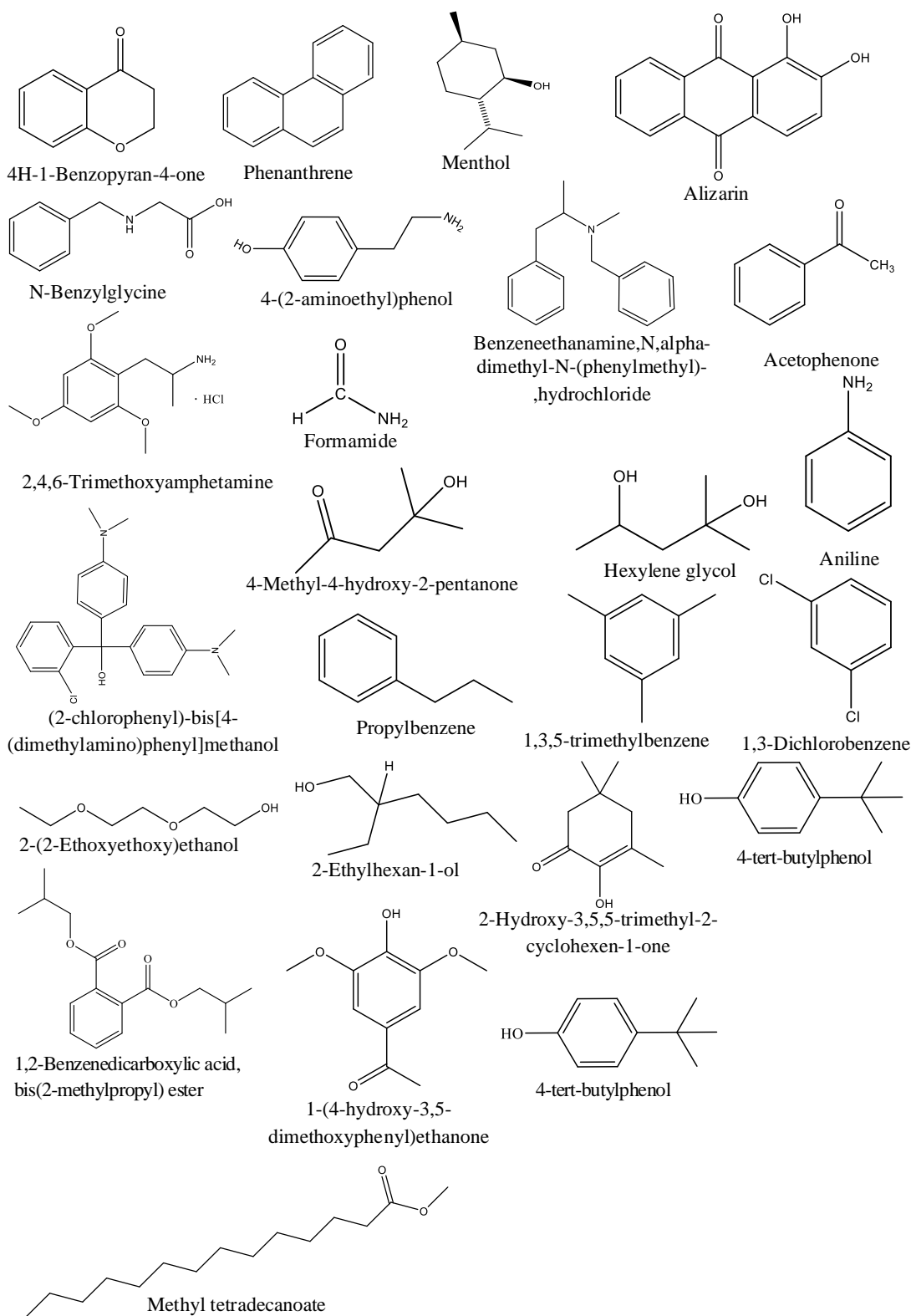


Figure 9: Some compounds identified from *Senna didymobotrya* root extract using GC-MS analysis.

4.3 Biosynthesis of Copper nanoparticles

Bio-reduction of Cu ions to Cu NPs on exposure to methanol plant root extract of *S. didymobotrya* was determined by observing the colour change and with UV-visible spectroscopy. There was a gradual colour change from light orange solution to dark brown indicating the formation of CuNPs after 4 hrs (Rajagopal *et al.*, 2021; Sharma *et al.*, 2018; Kalaimurugan *et al.*, 2019; Ghidan *et al.*, 2016; Vasantharaj *et al.*, 2019). Pre-trial runs indicated that no significant changes on colour and UV-Vis spectrum peaks observed after 3 hours. Metal nanoparticles usually absorb visible electromagnetic radiation through collective oscillation of conduction electrons at the surface-a phenomenon known as surface plasmon resonance (SPR) effect (Dang *et al.*, 2011). Thus, the dark colour observed during the reaction could be ascribed to the excitation of Surface Plasmon vibrations in the copper nanoparticles, indicating the formation of Cu nanoparticles (Sathiyavimal *et al.*, 2018; Krithiga *et al.*, 2013). Copper oxides are thermodynamically more stable than copper sulphates, which leads to the particle size growth and oxidation of copper without proper capping agents (Dang *et al.*, 2011). Thus, phytochemicals from *S. didymobotrya* root extract might have prevented the oxidation of copper, thereby acting as a reductants and capping agent for the CuNPs (Sathiyavimal *et al.*, 2018).

The UV spectrum of the methanolic root extract of *S. didymobotrya* (Fig. 10) shows bands at λ_{\max} 338 nm. The band at 338 nm can either be due to $n \rightarrow \pi^*$ transition or a combination of $n \rightarrow \pi^*$ and $\pi \rightarrow \pi^*$ transitions of heteroatoms linked in the double bond (Ogundipe *et al.* 2001). The observed transitions are probably related to phytoconstituents involved in the reduction process and formation of copper nanoparticles via π -electron interactions (Nasrollahzadeh *et al.* 2014, 2015). Hence, the methanolic extract of *S. didymobotrya* roots further acted as a reducing and stabilizing agent.

The UV–Vis spectrum of synthesized Cu NPs using root extract of *S. didymobotrya* (Fig. 11) showed changes in the absorbance maxima due to surface plasmon resonance (SPR), demonstrating the formation of Cu NPs (DeAlba-Montero *et al.*, 2017; Ramyadevi *et al.*, 2012). The surface plasmon resonance (SPR) peak, which is a signature of the formation of Cu nanoparticles, appears in visible region (Chan *et al.*, 2007; Liu *et al.*, 2015) at 545, 560, 571, 619, 641, 694, 763 and 792 nm with absorbances of 0.053, 0.053, 0.053, 0.054, 0.055, 0.062, 0.062 and 0.07, respectively (Fig. 11). According to Mei's theory, the occurrence of a single UV-visible peak in the UV-Visible spectrum of synthesized nanoparticles confirms that they are spherical in shape (Sharma *et al.*, 2018).

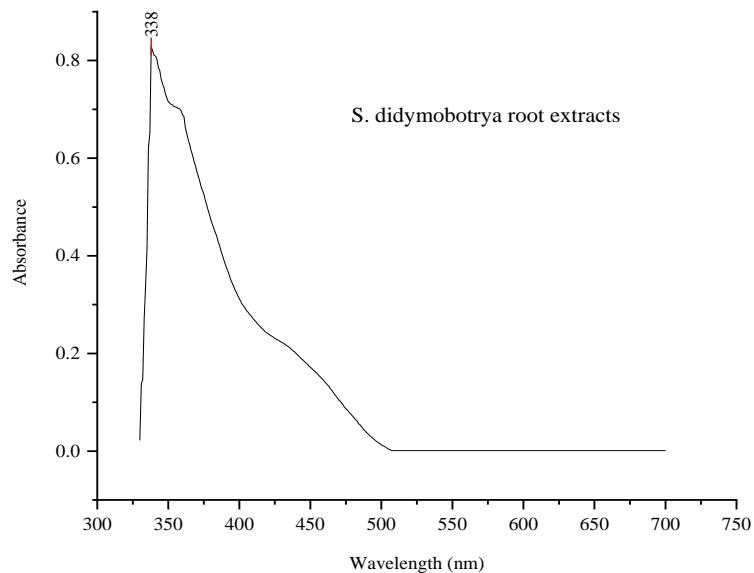


Figure 10: UV-Visible spectra of Senna didymobotrya root extract.

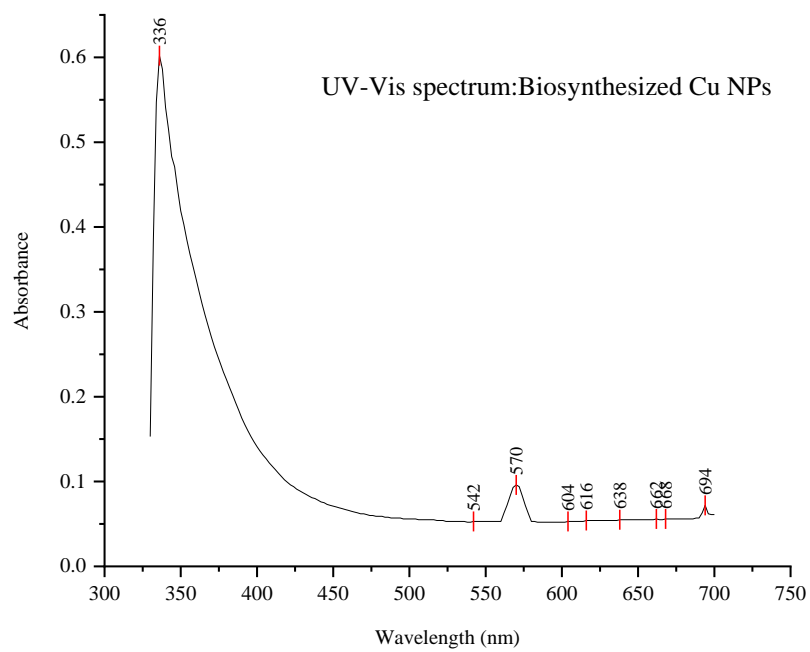


Figure 11: UV-Vis spectra of Cu NPs synthesized by Senna root extract.

4.3.1 Design of Experiments and optimization Analysis

Table 8 contains the list of experimental runs and the corresponding responses obtained from the experiments projected by Box Behnken design. The design optimized parameters that would yield CuNPs with the least average particle size. The experiments were done as per the run order to eliminate experimental bias. The mean particle size of Cu NPs were recorded on Particle Size Analyzer (Nanotracs)

Table 7: Box behnken design and response variables.

StdOrder	RunOrder	PtType	Blocks	Temp (°C)	Conc (M)	pH	Size(nm)
15	1	0	1	60	0.03125	6.5	53.59
1	2	2	1	40	0.0125	6.5	53.5
9	3	2	1	60	0.0125	3	21.63
5	4	2	1	40	0.03125	3	16.11
11	5	2	1	60	0.0125	10	63.6
14	6	0	1	60	0.03125	6.5	53.58
3	7	2	1	40	0.05	6.5	38.65
2	8	2	1	80	0.0125	6.5	36.59
8	9	2	1	80	0.03125	10	50.41
4	10	2	1	80	0.05	6.5	34.35
10	11	2	1	60	0.05	3	19.5
13	12	0	1	60	0.03125	6.5	53.57
12	13	2	1	60	0.05	10	55.4
6	14	2	1	80	0.03125	3	5.55
7	15	2	1	40	0.03125	10	53.18

A regression coefficient R^2 value of 0.9964 was obtained with a second order quadratic equation generated for the optimization process. The coefficients of the variables for the predicted models are shown in equation 4.

$$\text{Size} = -85.2 + 2.570 \text{ Temp} - 174 \text{ Conc} + 16.97 \text{ pH} - 0.02691 \text{ Temp*Temp} - 5813$$

$$\text{Conc*Conc} - 0.9391 \text{ pH*pH} + 8.41 \text{ Temp*Conc} + 0.0278 \text{ Temp} - 23.1 \text{ Conc*pH}$$

Equation 4

The values of the coefficients are calculated by regression analysis. The estimated values of the coefficients for the response is presented in Table 9.

Table 8: Calculated values of the coefficients of the model.

Term	Effect	Coef	SE Coef	T-Value	P-Value	VIF
Constant		53.580	1.020	52.65	0.000	
Temp	-8.635	-4.317	0.623	-6.93	0.001	1.00
Conc	-6.855	-3.427	0.623	-5.50	0.003	1.00
pH	39.950	19.975	0.623	32.05	0.000	1.00
Temp*Temp	-21.528	-10.764	0.917	-11.73	0.000	1.01
Conc*Conc	-4.088	-2.044	0.917	-2.23	0.076	1.01
pH*pH	23.008	-11.504	0.917	-12.54	0.000	1.01
Temp*Conc	6.305	3.153	0.881	3.58	0.016	1.00
Temp*pH	3.895	1.948	0.881	2.21	0.078	1.00
Conc*pH	-3.035	-1.518	0.881	-1.72	0.146	1.00

Conc = concentration and Temp = temperature

The adequacy of the model was checked by using the ANOVA technique. The predictor variables, that is pH, Concentration of Copper ion and temperature of the mixture were all

significant (Tamilvanan *et al.*, 2021). The value of ‘P’ less than the Alpha (α) 0.05 ($P < 0.05$) indicates that pH ($p < 0.0001$) is the most influencing factor when compared to concentration of copper ion ($p < 0.003$) and temperature of the mixture (0.001). The Variance Inflation Factors (VIF) value close to 1 indicate that the predictors are not correlated (Tamilvanan *et al.*, 2021). The ANOVA for average size of the Cu NPs is given in Table 10.

Table 9: Analysis of variance (ANOVA) for Size of Cu NPs Versus Temp ($^{\circ}$ C), Conc (M), pH

Source	DF	Adj SS	Adj MS	F-Value	P-Value
Model	9	4351.12	483.46	155.61	0.000
Linear	3	3435.11	1145.04	368.54	0.000
Temp	1	149.13	149.13	48.00	0.001
Conc	1	93.98	93.98	30.25	0.003
pH	1	3192.01	3192.01	1027.38	0.000
Square	3	851.88	283.96	91.40	0.000
Temp * Temp	1	427.78	427.78	137.69	0.000
Conc * Conc	1	15.42	15.42	4.96	0.076
pH * pH	1	488.63	488.63	157.27	0.000
2-Way Interaction	3	64.14	21.38	6.88	0.032
Temp*Conc	1	39.75	39.75	12.79	0.016
Temp*pH	1	15.17	15.17	4.88	0.078
Con*pH	1	9.21	9.21	2.96	0.146
Error	5	15.53	3.11		
Lack -of-Fit	3	15.53	5.18	51781.50	0.000
Pure Error	2	0.00	0.00		
Total	14	4366.66			

Table 11 gives the model summary. The qualities of the fitted models were evaluated based on the coefficients of determination (R^2) which was 0.9964. The model explains 99.64% of the variation in the average size data. The adjusted R^2 99.00%. R^2 (pred) is 94.31%, which indicate that the model explains 94.31% of the variation in average size of copper nanoparticles when used for prediction.

Table 10: Regression table - Model Summary

Model Summary			
S	Adj	R-sq(adj)	R-sq(pred)
1.76265	99.64%	99.00%	94.31%

Fits and Diagnostics for unusual observations

Obs	Size	Fit	Resid	Std Resid
2	53.5	51.67	1.83	2.08 R
10	34.35	36.18	-1.83	-2.08 R

R Large residual

Figure 12 presents the main effects plot for average size of copper nanoparticle. Temperature of reaction mixture, concentration of copper ion and pH of the medium affect the average size of copper nanoparticles. Comparing the slopes of the lines, it can be concluded that pH had the greater magnitude of effects.

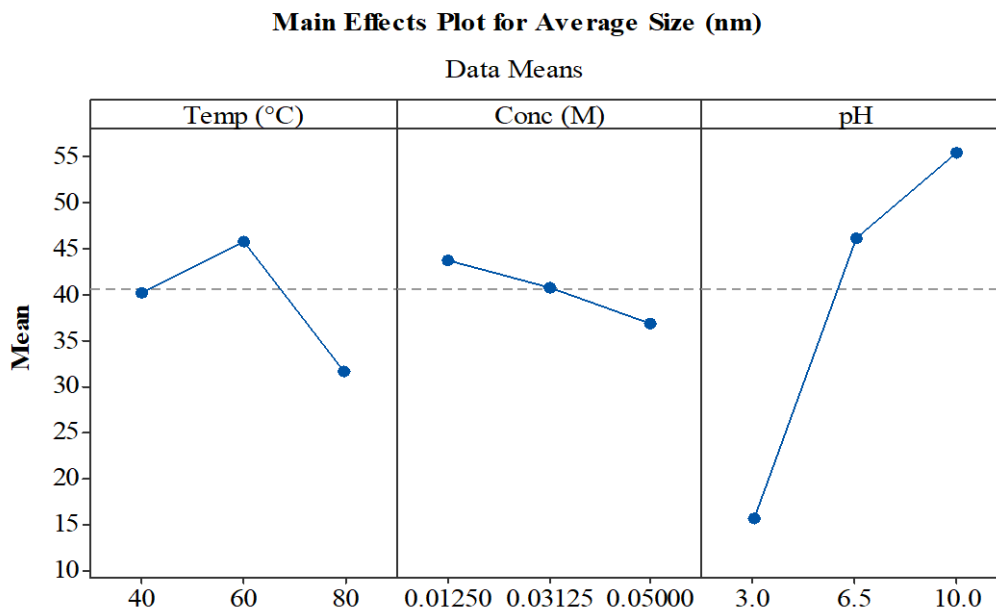


Figure 12: Main effects plot for mean particle size.

Figure 13 presents interaction effects plot for mean size for copper nanoparticles. From the plot, it is seen that there was interaction of temperature and concentration, interaction of concentration and pH as shown by lines intersecting at a point, but there was no possible interaction of temperature and pH as indicated by lines being approximately parallel from each other.

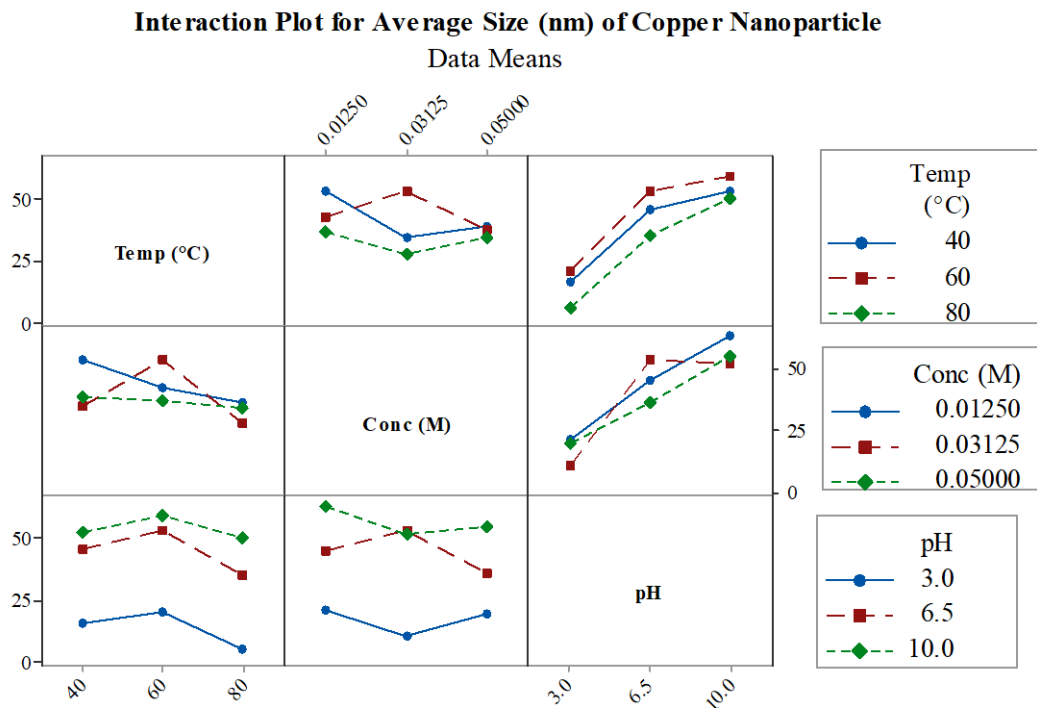


Figure 13: Interaction effects plot for mean particle size.

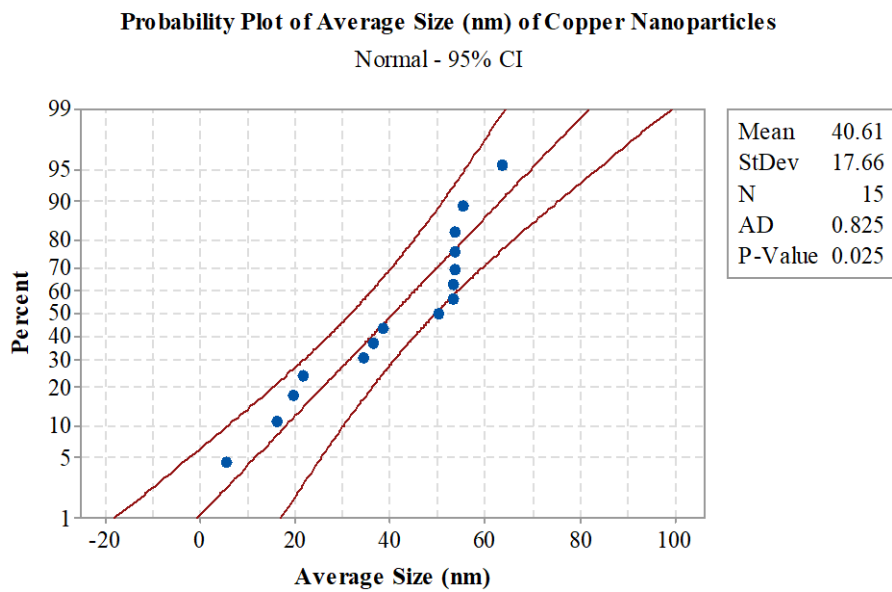


Figure 14: Probability plot for average size of copper nanoparticles.

Normal plot of residual for mean particle size is given in Figure 15. For the mean particle size data, the residuals are randomly scattered about zero hence follow a straight line indicating that the errors are normally distributed.

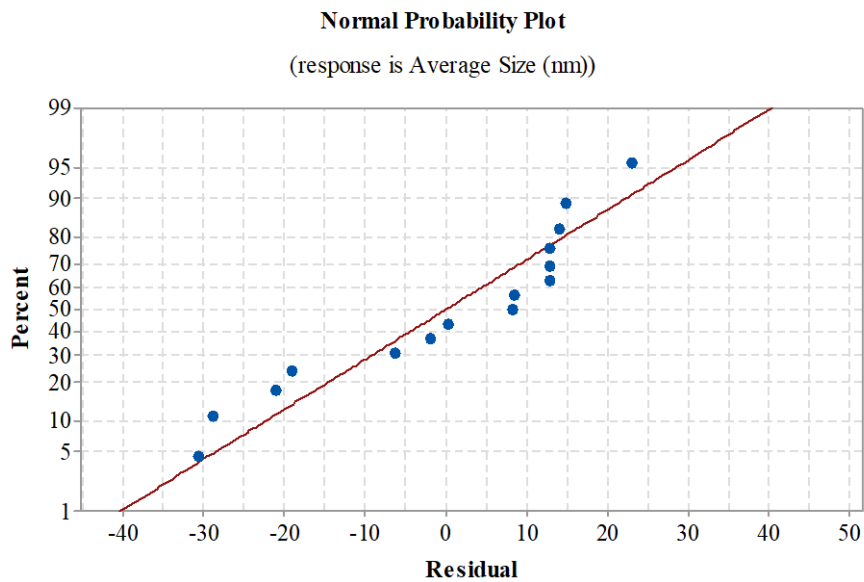


Figure 15: Normality plot of residual for mean particle size.

Figure 16 shows the plot of residual versus fitted values of mean particle size, it can be concluded that there is no obvious pattern and the proposed model is adequate.

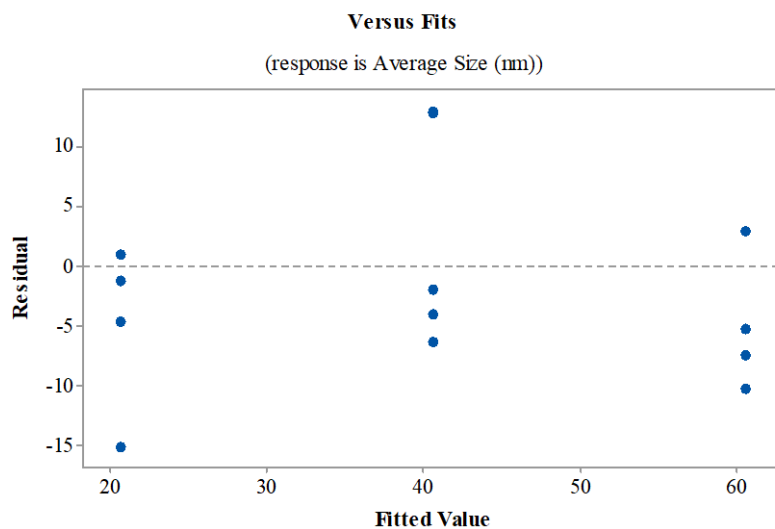


Figure 16: Plot of residual versus fitted values of mean particle size.

The three-dimensional (3D) surface plots for mean particle size of Cu NPs are shown in Fig.17-19. These surface plots were utilized to find out the desired mean particle size for Cu NPs for any suitable combination of input parameters. From Fig. 17, the least mean particle size of Cu NPs was reported at lower pH of the reaction mixture and less concentrated copper ion. Fig.18, revealed that least particle size was attainable at a higher temperature and lower pH. Fig. 19 indicated that higher temperature and medium concentration yielded the least mean particle size of Cu NPs.

Surface Plot of Size (nm) vs pH, Conc (M)

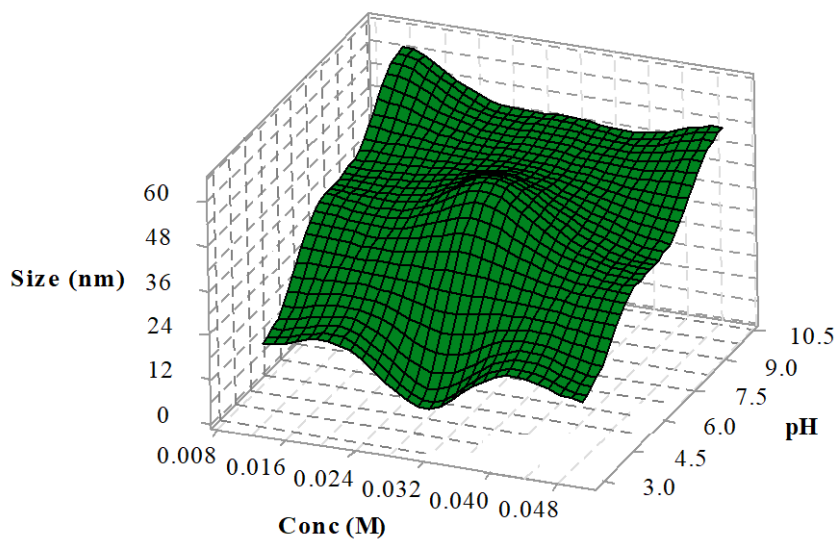


Figure 17: 3D Surface graph for mean particle size versus Copper ion concentration and pH of the mixture.

Surface Plot of Size (nm) vs pH, Temp (°C)

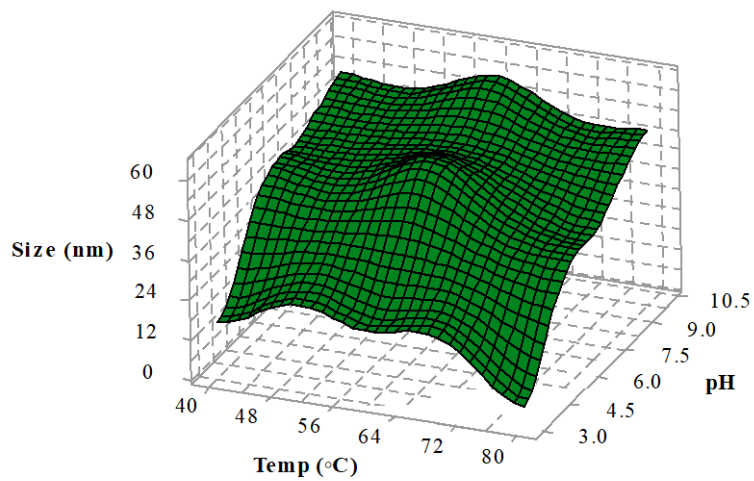


Figure 18: 3D Surface graph for mean particle size versus temperature and pH of the mixture.

Surface Plot of Size (nm) vs Conc (M), Temp (°C)

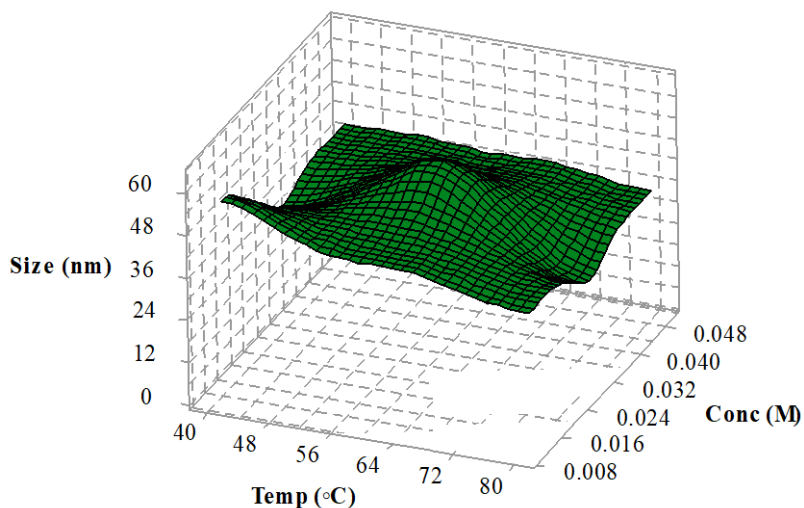


Figure 19: 3D Surface graph for mean particle size versus temperature and concentration of Copper ion

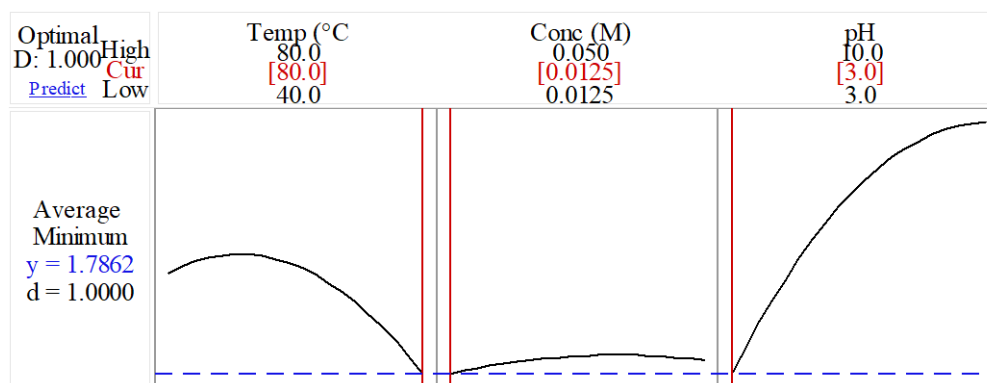


Figure 20: Response optimization for average particle size of Cu NPs.

According to Figure 20, the predicted average particle size is 1.7862 nm. Increasing temperature yields small particle size nanoparticle. Decrease in salt concentration and pH favours synthesis of Cu NPs of least mean size. These observations agree with those of Dang *et al.*, (2011). Previous studies (Zhang *et al.*, 2009; Park *et al.*, 2007) indicated that the pH of aqueous media influences copper reduction reaction in CuNPs synthesis.

Probable kinetic enhancement is thus conducive for reduction of crystallite size because of the enhancement of the nucleation rate (Dang *et al.*, 2011).

4.4 Characterization of Copper Nanoparticles

Based on objective three (3), the synthesized Cu NPs were characterized using UV-Vis spectrophotometer, Particle size analyser (PSA), zeta potential, X-Ray Diffractometer (XRD), and Fourier Transform Infrared Spectroscopy (FT-IR).

4.4.1 Particle Size Analysis

Particle size analysis was conducted using particle size analyser. The sizes of thirteen (13) samples of Cu NPs prepared at varied conditions of pH of the reaction medium, Copper ion concentration and temperature of the solution were determined. Data on particle sizes of Cu NPs are presented in Appendix A. The analysis revealed the influence of pH, copper ion concentration and temperature of reaction medium influence the particles of Cu NPs.

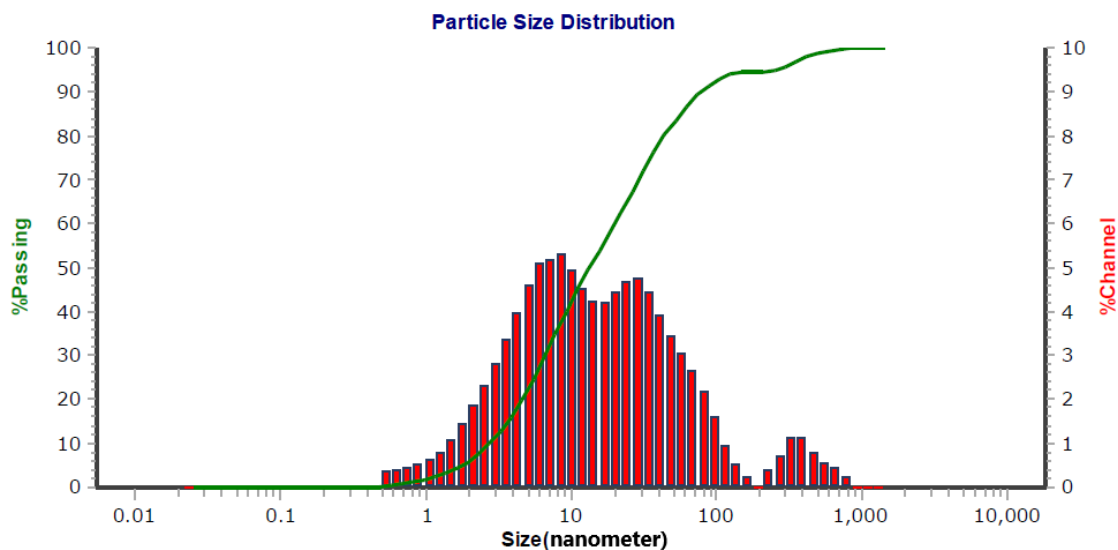


Figure 21: Particle Size of Cu NPs prepared at Temp 80 °C, pH 3.0 and Copper ion Concentration 0.03125 M.

4.4.1.1 Effect of pH

The pH of range 3-10 was varied during Cu NPs average size optimization process. The study revealed that pH as a parameter strongly influenced the size of Cu NPs as shown by Figure 11 of Main effects plot for mean particle size. The least average size of the nanoparticles was recorded at lower pH of 3.0. It was observed that increasing the pH increased the mean size of the nanoparticles. Similar observations have been reported by Honary *et al.* 2012 and Dang *et al.*, (2011). A possible explanation of this observation is that at pH of 3.0, nanoparticles were experiencing high electrostatic repulsion hence reducing agglomeration. Therefore, at alkaline pH, the nanoparticles were exhibiting lower electrostatic forces hence allowing particle growth.

4.4.1.2 Effect of Copper (II) sulphate concentration

Copper ion concentration of range 0.0125-0.05 M was varied for Cu NPs average size optimization. The least mean size of nanoparticles was recorded at lower concentrations of copper salt as revealed in Figure 20. This finding is in agreement with previous findings (Honary *et al.*, 2012; Erick and Nalini, 2015) who reported that large salt ion concentration lead to large particle size and broad size distribution. This could be because low concentration of salt reduced the probability of Cu-Cu interaction hence reducing agglomeration.

4.4.1.3 Effect of Temperature

Temperature in the range 40 °C to 80 °C was controlled for Cu NPs mean size optimization. The study showed that an increase of temperature between 40 °C and 80 °C led to decrease in the mean size of Cu NPs. Previous research has reported the similar findings (Erick and Nalini, 2015). This could be due to possible agglomeration at lower temperatures of 40 °C.

Higher temperature of 80 °C also speeds up the rate of Cu NPs formation as previously reported (Erick and Nalini, 2015).

4.4.2 X-Ray Diffraction Analysis

The XRD peaks were assigned in comparison with the standard powder diffraction card of Joint Committee on Powder Diffraction Standards (JCPDS card no. 89-2838). The peak positions were consistent with metallic copper of a crystalline nature. X-Ray diffraction (XRD) spectrum shown in Figure 21 revealed diffraction peaks at 2θ values of 43.30°, 50.02° and 73.41° corresponding to the Miller indices (111), (200), and (220), respectively which represent face-centered cubic Cu NPs (Ramya Devi *et al.*, 2012). Further, the peak at 30.0° showed that a small amount of copper is oxidised to copper (II) oxide, this is supported with the presence of peaks on the FT-IR spectrum at 650 cm^{-1} and at around 750 cm^{-1} . The average size of CuNPs as determined using Debye-Scherrer's formula was 6 nm, which is close to 5.55 nm as established by XRD analysis. The size of crystal under 100 nm suggested that the nanocrystalline nature of the biosynthesized CuNPs was below 15 nm (Rajagopal *et al.*, 2021). Similar results were reported by other researchers from the structure analysis of XRD for biosynthesized CuNPs (Rajagopal *et al.*, 2021; Sharma *et al.*, 2018; Ghidan *et al.*, 2016).

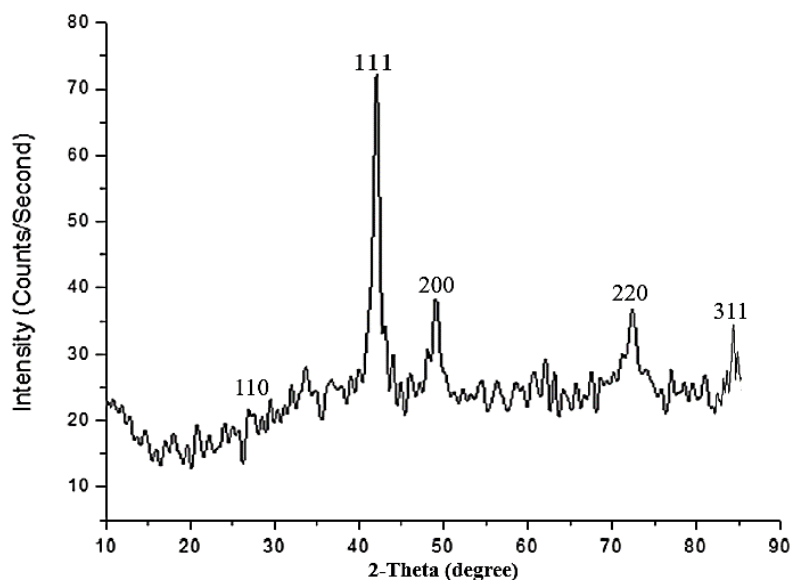


Figure 22: X-Ray Diffraction pattern of Cu NPs biosynthesized by *Senna* root extracts.

4.4.3 Zeta Potential Analysis

The zeta potential value of biosynthesized Cu NPs was -69.4 mV. This indicated the biosynthesized Cu NPs surfaces possessed strong electrostatic repulsion hence good stability. A recent study (Vasantharaj *et al.*, 2019) indicated that CuNPs of size 82.32 nm had a negative zeta potential of -11.9 mV. Such negative zeta potentials suggest that charge distribution of the nanoparticles as well as their sizes could play a role in promoting or enhancing their biological properties (Sankar *et al.*, 2014). In other words, high negative zeta potential translates into strong repulsion between the particles causing an amplification or enhancement of their stabilities (Salopek *et al.*, 1992).

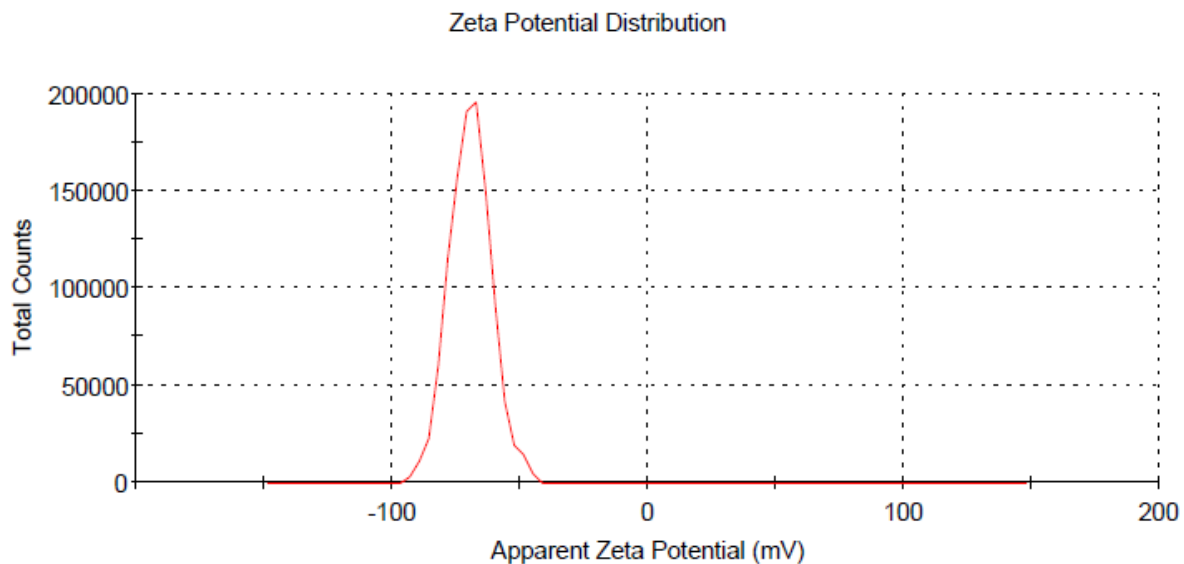


Figure 23: Zeta Potential Distribution of Cu NPs synthesized by *Senna* root extracts.

4.4.4 FT –IR Analysis

FT-IR analysis was done to identify the functional groups of the phytochemicals that participated in synthesizing copper nanoparticles and their stabilization. The spectrum shown in Figure 23 revealed a broad band in the range $3100\text{-}3500\text{ cm}^{-1}$ characteristic of N-H stretch of amines and amides, and a band of range $3400\text{-}2400\text{ cm}^{-1}$ indicating the presence of O-H of Carboxylic acids, alcohols and phenols. The band at 1612.25 is assigned to C=C of alkenes and aromatic compounds. The presence of aromatic compounds was confirmed by the two peaks at 988.30 and 830.60 known for C-H out-of-plane bend for aromatic compounds. A peak at 1271.13 cm^{-1} is attributed to C-O bond of alcohols, carboxylic acids and esters.

The presence of these functional groups indicated possible involvement of reductive groups on the surfaces of the CuNPs (Karimi et al, 2015). They are also involved in capping of the CuNPs, as observed in previous studies that synthesized CuNPs from plant extracts (Sathiyavimal *et al.*, 2018; Saif *et al.*, 2016). The spectrum indicated new chemical

linkages on the surface of CuNPs, suggesting that *S. didymobotrya* root extract can bind to CuNPs through hydroxyl and carbonyl groups of the amino acid residues in the protein of the extracts, therefore acting as reducing, stabilizing and dispersing agents for synthesized copper oxide nanoparticles and preventing agglomeration of the CuNPs (Ghidan *et al.*, 2016; Vasantharaj *et al.*, 2019).

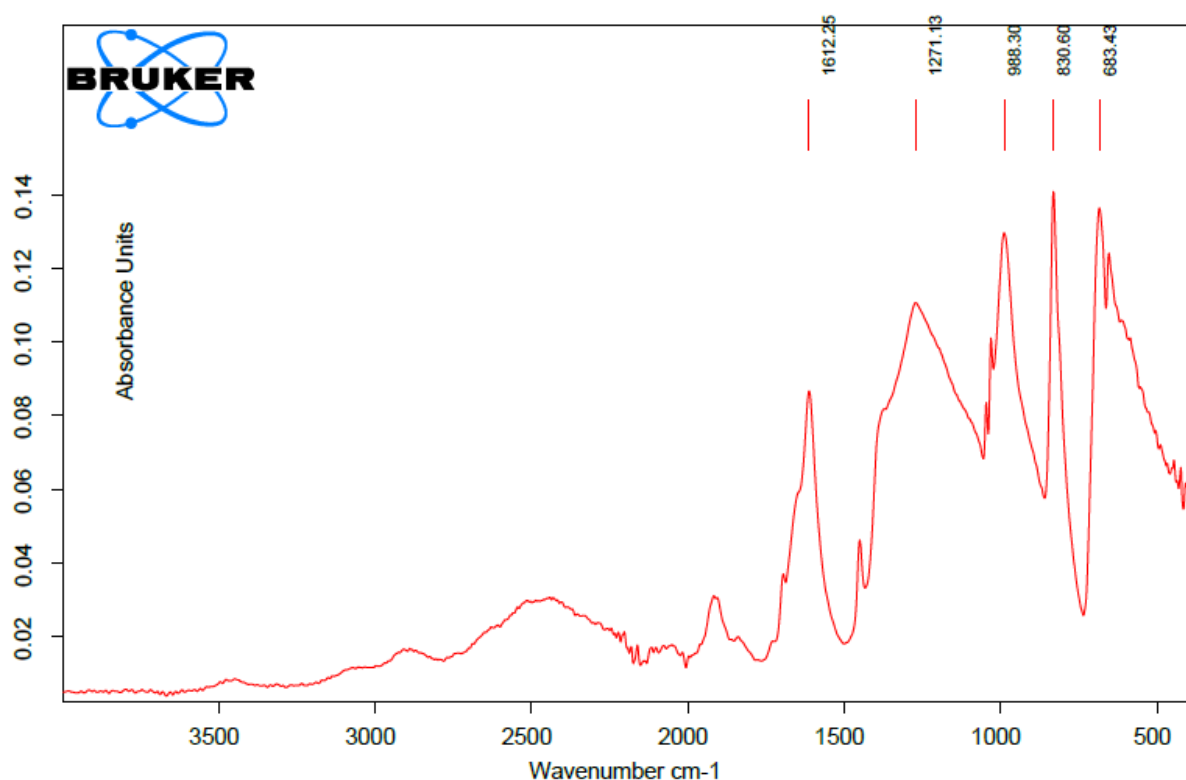


Figure 24: FT-IR Spectrum of Cu NPs synthesized by *Senna* root extract.

4.5 Anti-microbial activity of *Senna didymobotrya* copper nanoparticles

The antimicrobial action of *Senna didymobotrya* copper nanoparticles was observed by absence or presence of microbial growth inhibition or clear zones. Two bacteria strains were used in the analysis, *E. coli* and *S. aureus*, gram negative and gram positive bacterial strains respectively. Appendix B, presents the inhibition zones of *E. coli* and *S. aureus*.

Table 12 and Figure 24 shows that copper nanoparticles synthesized by *Senna didymobotrya* had antimicrobial activity against *E. coli* and *S. aureus*. Pearson's product-moment correlation was performed to evaluate the association between size of CuNPs and ZOI of CuNPs against *E. coli* and *S. aureus* (n = 13). The analysis showed that there was a negative correlation between size of CuNPs and zone of inhibition of *E. coli* ($r = -0.74$, $p \geq 0.01$). Similarly, a negative correlation was observed between the size of CuNPs and zone of inhibition of *S. aureus* by the CuNPs ($r = -0.74$, $p \geq 0.05$).

From the table, it can be seen that the highest zone of inhibition of 30 mm for *S. aureus* and 26 mm for *E. coli* was achieved for Cu NPs with the least mean particle size which was synthesized at optimum condition of temperature of 80 °C, Copper ion concentration of 0.03125 M and pH of 3.0. This indicated that Cu NPs of least mean particle size had high surface area to volume ratio hence effectively binding to the microbial membrane and probably altered its permeability which could have caused growth inhibition (Ahmadi et al, 2018). Sathiyavimal *et al.*, (2018) reported similar results in which 100 µL of CuNPs prepared from *Sida acuta* extract highly inhibited *E. coli* with a zone of inhibition maximum of 15 mm, showed a lower antibacterial activity against *S. aureus* while the lowest inhibition diameter was 11 mm against *P. vulgaris*. Previous authors (Ramyadevi *et al.*, 2012; Usman *et al.*, 2013; Chen *et al.*, 2019) have reported similar results, in which *E. coli* was the most inhibited bacteria when compared with *S. aureus* and other Gram-positive bacteria.

The higher inhibition of Gram-negative bacteria by CuNPs could be partially explained by the facilitated influx of smaller-sized nanoparticles into the cell wall of Gram-negative bacteria which consists of a unique outer membrane layer and a single peptidoglycan layer as compared to the cell wall of Gram-positive bacteria with several peptidoglycan layers

(Silhavy *et al.*, 2010; Hajipour *et al.*, 2012). Further, CuNPs have been speculated to adhere to Gram negative bacterial cell walls due to electrostatic interaction, or the copper ions facilitates rapid DNA degradation and reduction of bacterial respiration (Raffi *et al.*, 2010). In some Gram-negative strains, copper ions alter the conformation and electron transferase of the associated reductases, culminating into inhibition of cytochromes in the membrane (Warnes and Keevil, 2011).

Table 11: Antimicrobial activity of Cu NPs synthesized at different parameters.

S. NO	Test Drug	Z.O.I on E coli (mm)	Susceptibility (Amoxillin/Clavulanic acid) R (≤ 13) m (14-17) S (≥ 18)	Z.O.I on S aureus (mm)	Susceptibility (Amoxillin/Clavulanic acid) R (≤ 19) m (-) S (≥ 20)
1	CuNPs.T60.C0.03125.pH6.5	18 \pm 0.58	S	16 \pm 0.58	R
2	CuNPs.T60.C0.0125.pH3.0	19 \pm 0.58	S	21 \pm 0.58	S
3	CuNPs.T40.C0.03125.pH10	16 \pm 1.00	M	19 \pm 1.73	S
4	CuNPs.T80.C0.05.pH6.5	18 \pm 1.15	M	20 \pm 0.58	S
5	CuNPs.T40.C0.05.pH6.5	18 \pm 1.00	S	19 \pm 1.53	M
6	CuNPs.T80.C0.0125.pH6.5	15 \pm 1.53	M	16 \pm 0.58	R
7	CuNPs.T40.C0.03125.pH3.0	17 \pm 1.00	M	15 \pm 0.58	R
8	CuNPs.T40.C0.0125.pH6.5	15 \pm 1.00	M	14 \pm 0.58	R
9	CuNPs.T80.C0.03125.pH3.0	26 \pm 0.58	S	30 \pm 0.58	S
10	CuNPs.T60.C0.05.pH10.0	18 \pm 0.58	S	19 \pm 0.58	R
11	CuNPs.T60.C0.0125.pH10.0	15 \pm 0.58	M	16 \pm 1.15	R
12	CuNPs.T80.C0.03125.pH10.0	16 \pm 1.15	M	17 \pm 1.00	R
13	CuNPs.T60.C0.05.pH3.0	23 \pm 0.58	S	22 \pm 1.00	S
14	Amoxillin clavunilate (Standard)	20 \pm 0.58	S	28 \pm 0.58	S
15	Senna root extract	13 \pm 0.58	M	14 \pm 1.15	R
16	Copper sulphate solution	11 \pm 0.58	R	10 \pm 0.58	R

R – Resistant, M – intermediate, S – Susceptible

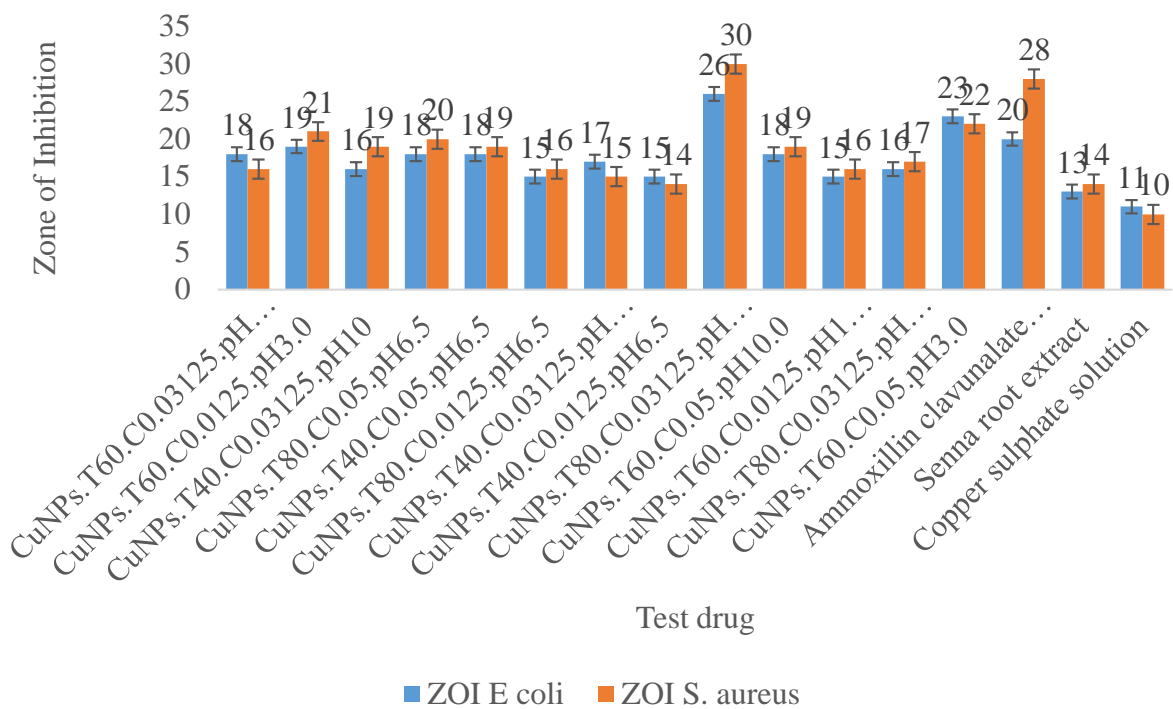


Figure 25: Graph of antimicrobial activity of Copper nanoparticles, Standard drug, copper sulphate solution and *Senna* root extract.

CHAPTER 5: CONCLUSIONS AND RECOMMENDATIONS

5.1 Conclusions

Phytochemical screening showed positive for phenols, alkaloids, anthraquinones, flavonoids, saponins, tannins, gladiac glycosides in the roots of *Senna didymobotrya*. *Senna* has high amounts of flavonoids and phenols. Gas chromatography analyses revealed that *Senna* roots consisted of 76 compounds and the main chemical constituents identified were Benzoic acid, Benzyl alcohol, Thymol, N-Benzyl-2-phenethylamine, Benzaldehyde, Vanillin, Phenyl acetic acid, Nonanoic acid, Benzothiazole.

Copper nanoparticles (Cu NPs) were synthesized using *Senna* roots extracts at optimized conditions of temperature, pH and concentration of copper ion. Box Behnken design was utilised to obtain the least particle size by optimizing pH of the medium, concentration of copper ion and temperature of the mixture. The design showed that the optimum synthesis conditions were temperature of 80 °C, pH of 3.0 and copper ion concentration of 0.0125 M. The mean particle size of Cu NPs predicted by the design at the optimum conditions is 1.7862 nm. According to the design, pH was the most influencing factor in determining the size of Cu NPs followed by temperature and the concentration of copper ion. UV-Vis analysis showed characteristic surface Plasmon resonance (SPR) peak 571 nm indicating the formation of Cu NPs. FT-IR analyses revealed that the nanoparticles were bound by carboxylic acids, amines and amides, phenols and esters. Particle size analysis showed that synthesized Cu NPs were of the range of 5.55 – 63.60 nm particle size. Cu NPs prepared at temperature of 80 °C, pH of 3.0 and Copper ion concentration of 0.03125 M were of least mean particle size. X-ray diffraction measurement confirmed the presence of cubic face-

centered Cu NPs. The measured zeta potential value of Cu NPs was -69.4 mV indicating that the synthesized nanoparticles were stable.

In conclusion the biosynthesized Cu nanoparticles are stable and displayed better antimicrobial activity against *E. coli* and *S. aureus* compared to amoxicillin clavulanate (standard).

5.2 Recommendations

Apart from *senna* roots, other parts of the plant such as the stem, leaves and flowers could be extracted using different solvents and their extractive yields compared. Different solvent mixture ratios can also be utilized to improve extractive yield.

Apart from optimized reaction conditions affecting the mean particle size of copper nanoparticles, other factors such as centrifugation speed, revolution per minute of the reaction mixture could also be investigated. This could improve size and stability of the biosynthesized copper nanoparticles.

The synthesized copper nanoparticles showed better antimicrobial activity *E. coli* and *S. aureus* compared to amoxicillin clavulanate (standard). Therefore, the study recommends the testing of biosynthesized copper nanoparticles against other potential multi-drug resistant microbes to enable their development into antimicrobial agents.

REFERENCES

- Aazam, E. S., & El-Said, W. A. (2014). Synthesis of copper/nickel nanoparticles using newly synthesized Schiff-base metals complexes and their cytotoxicity/catalytic activities. *Journal of Bioorganic Chemistry*, 57, 5-12
- Abd-Elkarem J. I., Bassuony H. M., Mohammed S. M., Fahmy H. M., & Abd-Elkader N. R. (2016). Eco-Friendly Methods of Copper Nanoparticles Synthesis. *Journal of Binanoscience*, 1-23. doi:10.1166/jbns.2016.1350
- Adewale, S.A., Folorunso S.A., Femi, A. F., Abel, K.O. (2020). Green synthesis of copper oxide nanoparticles for biomedical application and environmental remediation. *Heliyon*;6(7), e04508.
- Ahmad I, Yanuar A, Mulia K, Mun'im A. (2017). Application of ionic liquid as a green solvent for polyphenolics content extraction of *Peperomia Pellucida* (L) Kunth Herb. *Journal of Young Pharm.*, 9(4):486-90. DOI: 10.5530/jyp.2017.9.95.
- Ahmadi, O. Jafarizadeh Chakraborty, S. & Biswas, S. (2016). In Vitro–In Vivo performance of Bare and Drug Loaded Silica gel Synthesized via Optimized Process Parameters. *Journal of Applied Surface Science*, 360: 961-969.
- Alemayehu, G., Abegaz, B., Snatzke, G., & Duddeck, H. (1989). Quinones of *Senna didymobotrya* a. *Bulletin of the Chemical Society of Ethiopia*, 3(1).
- Alemayehu, I. Tadesse, S. Mammo, F. Kibret, B. & Endale, M. (2015). Phytochemical analysis of the roots of *Senna didymobotrya*,” *Journal of Medicinal Plants Research*, vol. 9, no. 34, pp. 900-907, 2015.
- Al-Hakkani, M. F. (2020). Biogenic copper nanoparticles and their applications: A review,” *SN Applied Sciences*, 2; 505.
- Ampaire L., Muhindo A., Orikiriza P., Mwanga-Amumpaire J., Bebell L., Boum Y. (2016). A review of antimicrobial resistance in East Africa. *African Journal of Laboratory Medicine*, 5(1). Retrieved from <http://dx.doi.org/10.4102/ajlm.v5i1.432>
- Anthony, S. T. Mutuku, C. N. Obey, J. K. Akumu, E. & Makau, E. N. (2014). Evaluation of in vitro antibacterial activity in *Senna didymobotrya* roots methanolic-aqua extract and the selected fractions against selected pathogenic microorganisms. *International Journal of Current Microbiology and Applied Sciences*, 3(5); 362-376.
- Anthony, S.T. Obey, K. J. & Mutuku, C. N. (2015). Assessment Of Antibacterial Activity Of Hot Aqua Extract Of *Senna Didymobotrya* Leaves,” *Baraton Interdisciplinary Research Journal*, 5;125-132.
- Arya, V. (2010). Living Systems: Eco-friendly Nanofactories, *Digest J. of Nanomaterials and Biostructure*, 5(1), 9-21.
- Asemani, M., & Anarjan, N. (2019). Green ayntesis of copper oxide nanoparticles using *Juglans regia* leaf ectract and assessment of their phisico-chemical and biological properties. *De Gruyter*,8: 557-567
- Awwad, M. A., Albiss, B. A., & Salem, N. M. (2015). Antibacterial Activity of Synthesized Copper Oxide Nanoparticles using *Malva sylvestris* Leaf Extract. *Smu Medical Journal*, 2.

- Barabadi, H. Honary, S. Ebrahimi P. et al. (2015). Microbial mediated preparation, characterization and optimization of gold nanoparticles,” *Brazilian journal of microbiology*, 45(4), 1493–1501.
- Barak M., Arzanlou M., Babapour B. & Ghorbani L. (2016, September 27). Antibiotic resistance pattern of bacterial enteritis among hospitalised children in Ardabil: a single center experience. *International Journal of Advances in Medicine*, 3(4), 991-993. Retrieved from <http://dx.org/10.18203/2349-3933.ijam20163736>
- Bashir, A., Saeed, B., Mujahid, Y.T. and Jehan, N. (2011). Comparative Study Of Antimicrobial Activities Of Aloe vera Extracts And Antibiotics Against Isolates From Skin Infections, *African Journal of Biotechnology.*, 10(19), 3835-3840, doi: 10.5897/AJB07.572.
- Bassetti, M., Trearichi, E. M., Mesini, A., Spanu, T., Giacobbe, D. R., Rossi, M., Shenone, E., Pascale, G. D., Molinari, M. P., Cauda, R. Viscoli, C. and Tumbarello, M. (2011). Risk factors and mortality of healthcare-associated and community acquired Staphylococcus aureus bacteraemia. *European society of Clinical Microbiology and infection*, 18; 862-869.
- Betancourt R., Rodriquez P. Y., Urbina B. A., Orta C. A., Rodriguez O. S., Cadenas, P., Saldivar R. H., and Cerda, L. A. (2014). Synthesis of Copper Nanoparticles by Thermal Decomposition and Their Antimicrobial Properties. *Journal of Nanomaterials*,5.
- Bharathi, D. Ranjithkumar, R. Chandarshekar, B. & Bhuvaneshwari, V. (2019). Bio-inspired synthesis of chitosan/copper oxide nanocomposite using rutin and their anti-proliferative activity in human lung cancer cells. *International journal of biological macromolecules*, 141; 476–483.
- Bhaskar A., RajaLakshmi A, Krithiga N, Gurupavithra S and Jayachitra A, (2014). Biosynthesis of copper Nanoparticles using *ocimum sanctum* leaf extract and its antimicrobial property. *International journal of biological and pharmaceutical research*, 5(6):511-515.
- Biswas, S. Chakraborty, S. and Mulaba-Bafubiandi, A. F. (2017). Optimization of copper nanoparticles biosynthesis process using aqueous extract of *Andrographis paniculata*,” *African Journal of Science, Technology, Innovation and Development*, 9(1); 131-138.
- Blosi, M., Albonetti, M., Dondi, M., Martelli, C., & Baldi, G. (2011). Microwave-assisted polyol synthesis of Cu nanoparticles. *Journal of Nanoparticles Resource*, 13: 127-138
- Buyela, D. K. (2017). Profiling and pathogenicity of *Ralstonia solanacearum* disease of tomato and it's control using *Senna didymobotrya* and *Moringa oleifera* plant extracts in Maseno (Kenya). MSc Thesis, Maseno University, Kenya.
- Caroling G, Priyadharshini MN, Vinodhini E, Ranjitham AM, Shanthi P. (2015). Biosynthesis of copper nanoparticles using aqueous guava extract. *International Journal Pharmacy and BioScience*. 5:25–43.
- Chakraborty, S., and Biswas, S. (2016). In Vitro – In Vivo performance of Bare and Drug Loaded Silica gel Synthesized via Optimized Process Parameters. *Journal of Applied Surface Science*, 360: 961-969.

- Chan, G. H. Zhao, J. Hicks, E. M. Schatz, G. C. & Van Duyne, R. P. (2007). Plasmonic properties of copper nanoparticles fabricated by nanosphere lithography,” *NanoLetters*, 7(7): 1947–52.
- Chatattikun M, Choabchalard A. (2013). Phytochemical screening and free radical scavenging activities of orange baby carrot and carrot (*Daucus carota Linn*) root crude extracts. *Journal of Chemical and Pharmaceutical Research*, 5(4):97-102.
- Chawla, R., Thakur P., Chowdhry A., Jaiswal S., Sharma A., Goel R., Sharma J., Priyadarshi S.S., Kumar V., Sharma R. K., & Arora R. (2013). Evidence based herbal drug standardization approach in coping with challenges of holistic management of diabetes: A dreadful lifestyle disorder of 21st century. *Journal of Diabetes and metabolic disorders*, 12,33-35.
- Chen, H. Wu, J. Wu, M. and Jia, H. (2019). Preparation and antibacterial activities of copper nanoparticles encapsulated by carbon. *New Carbon Materials*, 34(4); 382-389.
- Clinical Laboratory Standards Institute. (2010). Performance standards for antimicrobial disk susceptibility tests; Approved standard— 9th ed. CLSI document M2-A9. 26:1. Clinical Laboratory Standards Institute, Wayne, PA.
- Commission Recommendation of 18 October 2011 on the definition of nanomaterial (2011/696/EU)
- Dang, T. M. D. Le, T. T. T. Fribourg-Blanc, E. and Dang, M.C. (2011). Synthesis and optical properties of copper nanoparticles prepared by a chemical reduction method. *Advances in Natural Sciences: Nanoscience and Nanotechnology*, 2 (1) , 015009.
- de Kraker, M. E., Wolkewitz, M., Davey, P. G., Grundmann, H., BURDEN Study Group. (2011). Clinical impact of antimicrobial resistance in European hospitals: excess mortality and length of hospital stay related to methicillin-resistant *Staphylococcus aureus* bloodstream infections. *Antimicrobial Agents Chemotherapy*, 55; 1598–1605.
- DeAlba-Montero, I. Guajardo-Pacheco, J. Morales-Sánchez E. et al. (2017). Antimicrobial Properties of Copper Nanoparticles and Amino Acid Chelated Copper Nanoparticles Produced by Using a Soya Extract,” *Bioinorganic Chemistry and Applications*, 2017, Article ID 1064918.
- Deepak, K. D., Rajni, K. P., Anil, K. S., & Vaibhav T. (2020). Role of Nanobiotechnology in Drug Discovery, Development and Molecular Diagnostic. *Intechopen*. DOI: <http://dx.doi.org/10.5772/intechopen.92796>
- Din, M, I., Arshad, F., Hussain, Z. & Mukhtar, M. (2017). Green Adeptness in the Synthesis and stabilization of Copper Nanoparticles: Catalytic, Antibacterial, Cytotoxicity, and Antioxidant Activities. *Nanoscale Research Letters*, 12: 638
- Dominguez E., Zarazaga M., Saenzy Y., Brinas L., & Torres C. (2002). Mechanisms of Antibiotic Resistance in *Escherichia coli* Isolates Obtained from Healthy Children in Spain. *Microbial drug resistance*, 8(4).
- Dromigny J. A., Nabeth P., Juergens-Behr A., & Perrier-Gros-Claude J. D. (2005). Risk factors for antibiotic-resistant *Escherichia coli* isolated from community-acquired urinary tract infections in Dakar, Senegal. *Journal of Antimicrobial Chemotherapy*, 56(1), 236–239.

- Erb A., St'urmer T., Marre R., & Brenner H. (2007). Prevalence of antibiotic resistance in Escherichia coli: Overview of geographical. *European Journal of Clinical Microbiology & Infectious Diseases*, 26(2), 83-90.
- Erick, O. N. & Nalini, M. P. (2015). Green chemistry focus on optimization of silver nanoparticles using response surface methodology (RSM) and mosquitocidal activity: *Anopheles stephensi* (Diptera: Culicidae). *Spectrochimica Acta Part A Molecular and Biomolecular Spectroscopy*, 149:978-984.
- Espirito Santo B., Taudte S., Nies D. H., & Grass G. (2008). Contribution of copper ion resistance to survival of Escherichia coli on metallic copper surfaces. *Journal of Applied Environmental Microbiology*, 4, 977-986.
- Gakuubi, M. M. & Wanzala, W. (2012). A survey of plants and plant products traditionally used in livestock health management in Buuri district, Meru County, Kenya. *Journal of Ethnobiology and Ethnomedicine*, 8(39).
- Ganguanco L. M., Alejandria M., Karl E. H., Alfaraz L., Rona M. A., Maritess L., & Mediadora S. (2015). Prevalence and risk factors for trimethoprim-sulfamethoxazole resistant urinary tract infection in a developing country. *International Journal of Infectious Diseases*, 55-60. Retrieved from <http://dx.doi.org/10.1016/j.ijid.2015.02.022>
- Gayathi M., & Ashwini D. (2018). Green route of copper (Cu) nanoparticles synthesis using *Hemidesmus indicus* aqueous root extracts and its antimicrobial activity. *Research Journal of Chemistry and Environment*, 22 (11).
- Ghidan, A. Y. Al-Antary, T. M. and Awwad, A. M. (2016). Green synthesis of copper oxide nanoparticles using Punica granatum peels extract: effect on green peach Aphid, *Environmental Nanotechnology, Monitoring & Management*, 6; 95-98.
- Ghoto, S. A., Khuhawar, M. Y., Jahangir, T. M., Mangi, J. D. (2019). Applications of copper nanoparticles for colorimetric detection of dithiocarbamate pesticides. *Journal of Nanostructure in Chemistry*, 9; 77-93.
- Gini T. G & Jeya Jothi G., (2018). Column chromatography and HPLC analysis of phenolic compounds in the fractions of *Salvinia molesta* Mitchell
- Gondal, M.A., Qahtan, T.F., Dastageer, M.A., Maganda, Y. W. & Anjum, D. H. (2013). Synthesis of Cu/Cu₂O nanoparticles by laser ablation in deionized water and their annealing transformation into CuO nanoparticles. *Journal of Nanoscience and Nanotechnology*, 13(8):5759-66.
- Gopi M., Pearlin B., Kumar R. D., Shanmathy M., & Prabakar G. (2017): Role of Nanoparticles in Animal and Poultry Nutrition: Modes of Action and Application in Formulating Feed Additives and Food Processing. *International Journal of Pharmacology*, 13(7), ISSN 1811-7775. DOI: 10.3923/ijp.2017.724.731
- Gopinath M, Subbaiya R, Selvam MM, Suresh D. (2014). Synthesis of copper nanoparticles from Nerium oleander leaf aqueous extract and its antibacterial activity. *International Journal Current Microbiology and Applied Science*. 3(9):814-818.

- Granata, G., Yamaoka, T., Pagnanelli, F., & Fuwa, A. (2016). Study of the synthesis of copper nanoparticles: the role of capping and kinetic towards control of particle size and stability. *Journal of Nanoparticle Resource*, 18(133)
- Hajipour, M. J. Fromm, K. M. Ashkarran A. A. et al., (2012). Antibacterial properties of nanoparticles,” *Trends in biotechnology*, 30(10); 499–511.
- Honary, S. Barabadi, H. Gharaeifathabad, F. and Naghibi, F. (2012). Green Synthesis of Copper Oxide Nanoparticles Using *Penicillium aurantiogriseum*, *Penicillium citrinum* and *Penicillium waksmanii*. *Digest Journal of Nanomaterials and Biostructures*, 7; 999-1005.
- Hudzicki, J. (2009). Kirby-Bauer Diffusion Susceptibility Test Protocol. *American Society for Microbiology*.
- Hussein, H. J. Sahi, N. M. Saad, A. M. & Ali Malik Altameme, H. J. (2019). The Antibacterial Effect of bioactive compounds extracted from *Cassia didymobotrya* (Fresenius) Irwin & Barneby against Some Pathogenic Bacteria. *Annals of Tropical Medicine & Public Health*, 22; SPe117.
- Igunza, O. F. Ngeranwa, J. Orinda, G. and Mugo, P. (2019). In vitro modulation of clotrimazole, Ketoconazole, Nystatin, Amphotericin B and Griseofulvin by *Acmella caulirhiza* and *Senna didymobotrya* extract against *Candida* spp. *Journal of Applied Biosciences*, 142; 14478 - 14508.
- Jardon-Maximino, N., Perez-Alvarez, M., Cadenas-Pliego, G., Lugo-Uribe, L.E., Cabello-Alvarado, C., Mata-Padilla, J. M., & Barriga-Castro, E. D. (2021). Synthesis of Copper Nanoparticles Stabilized with Organic Ligands and Their Antimicrobial Properties. *Polymers (Basel)*, 13(17).
- Jeruto, P. Arama, P. F. Anyango, B. & Maroa, G. (2017). Phytochemical screening and antibacterial investigations of crude methanol extracts of *Senna didymobotrya* (Fresen.) H. S. Irwin & Barneby. *Journal of Applied Biosciences*, 114; 11357-67.
- Jeruto, P., Lukhoba, C., Ouma G., Mutai C., & Otieno D.,. (2008). An Ethnobotanical study of medicinal plants. *Journal of Ethnopharmacology*.
- Jesus M., Grazu V.,. (2012). *Frontiers of Nanoscience* (Vol. 4). (Richard E. P., Ed.) El sevier publications. Retrieved from www.elsevierdirect.com
- Kalaimurugan, D. Sivasankar, P. Lavanya, K. Shivakumar, M. S. and Venkatesan, S. (2019). Antibacterial and larvicidal activity of *Fusarium proliferatum* (YNS2) whole cell biomass mediated copper nanoparticles. *Journal of Cluster Science*, 30(4); 1071-1080.
- Kanninen, P., Johans, C., Merta, J., & Kontturi, K. (2008). Influence of ligand structure on the stability and oxidation of copper nanoparticles. *Journal of Colloid and Interface Science*, 318(1):88-95.
- Kareru, P. G. Kenji, G. M. Gachanja, A. N. Keriko, J. M. and Mungai, G. (2007). Traditional medicines among the Embu and Mbeere people of Kenya. *African Journal of Traditional, Complementary and Alternative Medicine*, 4; 75–86.
- Karimi, J. & Mohsenzadeh, S. (2015). Rapid, Green, and Eco-Friendly Biosynthesis of Copper Nanoparticles Using Flower Extract of *Aloe Vera*. *Synthesis and Reactivity in Inorganic, Metal-Organic, and Nano-Metal Chemistry*, 45:6,895-898

- Kato, H., in: S.C. Singh, H. Zeng, C. Guo, W. Cai (Eds.), Chapter 8 'Size Determination of NPs by Dynamic Light Scattering', in 'Nanomaterials: Processing and Characterization with Lasers' Wiley-VCH, 2012.
- Kavita, R., & Sharma, K. (2018). Biological Synthesis of Copper Nanoparticles and their Antimicrobial Properties: A Review. *World Journal of Pharmaceutical Research*, 7(7): 514-539
- Khan, A., Rashid, A., Younas, R., & Chong, R. (2016). A chemical reduction approach to the synthesis of copper nanoparticles. *Journal of International Nano Letters*, 6: 21-26
- Kigonde, E. V. Rukunga, G. M. Kerik J. M. et al. (2009). Antiparasitic activity and cytotoxicity of selected medicinal plants from Kenya. *Journal of Ethnopharmacology*, 123, 505–509.
- Killivalavan, A. Prabakar, A. C. Chandra Babu, K. et al. (2020). Synthesis and characterization of pure and Cu doped CeO₂ nanoparticles: photocatalytic and antibacterial activities evaluation. *Biointerface Research in Applied Chemistry*, 10(2), 5306–5311.
- Kitonde, C. K. Fidahusein, D. S. Lukhoba, C. W. and Jumba, M. M. (2014). Antimicrobial activity and phytochemical screening of *Senna didymobotry* used to treat bacterial and fungal infections in Kenya. *International Journal of Education and Research*, 2(1); 1-12.
- Kobayashi, Y., Ishida, S., Ihara, K., Yasuda, Y., Morita, T., Yamada, S. (2009). Synthesis of metallic copper nanoparticles coated with polypyrrole. *Coll. Polym. Sci.* 287, 877–880.
- Kolekar R, Bhade S, Kumar R, Reddy P, Singh R, Pradeepkumar K. (2015). Biosynthesis of copper nanoparticles using aqueous extract of *Eucalyptuss p.* plant leaves. *Current Science*. 109:255.
- Korir, R.K., Mutai, C., Kiiyukia, C. and C. Bii, C. (2012). Antimicrobial Activity and Safety of two Medicinal Plants Traditionally used in Bomet District of Kenya. *Research Journal of Medicinal Plants*; 6: 370-382.
- Kote R. J., Mulani M. R., Kadam S. A. and Solankar M. B., (2014). Anti-mycobacterial activity of Nanoparticles from *Psidium guajava* L. *Journal of microbiology and Biotechnology Research*, 4(5):14-17.
- Krithiga, N. Jayachitra, A. and Rajalakshmi, A. (2013). Synthesis, characterization and analysis of the effect of copper oxide nanoparticles in biological systems. *Indian Journal of NanoScience*, 1; 6-15.
- Lambert, M. L., Suetens, C., Savey, A. (2011). Clinical outcomes of healthcare- associated infections and antimicrobial resistance in patients admitted to European intensive-care units: a cohort study. *Lancet Infectious Diseases*, 11; 30–38.
- Lee H-J, Lee G, Jang N. R., Yun J. H., Song J. Y., Kim B. S. (2011) Biological synthesis of copper nanoparticles using plant extract. *Nanotechnology*. 1:371–4.
- Lim, J., Yeap, S. P., Che, H. X., & Low, S. C. (2013). Characterization of magnetic nanoparticle by dynamic light scattering. *Nanoscale Research Letters*, 8, 381.

- Linsinger, T., Roebben, G., Gilliland, D., & Calzolari L., (2011). Requirements on measurements for the implementation of the European Commission definition of the term “nanomaterial”, JRC Reference Report EUR 25404 EN
- Liu, Q., Zhou, D., Yamamoto, Y., Ichino, R., & Okido, M. (2012). Preparation of Cu nanoparticles with NaBH₄ by aqueous reduction method. *Trans. Nonferrous Met. Soc. China*, 22, 117 – 123
- Liu, R. Zhang, H. and Lal, R. (2016). Effects of Stabilized Nanoparticles of Copper, Zinc, Manganese, and Iron Oxides in Low Concentrations on Lettuce (*Lactuca sativa*) Seed Germination: Nanotoxicants or Nanonutrients?. *Water, Air, & Soil Pollutio*, 227; 42.
- Liu, X., Jiang, W., Su, M., Sun, Y., Liu, H., Nie, L., & Zang, H. (2019). Quality evaluation of traditional Chinese medicines based on fingerprinting. *Journal of Separation Science*, 43(1).
- M. Nasrollahzadeh, Z. Issaabadi, and S. M. Sajadi, “Green synthesis of a Cu/MgO nanocomposite by *Cassia filiformis* L. extract and investigation of its catalytic activity in the reduction of methylene blue, congo red and nitro compounds in aqueous media,” *RSC Advances*, vol. 8, pp. 3723-3735, 2018.
- Madureira, A. M. Ramalheite, C. Mulhovo, S. Duarte, A. and Ferreira, M. U. (2012). Antibacterial activity of some African medicinal plants used traditionally against infectious diseases. *Pharmaceutical Biology*, 50(4); 481-489.
- Maema, L. P. Potgieter, M. Masevhe, N. A. and Samie, A. (2020). Antimicrobial activity of selected plants against fungal species isolated from South African AIDS patients and their antigonococcal activity. *Journal of Complementary and Integrative Medicine*, 17(3); 20190087.
- Mahadevan, N., Upendra, B., Subburaju, T., Elango, K., & Suresh, B. (2002). Purgative and anti-inflammatory activities of *Cassia didymobotrya*, fresen. *Ancient Science of Life*, 22(1), 9.
- Maina, G. J. Maitho, T. and Mbaria, J.M. (2018). Antifleas Activity and Safety of *Tithonia diversifolia* and *Senna didymobotrya* Extracts. *Journal of Pharmacy and Pharmacology Research*, 2(3); 078-092.
- Makwana B., Parikh P, Zala D. (2014). Biosynthesis of copper nanoparticles and their antimicrobial activity. *Inst Post Studies Res KSV Uni. India*. 1–15.
- McGaw, L. J. Ja`ger, A. K. & van Staden, J. (2000). Antibacterial, anthelmintic and anti-amoebic activity in South African medicinal plants. *Journal of Ethnopharmacology*, 72; 247–263.
- Mining J., Lagat Z. O., Akenga T., Tarus P., Imbuga M., Tsamo M. K. (2014). Bioactive metabolites of *Senna didymobotrya* used as biopesticide against *Acanthoscelides obtectus* in Bungoma, Kenya. *Journal of Applied Pharmaceutical Science*, 4(9), 56-60. doi:10.7324/JAPS.2014.40910
- Mohammad, J. (2015), in *Experimental Design in Petroleum Reservoir Studies*. 1-8
- Molton J. S., Tambyah P. A., Ang B.S.P., Ling M. L., & Fisher D. A. (2013). The Global Spread of Health-care associated Multi Drug-resistant bacteria: a perspective from Asia. *Journal of Clinical Infectious Diseases*, 56.

- Mott, D., Galkowski, J., Wang, L., Luo, J., Zhong, C.J. (2007). Synthesis of size-controlled and shaped copper nanoparticles. *Langmuir* 23, 5740–5745
- Mourdikoudis, S., Pallares, R. M., & Thanh, N. T. K. (2018). Characterization Techniques for Nanoparticles: Comparison and Complementarity upon Studying Nanoparticle Properties. *Journal of Nanoscale*, DOI: 10.1039/C8NR02278J
- Mukungu, N. Abuga, K. Okalebo, F. Ingwela, R. and Mwangi, J. (2016). Medicinal plants used for management of malaria among the Luhya community of Kakamega East subcounty, Kenya. *Journal of Ethnopharmacology*, 194; 98–107.
- Mutuku, C. N. & Ndikiu, H. (2015). Assessment of antibacterial activity of senna didymobotrya leaves water extract as an Alternative remedy to curb nosocomial infections. *International Journal of Bioassays*, 4(4); 3783-87.
- Mworia, J. K. Mwitikibiti, C. Ngugi, M. P. and Ngeranwa, J. N. (2019). Antipyretic potential of dichloromethane leaf extract of Eucalyptus globulus (Labill) and Senna didymobotrya (Fresenius) in rats models. *Heliyon*, 5(12); e02924.
- Nagappan, R. (2012). Evaluation of aqueous and ethanol extract of bioactive medicinal plant, Cassia didymobotrya (Fresenius) Irwin & Barneby against immature stages of filarial vector, Culex quinquefasciatus Say (Diptera: Culicidae). *Asian Pacific Journal of Tropical Biomedicine*; 707-711.
- Nair R., Varghese S.H., Nair B. G. , Maekawa T., Yoshida Y., and Kumar D. S. (2010). *Plant Science*. 3, 154.
- Nankaya, J. Nampushi, J. Petenya, S. and Balslev, H. (2019). Ethnomedicinal plants of the Loita Maasai of Kenya. *Environment, Development and Sustainability*, 15(5).
- Nasrollahzadeh M, Sajadi SM. (2015). Green synthesis of copper nanoparticles using Ginkgo biloba L. leaf extract and their catalytic activity for the Huisgen [3 + 2] cycloaddition of azides and alkynes at room temperature. *Journal of Colloid Interface Science*. 457:141–7.
- Nasrollahzadeh M., Issaabadi Z., & Sajadi S. M. (2018). Green synthesis of a Cu/MgO nanocomposite by Cassytha filiformis L. extract and investigation of its catalytic activity in the reduction of methylene blue, congo red and nitro compounds in aqueous media. *Royal Society of Chemistry*, 8. doi:DOI: 10.1039/c7ra13491f
- Njoroge G. N. and Bussman, R. W. (2006). Diversity and utilization of antimalarial ethnophytotherapeutic remedies among the Kikuyus (Central Kenya). *Journal of Ethnobiology and Ethnomedicine*, 2(8); 7.
- Njoroge, G. N. & Kibunga, J. W. (2007). Herbal medicine acceptance, sources and utilization for diarrhoea management in a cosmopolitan urban area (Thika, Kenya). *African Ecology*, 45, 65–70.
- Njoroge, G. N. and Bussmann, R. W. (2006). Diversity and utilization of antimalarial ethnophytotherapeutic remedies among the Kikuyus (Central Kenya). *Journal of Ethnobiology and Ethnomedicine*, 2(8).
- Nyamwamu L. B., Ngeiya M., Mulaa M., Lelo E. A., Ingonga J., Kimutai A. (2015). Phytochemical constituents of senna didymobotrya Fresen irwin roots used as a traditional medicinal plant In kenya. *International Journal of Education and Research*, 3(6): 2411-5681

- Ocharo, C. M. (2005). Isolation and Identification of Antibacterial and Antifungal Compounds from Selected Kenyan Medicinal Plants. MSc Thesis, Kenyatta University, Kenya.
- Ochieng, C. O. Shrivastava, A. Chaturvedi U. et al. (2013). Effects of Senna didymobotrya Root Extract and Compounds on Tritoninduced Hyperlipidaemic Rats and Differentiation of 3T3-Li Preadipocytes. *The Natural Products Journal*, 3(3); 212-217.
- Ogundipe, O. O., Moody, J. O., Houghton, P.J., Odelola, H.A. (2001). Bioactive constituents from *Alchornea laxiflora* (benth) Pax and Hoffman. *Journal of Ethnopharmacology*, 74(3): 275-280
- Okello, S. V. Nyunja, R. O. Netondo, G. W. and Onyango, J. C. (2010). Ethnobotanical study of medicinal plants used by Sababots of Mt. Elgon Kenya. *African Journal of Traditional, Complementary and Alternative Medicine*, 7(1); 1–10.
- Olajire, A. A., Ifediora N. F., Bello, M. D. Benson, N. U. (2017). Green Synthesis of Copper Nanoparticles Using *Alchornea laxiflora* Leaf Extract and Their Catalytic Application for Oxidative Desulphurization of Model Oil. *Iran Journal of Science and Technology, Transaction A: Science*. [https://doi.org/10.1007/s40995-017-0404-9\(012345](https://doi.org/10.1007/s40995-017-0404-9(012345)
- Olala, C. N. (2014). Identification of plants used for treatment of malaria and factors influencing their use in Boro division, Siaya county, Kenya. MSc Thesis, Kenyatta University, Nairobi, Kenya.
- Omara, T. (2020). Antimalarial plants used across Kenyan communities,” *Evidence-Based Complementary and Alternative Medicine*, 2020.
- Omara, T. Kiprop, A. K. and Kosgei, V. J. (2021). Intraspecific Variation of Phytochemicals, Antioxidant, and Antibacterial Activities of Different Solvent Extracts of *Albizia coriaria* Leaves from Some Agroecological Zones of Uganda,” *Evidence-Based Complementary and Alternative Medicine*, 2021, Article ID 2335454.
- Orwa, C. & Njue, L. (2019). Efficacy of Crude Extract from Candle Brush (*Senna didymobotrya*) Leaves against *Aspergillus niger* in Reduction of Post-harvest Losses in Tomatoes. *Asian Food Science Journal*, (10)2; 1-8.
- Padma Naga P., Syed T. B., & Kumari C. S. (2018). Studies on Green Synthesis of Copper Nanoparticles Using *Punica granatum*. *Annual Research & Review in Biology*, 23(1). DOI: 10.9734/ARRB/2018/38894
- Park, B. K. Kim, D. Jeong, S. J. Moon, and J. S. Kim, (2007). Direct writing of copper conductive patterns by ink-jet printing,” *Thin Solid Films*, 515(19); 7706-7711.
- Patra, K. J., Das, G., Fraceto, L.F., Campos, E.V.R, Rodriguez-Torres, M.P., Acosta-Torres, L.S., Diaz-Torres, L.A., Grillo, R., Swamy, M. K., Sharma, S., Habtemariam, S., & Han-Seung, S. (2018). Nano based drug delivery systems: recent developments and future prospects. *Journal of Nanobiotechnology*, 16:71
- Poinern, G. E. (2015). *A Laboratory Course in Nanoscience and Nanotechnology*. (1. 978-1-4822-3104-5, Ed.) Boca Raton London New York, Western Australia: CRC Press (Taylor and Francis Group).
- Prema, P. (2010). Chemical mediated synthesis of silver nanoparticles and its potential antibacterial application,” In: *Progress in Molecular and Environmental*

- Bioengineering – From Analysis and Modeling to Technology Applications. *IntechOpen*; 151-166.
- Radu, G., Truică, G., Penu, R., Moroeanu, V., Litescu, S. C. (2012). Use of the fourier transform infrared Spectroscopy in characterization of specific Samples. *U.P.B. Sci. Bull., Series B*, 74(4).
- Raffi, M. Mehrwan, S. Bhatti T. M. et al. (2010). Investigations into the antibacterial behavior of copper nanoparticles against Escherichia coli. *Annals of Microbiology*, 60; 75-80, 2010.
- Rai M., Shende S., Avinash P. Ingle, Gade A. (2015). Green synthesis of copper Nanoparticles by *Citrus medical inn. (Idilimbu) juice* and its antimicrobial activity. *World journal of microbiology and biotechnology*, 31:865-873.
- Rajagopal, G. Nivetha, A. Sundar, M. et al. (2021). Mixed phytochemicals mediated synthesis of copper nanoparticles for anticancer and larvicidal applications,” *Heliyon*, 7(6); e07360.
- Ramyadevi, J. Jeyasubramanian, K. Marikani, A. Rajakumar, G. and Rahuman, A. A. (2012). Synthesis and antimicrobial activity of copper nanoparticles,” *Materials Letters*, 71; 114-116.
- Rasul, M. G. (2018). Extraction, Isolation and Characterization of Natural Products from Medicinal Plants. *International Journal of Basic Sciences and Applied Computing*, 2(6)
- Reddy, J.L., Anjana, J.C.B. and Ruveena, T.N. (2010). Evaluation of antibacterial activity of *Trichosanthes cucumerina*, L. and *Cassia didymobotrya* Fres. Leaves. *International J Pharm and Pharmaceut Sci.*; 2:153-155.
- Renganathan S., Saranyaadevi K, Subha V, Ravindran R. E. (2014). Synthesis and characterization of copper nanoparticle using *Capparis zeylanica* leaf extract. *International Journal of Chemical Technology Research*. 6:4533–41.
- Rozina SSM, Shaikh R, Sawant MR, Sushama B. (2016). Biosynthesis of Copper Nanoparticles using *Vitis vinifera* Leaf Extract and Its Antimicrobial Activity. *Der Pharm Lett*. 8(2016):265–72.
- Sahil, K., Sudeep, B., & Akanksha, M. (2011). Standardization of medicinal plant materials. *International Journal of Research in Ayurveda & Pharmacy*, 2(4), 1100-1109. ISSN 2229-3566
- Saif, S. Tahir, A. Asim, T. and Chen, Y. (2016). Plant mediated green synthesis of CuO nanoparticles: comparison of toxicity of engineered and plant mediated CuO nanoparticles towards *Daphnia magna*,” *Nanomaterials*, 6; 205.
- Salopek, B. Krasic, D. Filipovic, S. (1992). Measurement and Application of Zeta-Potential,” *Rudarsko-Geolosko-Naftni Zbornik*, 4; 147.
- Sandip, P., Shreewardhan, R., Sandeephan, M., Abhay, C., Debjani, D. (2014). Phytochemical evaluation and free radical scavenging potential of *Hugonia Mystax* (L) Leaf Extract. *Bionano Frontier*, 7(2).
- Sankar, R. Maheswari, R. Karthik, S. K. S. Shivashangari, and Rav, V. (2014). Anticancer activity of *Ficus religiosa* engineered copper oxide nanoparticles,” *Materials Science and Engineering C*, 44; 234-239.
- Sathiyavimal, S. Vasantharaj, S. Bharathi D. et al., (2018). Biogenesis of copper oxide nanoparticles (CuONPs) using *Sida acuta* and their incorporation over cotton fabrics

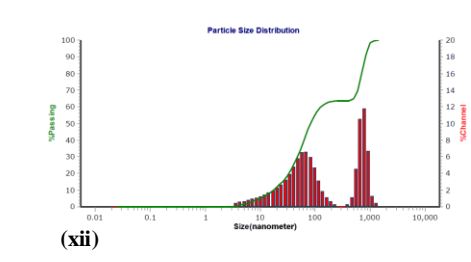
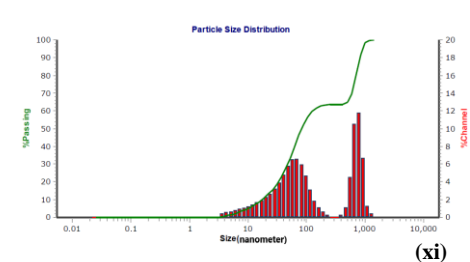
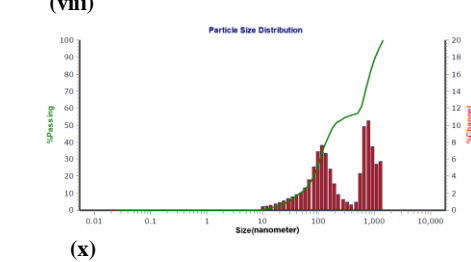
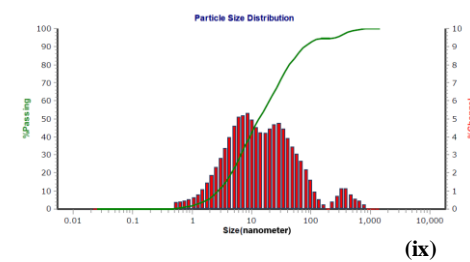
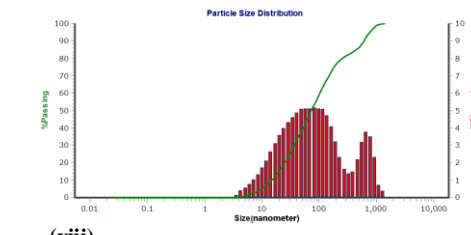
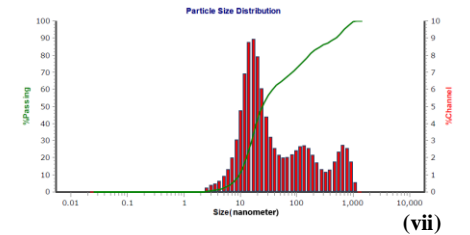
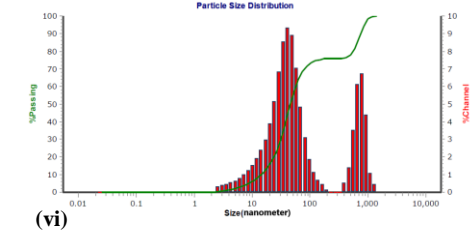
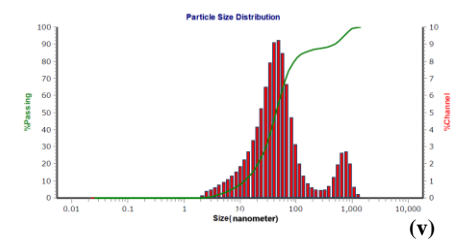
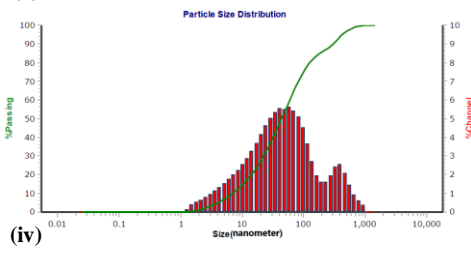
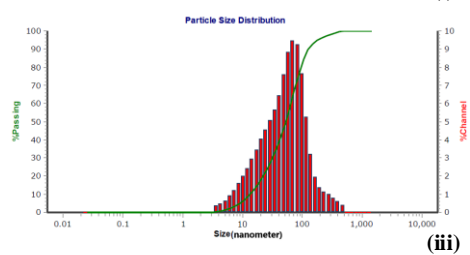
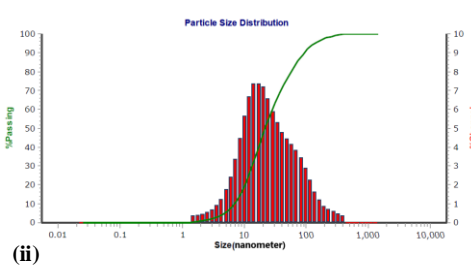
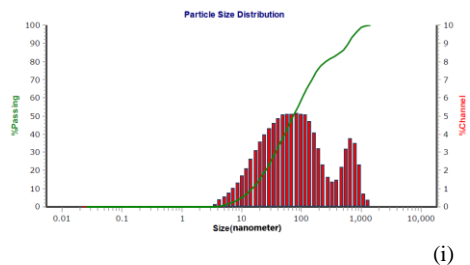
- to prevent the pathogenicity of Gram negative and Gram positive bacteria. *Journal of photochemistry and photobiology. B, Biology*, 188: 126–134.
- Sembiring, E. N., Elya, B., Sauriasari, R. (2018). Phytochemical Screening, Total Flavonoid and Total Phenolic Content and Antioxidant Activity of Different Parts of *Caesalpinia bonduc* (L.) Roxb. *Journal in the field of Natural Products and Pharmacognosy*, 10(1); 123-127
- Sergelidis, D., Papadopoulos, T., Komodromos, D., Isolation of methicillin-resistant *Staphylococcus aureus* from small ruminants and their meat at slaughter and retail level in Greece. *Letters in Applied Microbiology*, 61; 498-503.
- Shaikh S., Fatima J., Shakil S., Rizvi S.M.D., & Kamal, M.A., (2015). Antibiotic resistance and extended spectrum beta-lactamases types, epidemiology and treatment. *Saudi Journal of Biological Sciences*, 20(1), 90-101.
- Shailesh C. K., Parmar A., Tessy J. (2018). Green Synthesis of Copper Nanoparticles using *Mitragyna parvifolia* Plant Bark Extract and Its Antimicrobial Study. *Journal of Nanoscience and Technology*, 4 (4), 456-460, 2455-0191.
- Sharma, B. K. Shah, D. V. and Roy, D. R. (2018). Green synthesis of CuO nanoparticles using *Azadirachta indica* and its antibacterial activity for medicinal applications,” *Materials Research Express*, 5(9); 095033.
- Shobha G., Moses V., & Ananda S. (2014, August). Biological Synthesis of Copper Nanoparticles and its impact - a Review. *International Journal of Pharmaceutical Science Invention*, 3(8). Retrieved from <http://www.ijpsi.org>
- Sievert, D.M., Wilson, L. M., Wilkins, M. J., Gillespie, B. W., & Boulton, M. L. (2010). Public Health Surveillance for Methicillin-Resistant *Staphylococcus aureus*: Comparison of Methods for Classifying Health Care- and Community-Associated Infections. *American Journal of Public Health*, 100(9)
- Silhavy, T. J. Kahne, D. and Walker, S. (2010). The bacterial cell envelope. *Cold Spring Harbor perspectives in biology*, 2(5); a000414.
- Sofowara, A. (1993). Medicinal plants and traditional medicine in Africa. *Spectrum books ltd, Ibadan Nigeria*, 191-289.
- Tabuti, J.R.S. (2007). *Senna didymobotrya* (Fresen.) H.S. Irwin & Barneby. In: Schmelzer, G.H. and Gurib-Fakim, A. (Editors). *Prota 11(1): Medicinal plants/Plantes médicinales 1. PROTA*, Wageningen, Netherlands.
- Tadesse D. A., Zhao S., & Tong E. (2012). Antimicrobial drug resistance in *Escherichia coli* from humans and food animals, United States, 1950–2002. *Emerging Infectious Diseases*, 18(5), 741–749.
- Tamilvanan, A. Balamurugan, K. Mohanraj, T. Selvakumar, P. and Madhankumar, B. (2021). Parameter optimization of copper nanoparticle synthesis by electrodeposition process using RSM and CS,” *Materials Today: Proceedings*, vol. 45, no. 2, pp. 751-756, 2021.
- Tamilvanan, A., Balamurugan, K., Ponappa, K., & Kumar, M. B. (2015). Using Response Surface Methodology in Synthesis of Ultrafine Copper Nanoparticles by Electrolysis. *International Journal of Nanoscience*, 14 (5).

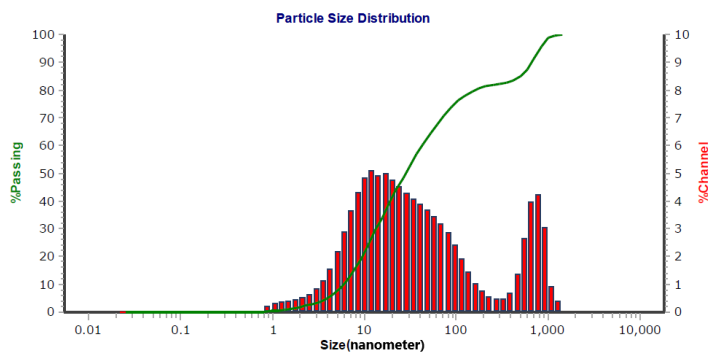
- Tenney J., Hudson N., Alnifaigy H., Cheung Li J. T., & Fung K. H. (2017). Risk factors for acquiring multidrug-resistant organisms in urinary tract infections: A systematic literature review. *Saudi Pharmaceutical Journal*, 26, 678–684. Retrieved from <https://doi.org/10.1016/j.jsps.2018.02.023>
- Thakkar, K. N., Mhatre, S. S., & Parekh, R. Y. (2010). Biological synthesis of Metallic Nanoparticles. *Journal of Biol. Med*, 6: 257-262
- Thangiah, A. S., & Ngule, M. C., (2013). Phytopharmacological analysis of methanolic-aqua extract (fractions) of *Senna didymobotrya* roots. *International Journal of Bioassays*, 2(11), 1473-1479.
- Tong, S. Y. C., Davis, J. S., Eichenberger, E. Holland, T. L., Fowler, V. G. (2015). *Staphylococcus aureus* Infections: Epidemiology, Pathophysiology, Clinical Manifestations, and Management. *Clinical Microbiology Reviews*, 28(3)
- Trease, G.E. and Evans, W.C. (1989). Pharmacognosy, 11th end, Brailliere tindall, London, pp 45-50.
- Tuem K. B., Gebre A. K., Atey T. M., Bitew H., Yimer E. M., Berhe D. F. (2018). Drug Resistance Patterns of Escherichia coli in Ethiopia: A Meta-Analysis. *Journal of BioMed Research International*. Retrieved from <https://doi.org/10.1155/2018/4536905>
- Umer, A., Naveed, S., Ramzan, N., Rafique, M.S. and Imran, M. 2014. A Green Method For The synthesis Of Copper Nanoparticles Using L-ascorbic Acid, *Matéria*, 19(3), 197-203, <https://dx.doi.org/10.1590/S1517-70762014000300002>.
- United States Pharmacopeia and National Formulary, USP 25, NF 19, United States Pharmacopeial Convention Inc., Rockville, 2002.
- Usman, M. S. El Zowalaty, M. E. Shamel K. et al., (2013). Synthesis, characterization, and antimicrobial properties of copper nanoparticles,” *International journal of nanomedicine*, 8; 4467–79.
- Vaidehi, D. Bhuvaneshwari, V. Bharathi, D. & Sheetal, B. P. (2018). Antibacterial and photocatalytic activity of copper oxide nanoparticles synthesized using Solanum lycopersicum leaf extract. *Materials Research Express*, 5(8); 085403.
- Vasantharaj, S. Sathiyavimal, S. Saravana M. et al., (2019). Synthesis of ecofriendly copper oxide nanoparticles for fabrication over textile fabrics: Characterization of antibacterial activity and dye degradation potential,” *Journal of Photochemistry and Photobiology B: Biology*, 191; 143-149.
- Vasantharaj, S. Sathiyavimal, S. Saravana M. et al., (2019). Synthesis of ecofriendly copper oxide nanoparticles for fabrication over textile fabrics: Characterization of antibacterial activity and dye degradation potential. *Journal of Photochemistry and Photobiology B: Biology*, 191; 143-149.
- Wagate, C. G., Mbaria, M. J., Gakuya, D.W., Nanyingi, M. O., Kareru, P. G., Njuguna, A., Gitau, N., Macharia, J. K. and Njonge, F. (2012). Screening of some Kenyan medicinal plants for antibacterial activity. *Phytotherapy Research*, 24.
- Wang, H. K., Yi, C. Y., Tian, I., Wang, W. J., Fang, J., & Zhao, J. H. (2012). Ag-Cu bimetallic copper nanoparticle prepared by microemulsion method as catalyst for epoxidation of styrenes. *Journal of nanomaterials*, 8.

- Warnes, S. and Keevil, C. (2011). Mechanism of copper surface toxicity in vancomycin-resistant enterococci following 'wet' or 'dry' contact. *Applied and Environmental Microbiology*, 2011. 77; 6049-6059.
- Williams, D. N., Ehrman, S. H., and Holoman, T. R. P. (2006). Evaluation of the microbial growth response to inorganic nanoparticles. *Journal of Nanobiotechnology*; 4: 3
- Wongpisutpaisan, N. Vittayakorn, N. Ruangphanit, A. & Pecharapa, W. (2013). Cu-Doped TiO₂ Nanopowders Synthesized by Sonochemical-assisted Process. *Sains Malaysiana*. 42(2), 175-181.
- Wu, S. H., & Chen, D. H. (2004). Synthesis of high-concentration Cu nanoparticles in aqueous CTAB solutions [J]. *Journal of Colloid and Interface Science*, 273(1): 165-169.
- Yadav, P., Mahour, K., & Kumar, A. (2011). Standardization and evaluation of herbal drug formulations. *Journal of Advanced Laboratory research in Biology*, 2(4).
- Yoon, K., Byeon, J. H., Park, J. and Hwang J., (2007). Susceptibility constants of *Escherichia coli* and *Bacillus subtilis* to silver and copper Nanoparticles". *Sci Total Environ* 373:572-575.
- Zhang, H. Siegert, U. Liu, R. and Cai, W. (2009). Facile Fabrication of Ultrafine Copper Nanoparticles in Organic Solvent. *Nanoscale Research Letters*, 4; 705.

APPENDICES

Appendix A: Particle Size Analyzer Data





(xiii)

Key: Particle size of CuNPs prepared at: (i)Temp 80 °C, pH 3.0 and Copper ion Concentration 0.03125 M, (ii) Temp 60 °C, pH 3.0 and Copper ion Concentration 0.0125 M, (iii) Temp 40 °C, pH 10.0 and Copper ion Concentration 0.03125 M (iv) Temp 80 °C, pH 6.5 and Copper ion Concentration 0.05 M, (v) Temp 40 °C, pH 6.5 and Copper ion Concentration 0.05 M, (vi) Temp 80 °C, pH 6.5 and Copper ion Concentration 0.0125 M, (vii) Temp 40 °C, pH 3.0 and Copper ion Concentration 0.03125 M, (viii) Temp 40 °C, pH 6.5 and Copper ion Concentration 0.0125 M, (ix) Temp 80 °C, pH 3.0 and Copper ion Concentration 0.03125 M, (x) Temp 60 °C, pH 10.0 and Copper ion Concentration 0.05 M, (xi) Temp 60 °C, pH 10.0 and Copper ion Concentration 0.0125 M, (xii) Temp 80 °C, pH 10.0 and Copper ion Concentration 0.03125 M, (xiii) Temp 60 °C, pH 3.0 and Copper ion Concentration 0.05 M.

Appendix B: Growth Inhibition Zones of Cu NPs biosynthesized at different conditions of temperature, pH and Copper ion Concentration

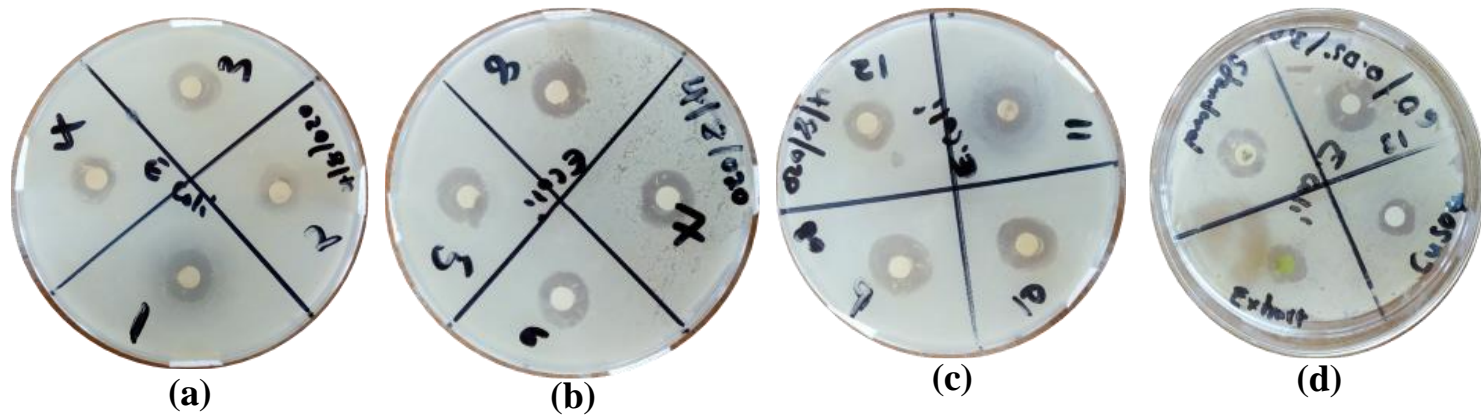


Figure 26: The growth inhibition zones of CuNPs biosynthesized at different conditions of temperature, pH and copper ion concentration against *Escherichia coli* in Luria betani (LB) disk diffusion

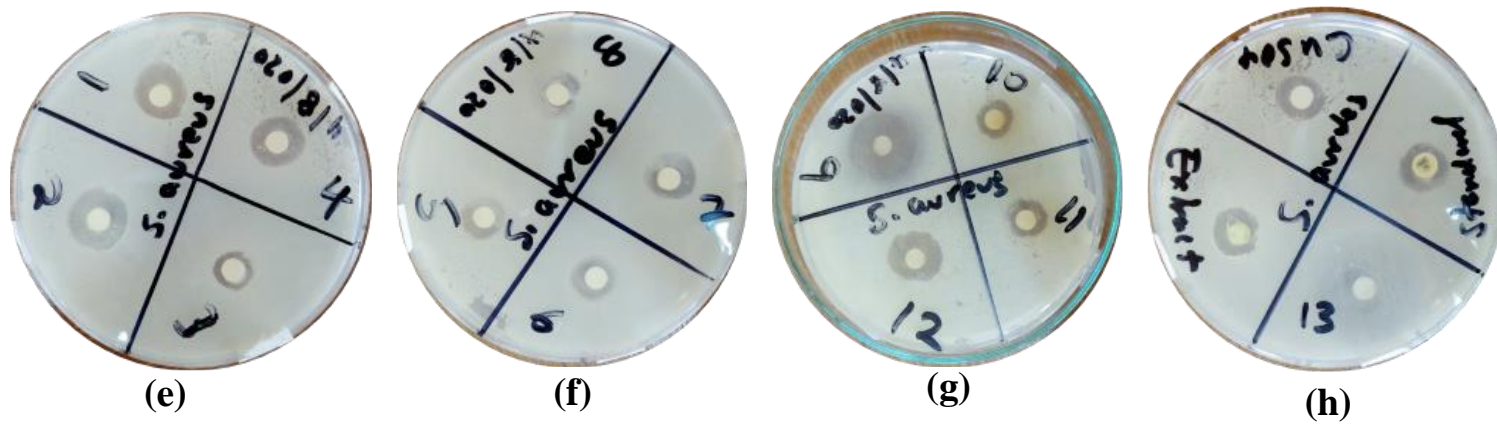


Figure 27: The growth inhibition zones of CuNPs biosynthesized at different conditions of temperature, pH and copper ion concentration against *Staphylococcus aureus* in Luria betani (LB) disk diffusion